Development of a parametric model for analysing temperature effects of solar radiation on yachts

Vivek Kumar

Master Thesis

presented in partial fulfillment
of the requirements for the double degree:
"Advanced Master in Naval Architecture" conferred by University of Liege
"Master of Sciences in Applied Mechanics, specialization in Hydrodynamics,
Energetics and Propulsion" conferred by Ecole Centrale de Nantes

developed at the University of Genoa in the framework of the

"EMSHIP"
Erasmus Mundus Master Course
in "Integrated Advanced Ship Design"

Ref. 159652-1-2009-1-BE-ERA MUNDUS-EMMC

Supervisor :   Prof. Dario Boote, University of Genoa, Italy

Reviewer   :   Prof. Maciej Taczała, ZUT University, Szczecin, Poland

Genoa, February 2014

DECLARATION OF AUTHORSHIP

I declare that this thesis and the work presented in it are my own and have been generated by me as the result of my own original research. Where I have consulted the published work of others, this is always clearly attributed. Where I have quoted from the work of others, the source is always given. With the exception of such quotations, this thesis is entirely my own work. I have acknowledged all main sources of help. Where the thesis is based on work done by myself jointly with others, I have made clear exactly what was done by others and what I have contributed myself. This thesis contains no material that has been submitted previously, in whole or in part, for the award of any other academic degree or diploma. I cede copyright of the thesis in favour of the University of Genoa, Italy.

Date: 15 JANUARY 2014   VIVEK KUMAR

ABSTRACT

The perfection of a yacht's beauty is that nothing should be there for only beauty's sake.
-John MacGregor, Scottish explorer and designer of the first modern sailing canoes

The two most important characteristics of a motor yacht are its performance and high quality aesthetics. While the former is measured by attributes such as speed, range and the power-to-weight ratio, the latter is measured essentially by the hull's fairness and lack of visually observable defects. In practice, however, environmental loads such as solar radiation have a detrimental effect on these two characteristics. It causes high temperatures on the hull and deck, leading to deformations and increased energy needs to cool the ship. The ship then needs to be built with a stronger scantling to resist thermal expansions, and larger cooling systems for maintaining internal comfort. More systems mean more ship weight and cost.

The classic colour of the motor yacht fleet is thus unsurprisingly white. However, recent trends see owners opting for darker colours, which absorb much more heat from the sun. Consequently, uneven thermal expansions causes a very unaesthetic "wavy" pattern along the ship when seen longitudinally. This may be due to thermal stresses combined with global ship loads that cause local stresses in ship sections. Currently, an overly thick epoxy layer is used to mask the aluminium hull of the ship along with a shorter transversal and longitudinal framing system. This conservative approach makes the vessel heavier and more expensive.

This thesis is in response to the need for a naval architect to deal with the engineering challenge of implementing solutions that will enable painting with dark colours, and still obtain excellent aesthetics. It contains an analytical study from experimental investigations, combined with a theoretical model for predicting temperatures. Parametric modelling has been used to study the effects of seasonal variations, different colours, different materials, and various solutions have been proposed to negate the detrimental effects of high temperatures. This thesis work was carried out in close cooperation with Baglietto Shipyards, Italy.

Vivek Kumar
vivek.kumar.mailbox@gmail.com

CONTENTS

List of Tables

1   SUMMARY

This work has been done in response to the critical need for a naval architect to analyse the effect of solar loads that destroy the aesthetic appeal of a motor yacht. To begin with, it was important to know the fundamental input to the problem – the behaviour of solar radiation and its influence on surface temperatures. The project began with a data acquisition of hull temperatures over the target yacht, using infrared thermal imaging as shown in Figure 1.
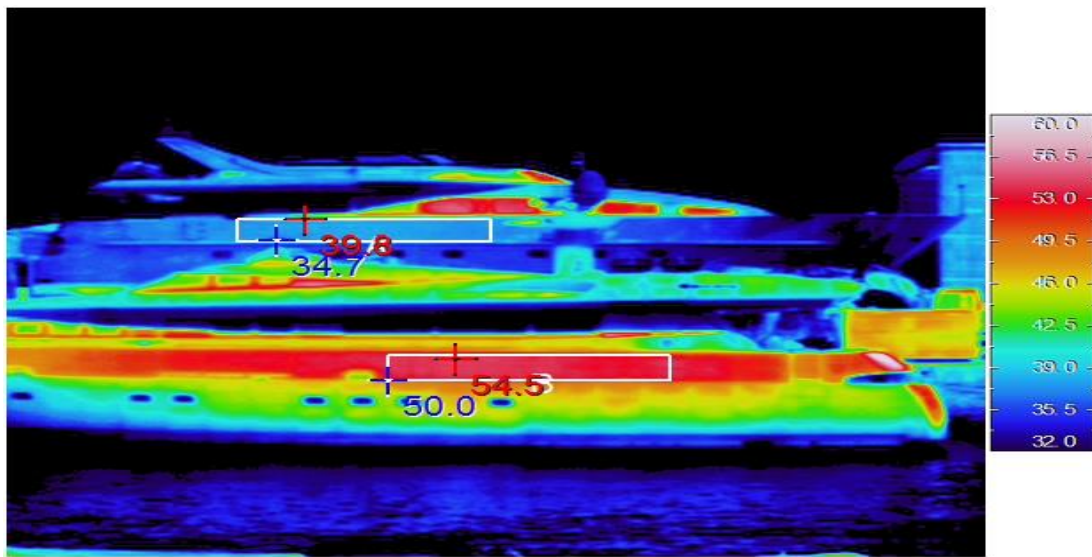
Figure 1: The white ship at 35-40^{0}C is much cooler than the dark-blue ship at 55-60^{0}C even while out of water (windows are ignored since they reflect sunlight and show up as red regions)

However, such extensive measurements would have been needed throughout the year, in different ship positions, for sufficient data. Thus, specific calculations on Solar Ray Tracing and Classical Heat Transfer theory have been used to create a theoretical model.

Lastly, these results have been used to conduct a system analysis, to determine likely solutions for reducing temperatures, and resulting effects such as deformations seen on the metal plating. The most effective way of reducing thermal deformations was found to be the structural reinforcement of the intermediate section between bulkheads. This can be done by increasing the web height of the frames and longitudinals, which have the biggest effect on increasing the strength of the affected region. Changing the paint colour to silver grey also had a very big impact on surface temperatures. New technologies such as heat reflective paints have been suggested since they have started finding use as thermally insulative applications, in the marine

industry. For a detailed analysis, Section 8.5 lists a complete concept evaluation and implementation plan.

Paint colour was found to be the most important parameter in deciding the surface temperature of the hull under intense solar radiation. In turn, the fairness of the hull and increased loads to cool the ship are dependent on surface temperatures. The stiffness of the structure and the materials used in the hull are the next most important parameters.

Optical effects were studied and it was determined that apparent deflections are very important when evaluating the fairness of a yacht visually, which is usually the case. Recommendations to adopt objective evaluation criteria have been put forth based on existing draft proposals. This will enable both the shipyard and the owner to look forward to a high degree of aesthetic quality, which can be measured and thus avoid unnecessary disputes. In conclusion, detailed solutions presented in the Chapter 8 offer a very useful insight into possibilities of overcoming the detrimental effects of high temperatures.

There seems to be a consensus from studied literature that comprehensive data publicly available on such research is limited. Jasper (1955) states that limited quantative data is available which would indicate the actual stress and temperature variations that might be expected of a ship in service. There also seems to be a lack of publicly available literature over the last 25 years treating this subject in detail. This work thus, holds importance in disseminating information developed from independent research work, involving several experimental and theoretically ratified models.

The parametric model can be adapted to predict hull surface temperatures for a ship of any size, geometry and colour, operating anywhere in the world. Rigo & Rizzuto (2002) state that it is very difficult to quantify thermal loads due to the identification of temperature distributions and boundary conditions. It is hoped that this thesis is a step in the right direction, to fill the much needed research gap in evaluating thermal loads. These are normally only restricted to fire loads, while dealing with solar radiation only qualitatively.

2   INTRODUCTION

Aesthetics – It's all about engineering. To put this point in perspective, we must begin with a question. *Why is a yacht typically white?* Several reasons can be put forth such as, "It is cheaper than coloured paints due to the additional cost of pigments". Some would say, "White forgives imperfections and does not glitter and reflect so much, which makes it an easy choice for boat owners" or "dark surfaces show dirt, salt splashes and other defects quite easily". On the other hand, white neither fades as fast as other colours, nor does it need as much maintenance. Many owners even paint their boat white just because it has long been a pseudo standard in the industry. However, recent trends see many yacht owners opting for darker colours such as black or dark-blue.

And then they realize that *there is one more reason* why the classic colour of the fleet is white.

White boats, especially if built out of aluminium, are much cooler than if they were painted black. In the latter, this not only translates to distortion of the hull plating, but it also destroys the aesthetic appeal of the yacht. There will also be increased energy requirements to cool the ship. In fact on a clear day, external hull surface temperatures can reach an intense 50-60°C degrees, *even in winter*!

Over the last several years, the increasing demand for superyachts and megayachts has seen substantial demands being placed on yacht builders, for delivering the most exquisite shapes and designs. To keep up with this demand for the best aesthetics, the engineering behind coatings and materials has not fully kept up to speed. It is foreseen that this trend is going to continue in future, prompting the shipyard to implement solutions that are able to deliver this requirement. To keep the yacht looking good, the designer, the shipyard, the owner, the paint supplier, the contractors, the paint inspector, the crew and the maintenance facility must all work together. However, it is in the design stage, where the most potential for improvement exists.

The naval architect hence has to devise innovative solutions, to allow the ship to be painted black, and still avoid associated problems – a technical contradiction!

2.1   The Problem: Circumstances in Aluminium Motor Yachts

A motor yacht is a sophisticated ship meant for luxury cruising and recreation. To remain aesthetic, the fairness of the hull is paramount and *any deviations causing the hull to develop deformations instead of being smooth are considered unacceptable.* Figure 2 below illustrates an easily observable "wavy" profile on the side hull surface of a motor yacht. Even the reflection of the straight rope and the waves over the hull are seen to be highly undulating.

Figure 2: Image of the port side of a motor yacht with an aluminium hull, showing warping-distortions seen along the longitudinal direction, due to uneven thermal expansions

This undulation can be attributed to thermal expansion due to thermal gradients. Several factors combine to produce temperature differentials in a ship's hull (Gerard, 1959) and (Zubaly, 1973)

- *The colour of the hull paint*
- *The intensity of solar radiation*
- The effects of shading from the sun
- The temperatures of the surrounding water and air
- The temperature of air and liquids within the ship
- The effects of wind and waves in dissipating heat
- Extremely high temperatures of the welding process during fabrication

Yachts typically spend a majority of their time docked at the marina. Here, they might be sheltered from the high seas but they are still exposed to some vagaries of the environment, principally solar radiation. It is also important to note that the side shell of the hull is the most affected region and this exposed surface can be divided into different areas. For example, based on how the ship is berthed (or headed at sea) - port and starboard may be *asymmetrically exposed to solar radiation* (Figure 3). There is also a thermal discontinuity at the waterline, which sets up thermal gradients vertically on the hull surface. The top of the superstructure is usually in a lighter colour and in any case cannot be easily seen. Hence only hull temperatures have been treated in this thesis report.
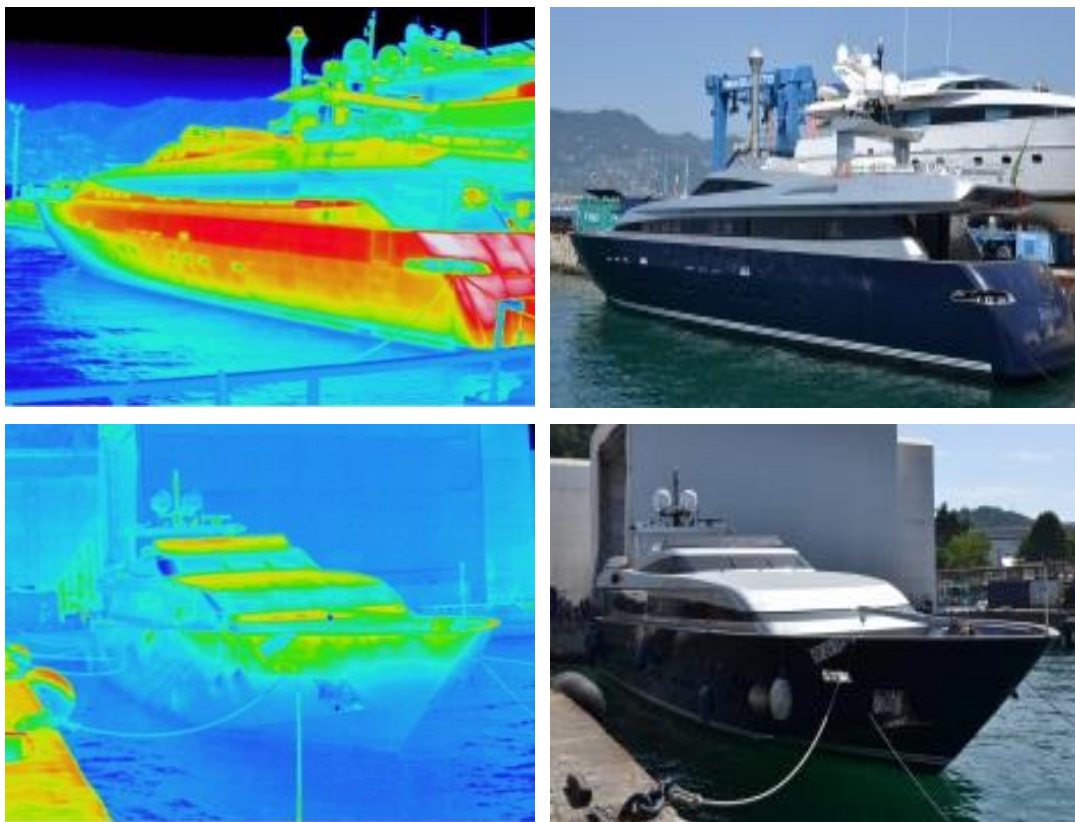
Figure 3: Thermal Imaging showing differential exposure to the sun between Port and Starboard

If the temperature distribution is uneven, temperature gradients produced by the thermal environment can contribute to the state of stress in the structure. Because of the complex nature of ship structures, *each part of the structure exercises some restraint or contraction on adjacent structures*. Thus the ship plating is not completely free to deform and the expansion or contraction of the plating occurs as a function of temperature and thermal gradients, causing distortions.

In addition, due to the loads exerted by hydrostatic forces, stresses are induced in the side shell, which are manifested as secondary and tertiary stresses in the frames, stiffeners and plates. It is also likely that the section between two bulkheads acts like a beam with maximum deflection in the mid span. Moreover, the vertical thermal gradient will cause region between the deck and the waterline to exhibit another mode shape. Lastly, the plate itself will deform. This phenomenon is very complex, especially with regard to ascertaining boundary conditions for calculations. It must also be kept in mind that high temperatures cause materials to expand, making the analysis thermo-structural. Thermal and structural stresses interact, with material properties changing with temperature, and a linear approximation of this behaviour is not available. Section 7.1.2 provides a useful insight into this problem.

2.2   Current Solutions and Limitations

Currently an epoxy filler layer is used to coat the entire aluminium hull surface over which the paint is applied. An epoxy filler is used normally to improve the finish of a surface. Thus, the bare metal of the boat is coated with a coarse epoxy layer and then a fine one to create a smooth surface, over which the paint is applied, in several coats.

Figure 4: Image of a ferry (taken at the marina) without any epoxy filler layers. Deflections are clearly visible in the blue painted region and justify the need for epoxy layering (taken in Aug, 2013)

This epoxy layer has to be made thicker than required (e.g. 15-20mm instead of 5-10mm) in order to mask the warping-distortion of the plates. However, the epoxy being thermally insulating, sets up a big temperature difference across itself and expands twice as much as the aluminium hull. It also makes the ship heavy, on the order of 1ton/mm of epoxy for a 40 metre yacht. The fact remains that the epoxy filler is essential in delivering a smooth finish to the motor yacht as Figure 4 illustrates, however its application must be carefully controlled to minimize the temperature distribution over it.

In addition, the transversal scantling frame spacing has to be reduced to increase the stiffness of the panel and reduce the degree of bending (e.g. 900-1000mm instead of 1100-1200mm). Even the longitudinal spacing has to be modified (e.g. 300-350mm instead of 350-400mm).

Both approaches above are conservative and make the vessel heavier and more expensive to build. Furthermore, even after these procedures, one can continue to see plate deformations.

2.3   Research Objectives and Methodology

To determine a way of predicting the ship surface temperature was the most important objective. Reducing temperatures and its negative effects such as deflections and increased air-conditioning energy needs was the outcome desired from the thesis, after the completion of a detailed analysis.

Different parameters that affected the thermal loading were studied. All these studies were then compared with each other and later with other external references, where applicable. As a concluding note, solutions to overcome the problem were conceptualized.

A detailed chapter on the effects of temperature has been included. Here, deformations have been analysed including a section on optical analysis and hull coating defects. This has been included since the overall purpose is to improve aesthetics, which is a visual parameter. This chapter presents a very interesting discussion on distinguishing apparent deflections from real deflections which occur due to the highly reflective nature of the motor yacht's surface. Heat, Ventilation and Air conditioning Analysis (HVAC) focusses on a brief discussion of the relation between the yacht's energy consumption to the colour of its hull paint.

Primary Objective :		
Measure surface temperatures	Create temperature prediction model	Analyse parameters and suggest solutions

Secondary Objective :

Analysis of Deformations and Hull Coating Defects	Energy Efficiency & Thermal Comfort Analysis
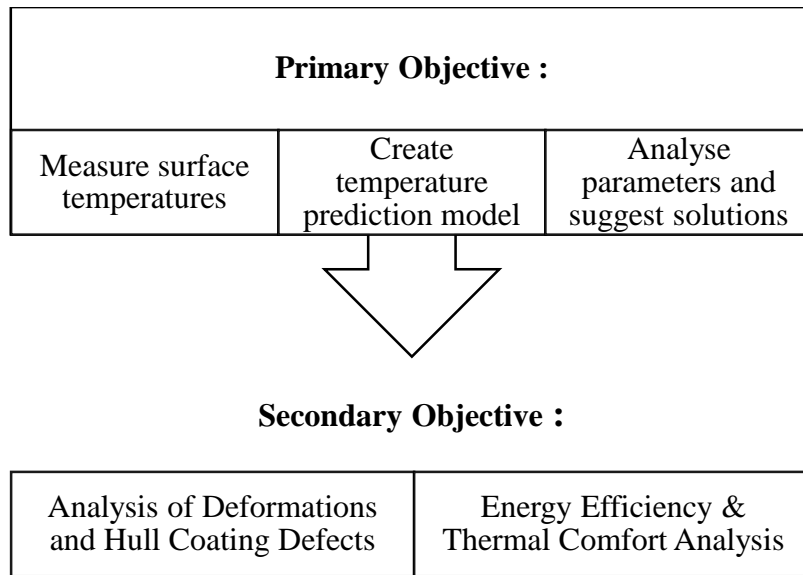
Figure 5: Block diagram of thesis objectives

The research plan adopted is briefly outlined below in a work breakdown structure. In subsequent pages, each element is elaborated upon with work carried out and corresponding justifications.

- Collect temperature distribution data on aluminium hull plating.
- Collect stress and deflection distribution data on aluminium hull plating.
- Define conditions where the problem is most located.
- Develop theoretical models to predict the surface temperatures.
- Develop theoretical models to predict the plate bending phenomena.
- Carry out a parametric analysis to find the critical factors causing the phenomena.
- Develop FEM models if time permits to predict the plate bending behaviour.
- System analysis to design conceptual solution to the problem.
- Experimentally analyse different epoxy-aluminium plates under different conditions.
- Discussions and implementations of solutions.

The project plan was divided into three stages of two months each as described in Figure 6.

STAGE-1	STAGE-2	STAGE-3
•Preliminary Study & Observations •Structural Analysis Research •Materials Research : Aluminium alloys & epoxy fillers •Study of Existing Solutions to reduce hull plate distortion •Theoretical Study : Heat Transfer & Thermal Stresses •Plan for experiments to be conducted •Project Technical Checkpoint	•Experiments & Observations • Create Solar Ray Tracing Model •Use Model to predict surface temperatures •Compare and correlate model and measurements •Use model to conduct a parametric analysis •Theoretical Analysis: Plate deformation •Project Technical Checkpoint	•Theoretical Ship Section Stress Analysis •Energy Efficiency Analysis •Conceptualize Solutions •Solution Implementation plan •Experimental Validation •Parametric Analysis : Input (Materials...) Output (Aesthetics, Cost...) •Project Conclusion

Figure 6: Stage-wise representation of the project plan

2.4 Measurements

A problem in plate warping-distortion has about 7 main variables − material(s), paint colour, panel/plate length and width, material thickness, stress/strain and temperature. Since a normal design sequence will define material choice and plate dimensions beforehand, only temperature and deformations (strain) need to be measured.

For an in-depth analysis, there were various measuring techniques available. To measure temperatures, portable thermocouples could have been used to obtain temperature data on outside and inside plating allowing us to construct temperature distribution curves. For deflections, three-dimensional calculations could be verified by tests carried out on a laid-up ship having strain gauges disposed longitudinally on the hull and on bulkheads, and other members (Hechtman, 1956). *However the above methods were not practical in terms of ship inspection availability, laboratory resources, budget and the short time (6 months) available* for this project, and thermal imaging and manual measurements were chosen instead.

2.4.1   Temperature

In light of the above challenge, the best method to measure temperature in terms of time, cost, convenience and accuracy was *Thermography*. This involves the use of thermal imaging

cameras to inspect the hull and provides a detailed temperature gradient of the analysed surface. Since they are based on the principle of detecting radiations, they are an excellent tool for detecting thermal variations caused by solar radiation (Figure 7). They are already used for marine inspections on commercial ships for features such as engines, compressors, boilers etc. *Thermography offers the advantage of not interfering with the vessel's operation.*

At the time of starting this thesis, it was summer when atmospheric temperatures were around their peak and a quick plan was necessary for data collection. Thermal imaging was immensely helpful in conducting a large amount of measurements in a short time, in the midst of a busy shipyard. Periodical checks to note the effect of seasonal variations have yielded some very remarkable observations.

Motor yachts spend a majority of their time at the marina. This implied collecting temperature data on the aluminium hull from solar radiation, when the ship was in dock. This also meant that the geographical location of the marina played an obvious role in deciding the intensity of solar radiation. A marina in the Mediterranean will have significantly more solar exposure than one in Scandinavia for instance, however the latter might have a greater thermal gradient.
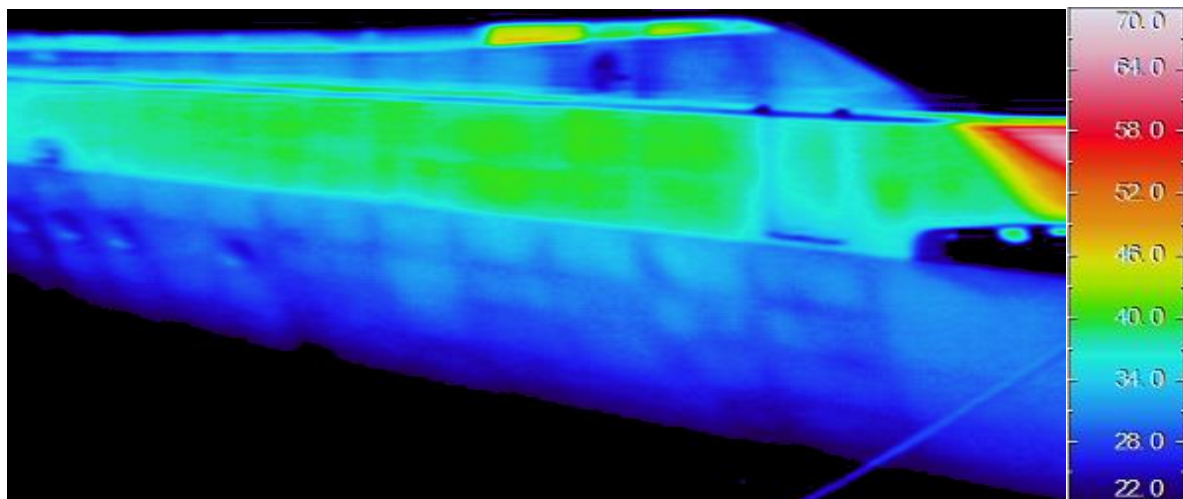

Figure 7: Thermal imaging of the target ship - temperature distribution over various surfaces can be clearly seen including inside the scantling of a ship

2.4.2   Effects of Temperature

Most solid materials expand upon heating and contract when cooled. In fact, the *thermal expansion* of the epoxy filler is about twice that of aluminium. The average coefficient of linear

thermal expansion (α) is a material property that is indicative of the extent to which a material expands on heating. For commercially pure aluminium metal it is 24×10^{-6}/Kelvin while it is 55×10^{-6}/Kelvin for epoxy. This thermal expansion can generate internal stresses when a structural part is heated but is fixed or not allowed to move freely.

In addition, the thermal resistivity of the epoxy (0.1-0.2 W/m/K) is a thousand times more than aluminium (150-230 W/m/K). This means that the thicker the epoxy, the greater will be the temperature difference across it. A very interesting result from this study was that at the beginning, it was assumed that the metal bent because of a large temperature difference over it. In fact, common sense soon dictated that metals are very good conductors of heat and the temperature difference over thin plates is negligible. Thus, there had to be another reason behind the plate deflection and it was suggested that that there are three mechanisms at work:

- The expansion of the epoxy (20mm) tries to bend the thin metal plate (5mm).
- The uneven expansion of the aluminium, where the plate is free to deform much more than the stiffeners (which restrict the plate edges).
- The global bending loads which appear as a local component in terms of secondary and tertiary stresses in the plate and section causing multiple deflection modes shapes.

However, measuring deformations was a very difficult proposition as the test ship was in water. It is practically very difficult to measure an object moving with respect to a fixed reference at all times, the way a ship does by heaving, rolling and pitching. Thus to measure deformations, modern techniques like 3D laser scanning have been suggested, which are becoming both cost effective as well as reliable. Paoli, Razionale, & Saba (2011) present an excellent paper for an automatic scanning process for yacht hulls. Moreover, some software-based inexpensive solutions can simply use multiple-angle standard camera images and generate a point cloud measurement field (3D model) of the object they scan. This method is called *stereo-scanning*. For this research, it was not possible to procure such tools and instead, manual measurements have been made on the target ship as described in Section 7.1.1.

Optical distortion effects are presented in Section 7.2 and very pertinent to this research project. Motor yacht hulls have glossy and reflective surfaces. Any curvature on a highly reflective surface cause a spherical mirror effect, magnifying reflections (Pedrotti L. , 2013). Hot surfaces will also cause heating of air nearby resulting in refraction of light through this heated layer.

Both effects will cause deflections to look even more obvious. Besides this, high hull temperatures also damage the surface coating. (Kattan, 2009). (ISO11347:2012) reference provides a recently published reference for the measurement and assessment of yacht coatings. Section 7.3 contains additional discussions on the subject.

2.5 Modelling

While measurements are a source of actual data, they are time consuming and a large amount of data is needed to see the effect of every parameter. Modelling the phenomena however, provides an alternative. It involves the use of quantitative mathematical models or scaled experimental models of physical systems, to describe system output behaviour subject to input variables. Since they are built on system parameters, they allow the possibility of simulating a real system both in the present and future scenarios. This is essential for enabling rapid parametric studies in a short time.

To perform a theoretical analysis, a thorough search had to be performed of various solar models (ASHRAE, 2009); heat transfer literature (Krieth, Manglik, & Bohn, 2011), (Cengel, 2002) and material mechanics (Beer, 2012) to determine the applicability of the right methods. Available theories and methods of calculation of heat transfer had to be applied to the complex geometry and thermal-structural boundary conditions on ships. Conduction within the structure, convection to and from the surrounding air and water, and radiation to and from the ship had to be considered. Based on these heat transfer principles, a thermal model based on an e*nergy-balance method* was set up, described in Section 5.2.

Ship specific studies of this kind have been found to be far and few and dated several decades ago. However, many of the same principles still hold and the works of (Hechtman, 1956), (Lyman & Meriam, 1964) and (Jasper, 1955) represent pioneering work in this regard. From these studied literature, it is also understood that calculation of thermal stresses in girders and ships can be made by theoretical methods proposed by several authors, notably (Timoshekno, 1987), whose methods have been applied in the past to ship structures.

However these theoretical thermal stress calculations are for 2-dimensional cases, and the problem could be extrapolated to a 3-dimensional case using finite element methods. Moreover, thermal analyses can be steady state or transient. In this case, while the sun's path

in the sky keeps changing with time, it can be discretized into hourly segments, where the effects of thermal effects can be considered as steady state at every hour mark. This greatly simplifies the modelling procedure, while being more than sufficient for conducting an informed analysis.

2.6   Analysis and Solutions

Chapter 6 deals with a detailed explanation of the results of the theoretical modelling and its performance with thermal imaging measurements, additionally described in Appendix 1. This correlation process not only allowed the theoretical model to be validated but inversely, interesting insights into actual thermal imaging measurements have also been found. As an example, the effect of the heat radiated from concrete dock on the yacht was found to be significant, since the concrete give off a lot of heat in summer and heated up the yacht. On the other hand, the same dock blocked sunlight from reaching the lower parts of the hull, cooling it, but creating a steeper thermal gradient.

Section 6.3 focus on parametric modelling which was carried out to test the effect of variance of different parameters, with the overall objective to reduce surface temperature and its negative effects such as deformations. The secondary purpose of this stage was to perform an analysis with the aim to find solutions with the most optimum criterion, subject to various constraints.

Chapter 8 consolidates information from all measurements, modelling and analysis and presents a structured procedure for obtaining solutions, to the problem of reducing surface temperatures even on black coloured hulls. A methodology called TRIZ or Theory of Inventive Problem Solving has been applied. This is widely used for effective brainstorming and conceptualization of technical solutions. An overview of the system has been discussed in the chapter to assist the reader in understanding the process. This will allow future researchers to use appropriate design and conceptualization methods prescribed in this method.

3   EXPERIMENTAL MEASUREMENTS

The development of theoretical and computational methods for scientific and engineering simulations provides us with tools to virtually analyse the behaviour of physical systems. However, *it is necessary to corroborate such simulations with experimental measurements* to accurately predict real life behaviour. Thus, in order to understand thermal behaviour over yachts, it was necessary to know the environments in which they are subjected to, during normal service. Here, since *motor yachts spend the majority of their time at the marina,* this implied collecting temperature data when the ship is in dock. The measurement of meteorological data, temperatures and deflections are described in the sections below:
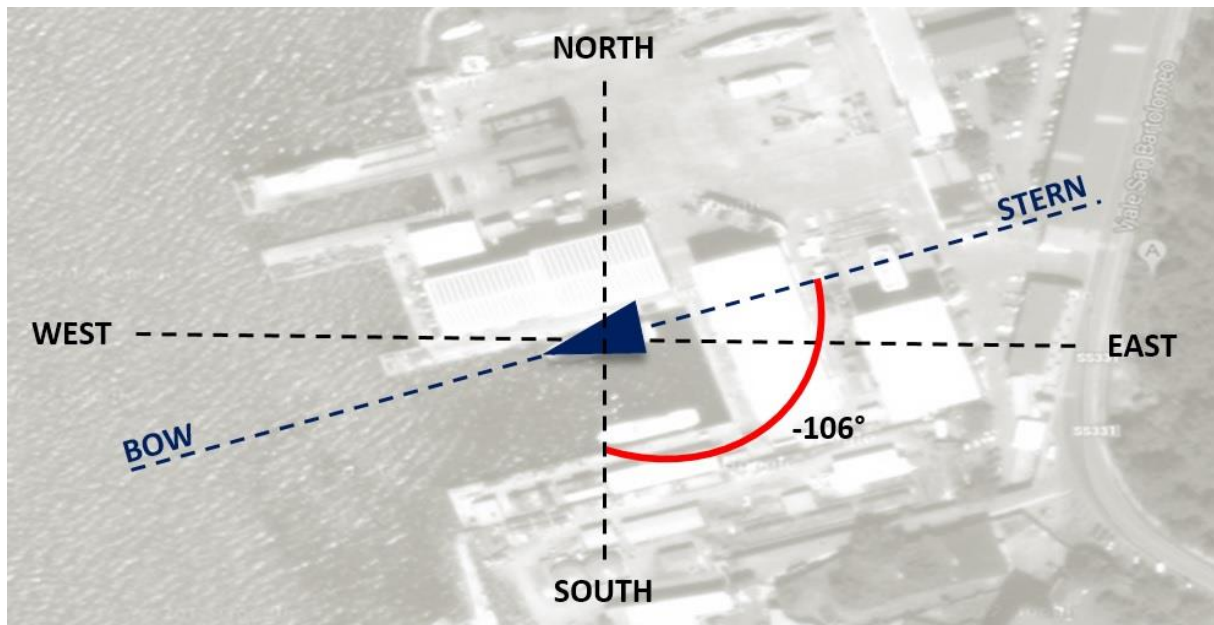
Figure 8: The angular position of the target ship was 106° east of South

3.1   Target Ship

The main target ship which was the basis of this study was a dark-blue coloured yacht, 34 metres in length and 10 years old. (Figure 9). It was moored in water by the starboard side. The orientation of the ship was roughly perpendicular (Figure 8) to the north-south direction, about -106° (it is considered negative by convention of the ASHRAE solar model described later). The sun shone only on the port side (left) and the starboard side (right) was almost always in shade, except in the evening for a few hours in summer (when the sun path is longer). There were also other ships for comparative purposes. These were two white ships (one on land and

the other in water) and one grey ship. These ships were also in the same length category, between 35-45m. Only the hull was analysed for this project and not the superstructure, based on the shipyard's directives.

Figure 9: The dark blue 34m "Revitality" moored on its starboard side (Aug, 2013)

3.2 Meteorological Observations

As stated before, the geographical location of the marina plays an obvious role in deciding the hull surface temperatures. For the purpose of this thesis, the target ship was in La Spezia, Italy (located at 44.10° N, 9.81° E). However, solar data for the city of Genoa, Italy (44.41° N, 8.93° E) was used as it was the nearest weather station data available for use in the ASHRAE solar model (described in Section 5.1.1) and was sufficiently accurate.

Meteorological observations for La Spezia were used at shore. Statistical analysis of weather data was already available from the local weather station's website (MeteoSpezia, Meteorologial Weather Station website, La Spezia, 2013) which yielded reliable information on mean and extreme thermal environmental conditions that a motor yacht may be expected to

encounter here. Both past averages and present conditions of humidity, wind speed and air temperatures were used for correlating the theoretical model.

3.3 Temperature Measurement

Thermal loads are a function of temperature and this was the starting point of the investigation. Here, temperature distributions could have been assumed or measured in the hull plating. Assumptions are suitable for a theoretical analysis while measurements are more indicative of the actual phenomena, and necessary to conduct the FEM analysis. As mentioned previously non-contact radiometric techniques such as thermal imagers and infrared thermometers were used to measure the hull surface temperatures. These techniques include *infrared thermometry* and *thermal imaging*.

The advantages of these devices are that they enable very quick "point-and-shoot" non-contact measurement, allow easy software based visualization of temperature gradients, focus only on measuring radiation heat signatures, and do not interfere with regular ship operations. They are already used in HVAC surveys and many other industries. On the down side, this technology is still quite expensive, and needs calibration with the ambient temperature and surface emissivity to be sufficiently accurate, to measure small temperature differences. However, the benefits far outweigh the challenges and these are fast becoming an industrial norm.

3.3.1 Infrared Thermometry

Infrared Thermometers work much like a thermal imager; however, instead of an array of sensors to create an "image", they only provide the temperature of the specific point that they are focussed at. Thus, they are also referred to as 'temperature guns'. Obviously, these guns are meant for point measurements and are not suitable for measuring objects the size of ships, in this case of the order of 30-50 meters. Thus, thermal imaging was used extensively on selected days with IR thermometer as a secondary tool for quick daily correlation between the theoretical model and experimental observations for extreme and average temperatures.

3.3.2 Thermal Imaging

Thermal cameras detect heat signatures of objects that emit radiation. Knowing that light is made up of visible and infra-red components, using such cameras help one to focus clearly on

only the heat transfers taking place in the test environment and determine temperatures accurately. Thermal cameras are very versatile and are also quite simple to operate, with the one used in this thesis being very similar to a camcorder (Figure 83). As a shipyard is always extremely busy, with material, cranes and even ships moving about, thermal imaging was vital in providing quick measurements in a single capture. It was necessary to use the bundled software that enabled deeper analysis of the thermal images, and generated several important graphs that have been described in the adjoining results page. Several measurements were carried out over the course of six months. Primarily,

- In August 2013, a dark-blue ship in water and a white ship on land.
- In October and November 2013, comparative measurements were made between a dark-blue ship, a grey ship and a white ship.
- Experiments on a full scale panel in January 2014
- Correlation measurements were made periodically from August to December 2013 with the IR thermometer to verify the theoretical model.

3.3.3   Challenges Faced

Typical challenges faced during the measurements were finding clear sky days (winter is the rainy season in La Spezia), availability of the thermal camera (it was leased) and acceptable viewing angles to measure ships. The typical measurement distance ranged from 3-40metres from port, starboard, stern and bow angles. Thermal cameras are most accurate when they are held perpendicular to the surface. It was also necessary to use calibration tapes of known emissivities, to find the correct hull surface temperature. This has been described in the next chapter. Ideally, it would have been useful to have contact based thermometric equipment. This would have helped to develop a more robust measurement system analysis (MSA)

Another challenge was that the shipyard was in a constant state of work and sometimes ships would be moved from one location to another, posing a hindrance to continuous observations. The presence of nearby buildings and natural terrain also cast a shadow on ships, which had to be duly noted and accounted for in the temperature correlations.
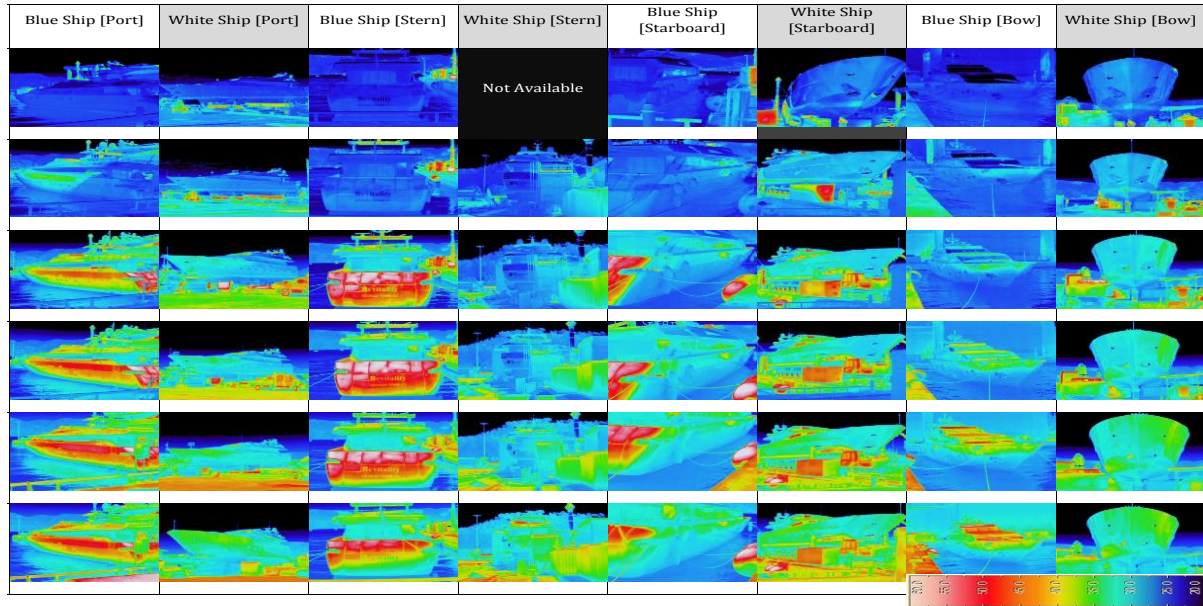
3.4   Observations and Inferences

Figure 10: Hourly measurements showing heating up of the dark blue and white ship (Aug, 2013)

Thermal Imaging on a dark-blue 34m motor yacht (in water) and a reference white boat (on land) were carried out over a 10 hour period, from 0800h in the morning to 1800h in the evening, on a clear sky day in August, 2013. A snapshot of the thermal imaging measurements is seen in Figure 10 showing the gradual heating up of the dark blue and the white yachts. One can clearly see that as the sun rises on the port side, the dark blue ship begins to heat up rapidly, while the white ship is, in contrast, much cooler. Detailed tabular information has been provided in Appendices 5, 6 and 7.

Table 1: Summary of temperature variations over the ship in August 2013

No	Remarks
1	The Dark blue ship is about 52^0C on the bulwark compared to 38^0C for the white ship
2	There are steep thermal gradients around portholes. Deflections were also seen near portholes
3	A 10^0C temperature difference exists at the waterline
4	Transverse Frames conduct heat away from the surface, thus acting as 'fins'
5	There is no significant temperature variation over longitudinal stringers
6	The stern is the hottest region with temperatures reaching 61^0C

The side exposed to the sun sees elevated temperatures primarily over the bulwark and between bulkheads. The side in shade is, in contrast, much cooler. The thermal gradient for ships standing in water is from top to bottom, i.e. higher temperatures at the top and cooler as we reach the waterline due to the cooling effect of water. These gradients set up thermal loads

which replaces the fair hull with a very un-aesthetic "wavy" pattern on the plating. Temperatures are slightly higher in the centre of the plating than at the edges (weld-lines) with transverse frames or bulkheads, while longitudinal stringers do not seem to have much effect on the temperature distribution.
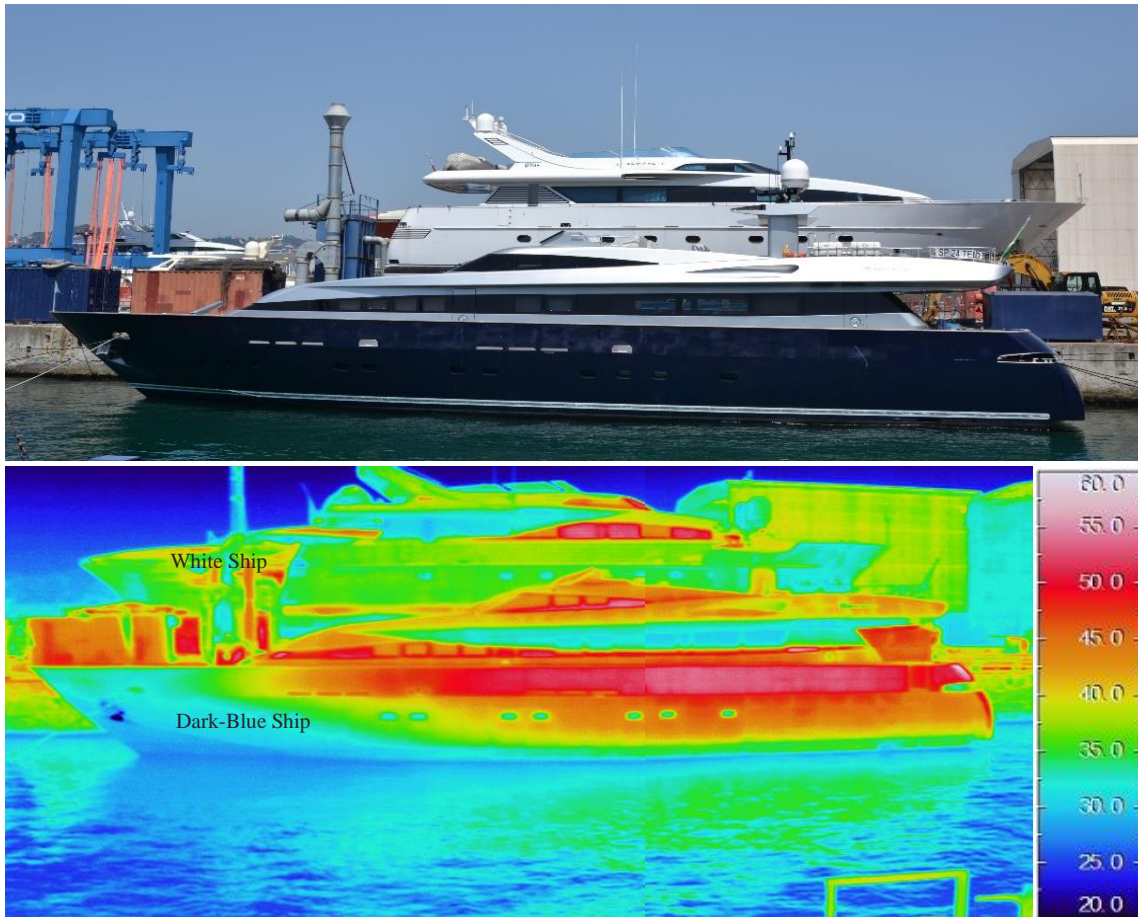
Figure 11: Thermal image comparison of a dark blue ship and a white ship at 1200h, August 2013 (Note: Windows show false reflections and should be ignored)

The bulwark temperature of the dark-blue yacht in the foreground is 55-60 ^{0}C while the white ship in the background is much cooler at 35-40 ^{0}C. The thermal gradient from the waterline (cooler) to the bulwark (hotter) is quite noticeable for the ship in water. When compared with the 40m white ship dry docked (standing on land) exposed to the sun under the same conditions, two significant observations were noted. Surface temperatures due to the colour white are much lesser than dark-blue. Also, since the white ship was on land, there was no cooling effect due to water which meant a much lesser thermal gradient or in other words, a more uniform heating.

3.4.1   Longitudinal Temperature Variation

In Figure 12, probe line A (in red) represents the white ship temperature while probe line B (in blue) is for the dark-blue ship. Both measurements are on the bulwark from stern to bow. The highest temperatures for both yachts are noted in the stern region but there is marked difference between the yachts. The minimum, maximum and average temperatures are presented in Table 2 below. The white ship is about 14^0C cooler when comparing maximum temperatures.

Table 2: Temperature data along the ship bulwark

Number	Max	Min	Ave	Emissivity
A	37.57	31.88	36.14	0.95
B	51.68	32.18	42.93	0.95
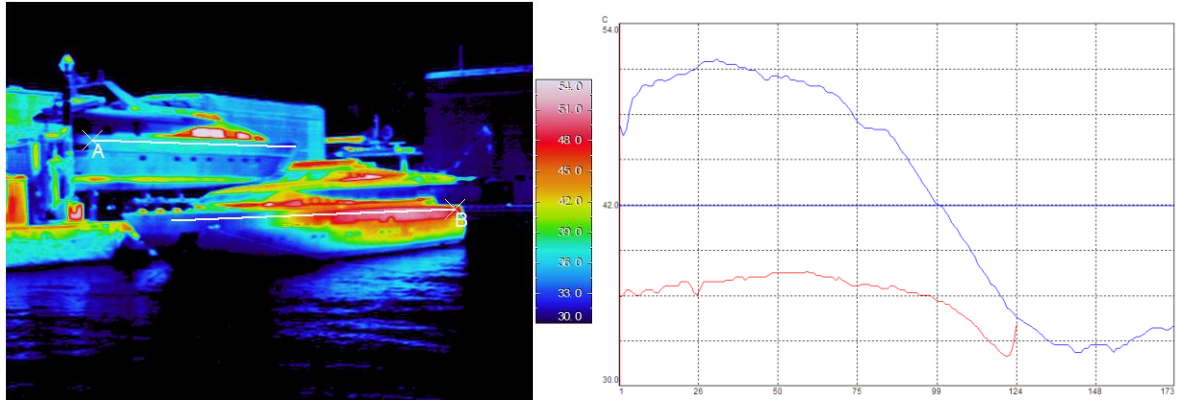
Figure 12: Longitudinal temperature variation along the bulwark of the white & dark blue ship. Probe lines A (red) & B (blue) from stern to bow [Graph: each vertical division in 3^0C]
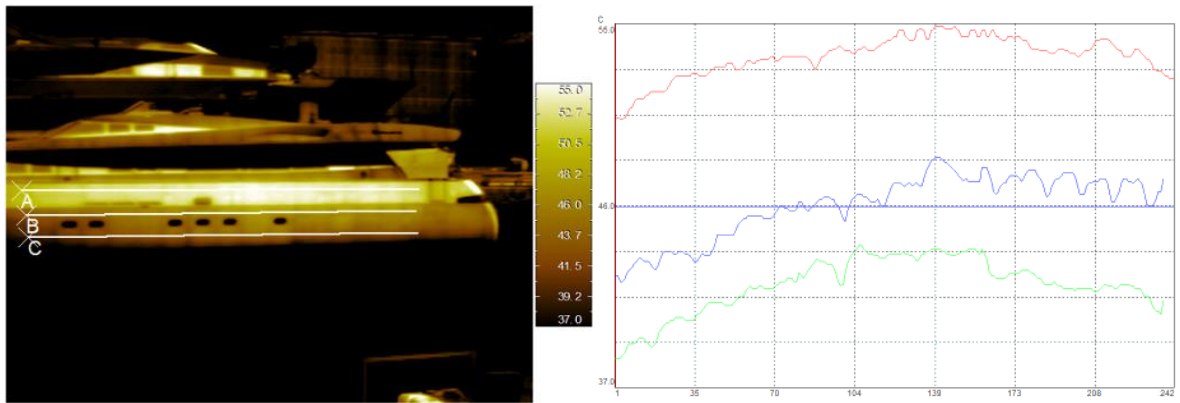
Figure 13: Longitudinal temperature variation of the dark blue ship along the bulwark-plating, mid-plating and waterline-plating [Graph: each vertical division is 2.25^0C]

In Figure 13, probe lines A (red), B (blue) and C (green) along the ship length show the temperatures along the bulwark, the mid-plating and the waterline-plating. As clearly seen, the bulwark temperature is the highest. The regular pattern of temperature "dips" along the

probe lines are where the transverse frames connect to the plating and conduct the heat away. Similar to the figure above, a close-up of the stern is shown below in Figure 14.
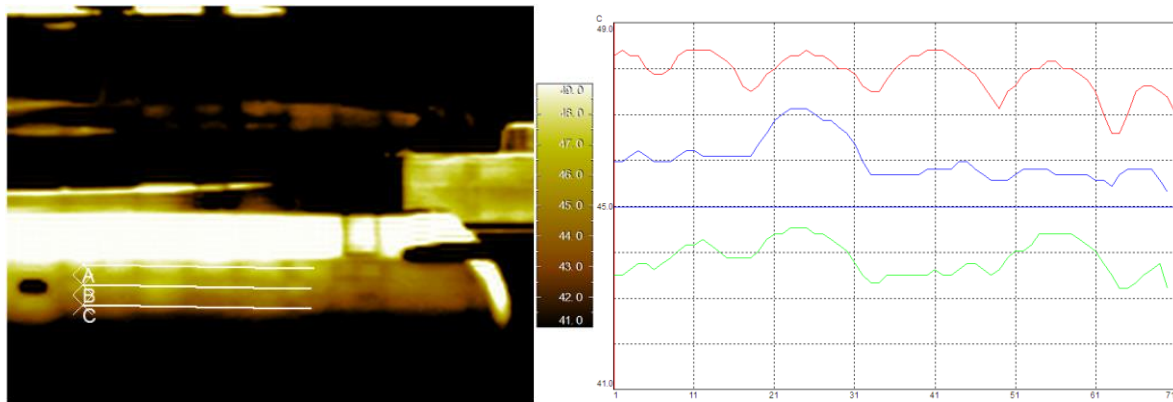
Figure 14: Close up of the longitudinal temperature variation along the bulwark-plating towards the aft of the ship [Graph: each vertical division is 1^{0}C]

The transverse frames are easily seen both visually and graphically as shown in Figure 14, where there is a clear temperature drop over them. This temperature drop is on average of the order of 1^{0}C [pt.1]. However, just under the bulwark, the temperature difference over the transverse frames is of the order of 2.5^{0}C as shown below in Figure 15.
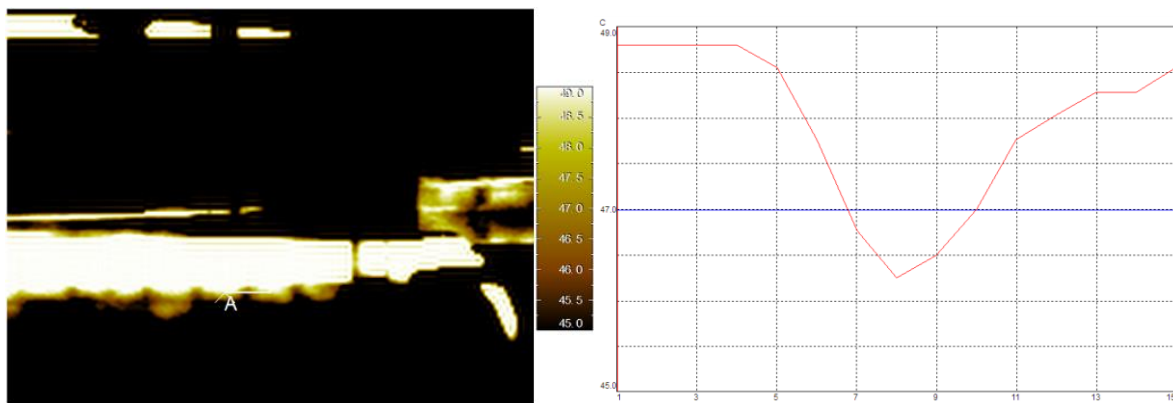
Figure 15: Longitudinal temperature variation (close-up) across a transversal frame just under the bulwark-plating towards the aft of the ship [Graph: each vertical division is 0.5^{0}C]

Figure 16 shows a horizontal probe across portholes on the sun-exposed side to visualize the distribution of temperature. There is a variation from 45^{0}C to 36^{0}C across the porthole. Thus, uneven thermal stresses would be concentrated around this area and indeed, this was visually confirmed by the presence of uneven plate warping. Since these portholes are also present in the middle of two bulkheads, the plate warping is quite noticeable.
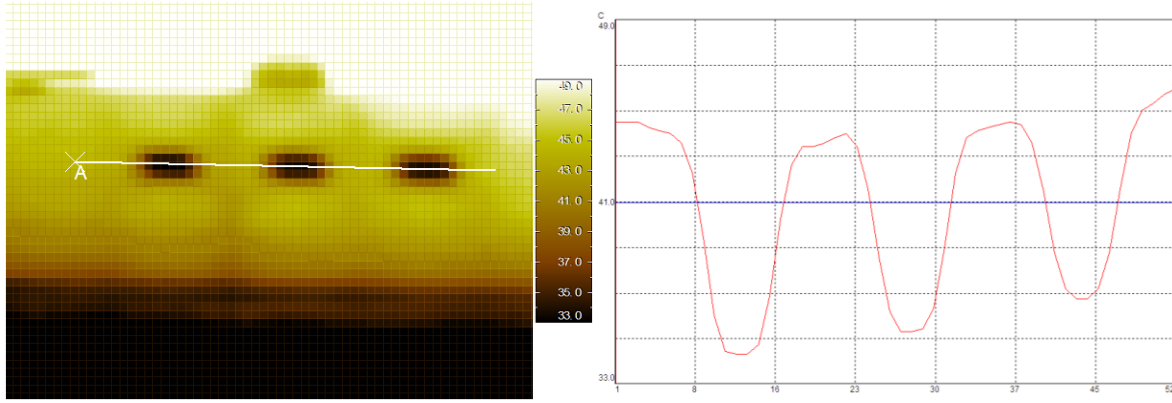
Figure 16: Close up of the longitudinal temperature variation across portholes on the sun-exposed side [Graph: each vertical division is 2^{0}C]
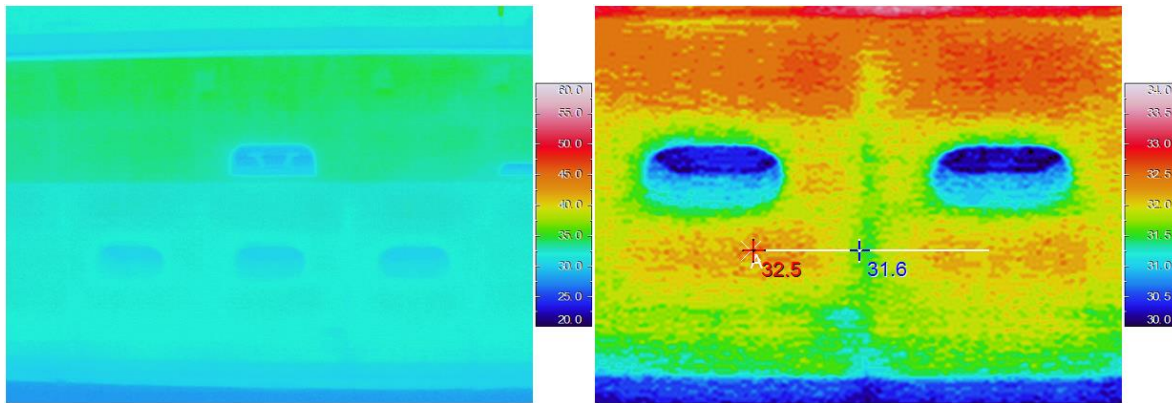
Figure 17: Longitudinal temperature variation (close up) along portholes on the shade side

On the shade side, a close up of the thermal gradients around the portholes is shown in Figure 17 . Since this side is away from the sun, the temperature differences are very low. It can be seen that there is a transverse frame passing between the portholes, as visualized by the temperature difference.

3.4.2 Vertical Temperature Variation
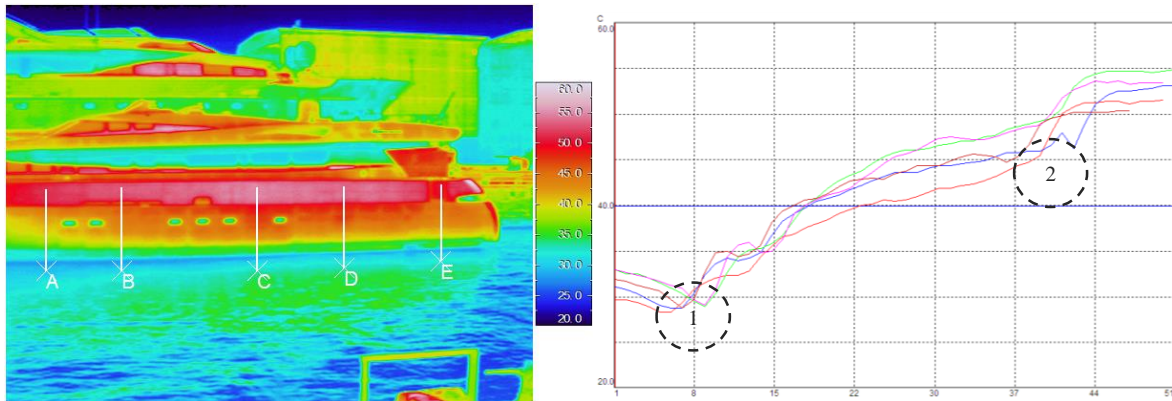
Figure 18: Vertical temperature variation along various probes along the ship [Graph: Each vertical division is 5^{0}C]

Probe lines A, B, C, D, and E represent temperature gradients across the longitudinal direction of the yacht shown in Figure 18. At the waterline [Zone-1] there is an abrupt fall in temperature of 3^0C from the average of 33^0C in the graph. To keep in mind is that the actual far field water temperature is about 24 degrees, but the reflection of the heat radiated from the ship can be seen in the water. Thus, the actual temperature difference is about 8-9^0C.

There seems to be a linear rise in temperature from the waterline (30^0C) to (50^0C) where the bulwark starts, and Zone-2 shows an abrupt temperature rise of 5^0C. This maybe because the bulwark is a vertical surface and is therefore more exposed to the sun. The hull is more curved causing lesser solar radiation to be absorbed, especially at the bow (Figure 12) .This could also be due to the fact that there is no structure behind the bulwark (unlike the hull which has transverse frames and bulkheads, which conducts the heat away). A second image below in sepia colour helps to visualize the temperature gradient at the waterline region (Figure 19).
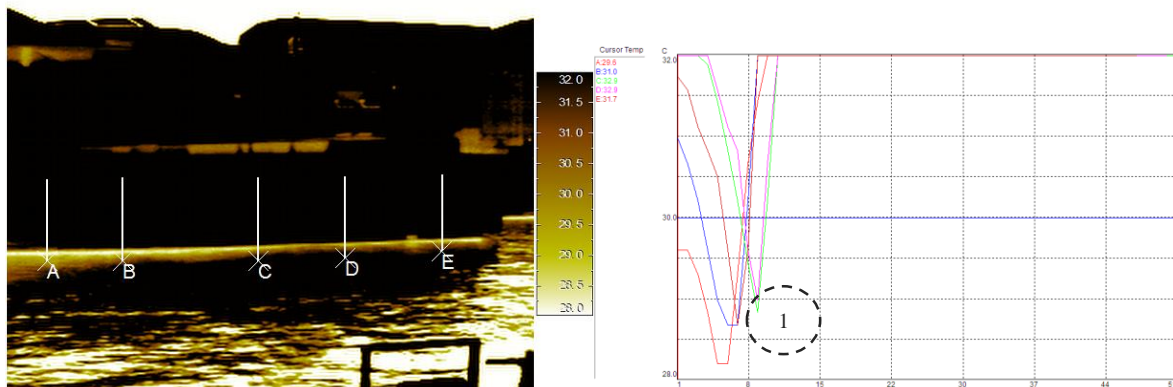
Figure 19: Vertical temperature variation along the ship with a close up of the waterline [Graph: each vertical division is 2^0C]
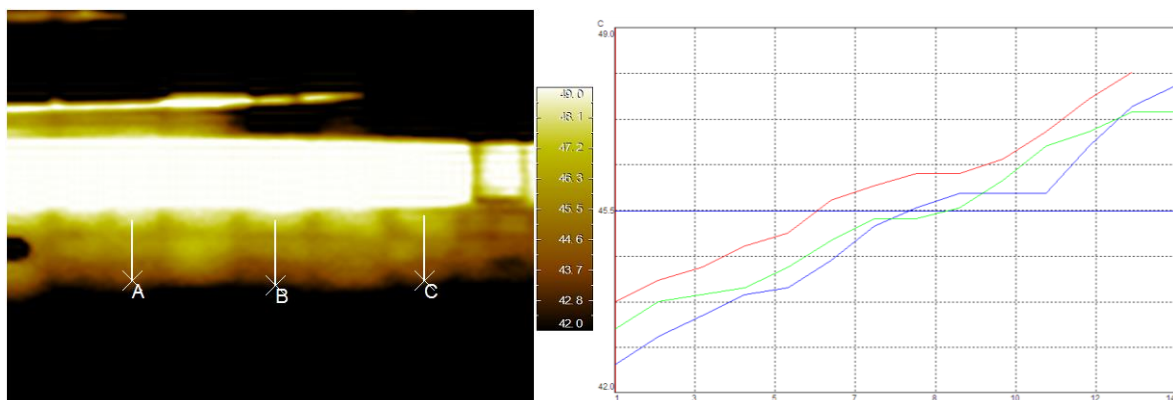
Figure 20: Vertical temperature variation along the longitudinal stringers [Graph: each vertical division is 0.875^0C]

Contrary to the transverse frames, there is no significant temperature variation due to the longitudinal stringers as seen in the temperatures graphs where the temperature rise is nearly constant over them with no sharp rises or falls. (Figure 20). To demonstrate the thermal stresses due to openings in the structure, a vertical line probe A passes from the waterline to the bulwark through a window porthole, while line B passes over a continuous hull structure. There is a sharp fall in temperature from 45^0C to 33^0C, thus creating a sharp local thermal gradient which will lead to increased thermal stresses and uneven expansions due to stress concentrations. Note that this is the window on the side exposed to the sun.
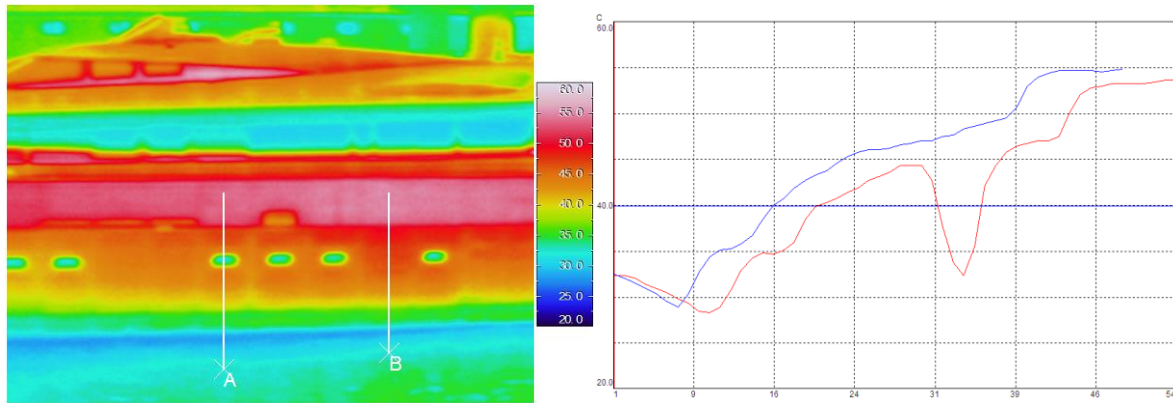
Figure 21: Vertical temperature variation along the ship across portholes on the sun side [Graph: each vertical division is 5^0C]

The target ship was positioned in such a way that the morning sun directly hit the stern. As seen in Figure 22, the highest temperatures were recorded near the stern, again at the bulwark. Also, at the stern, the hull is in contact with the water at pt.1 but lifts out of the water at the transom [pt.2]. Thus, the cooling effect of water is no longer available and probe line A at pt.1 sees a larger thermal gradient than line B.
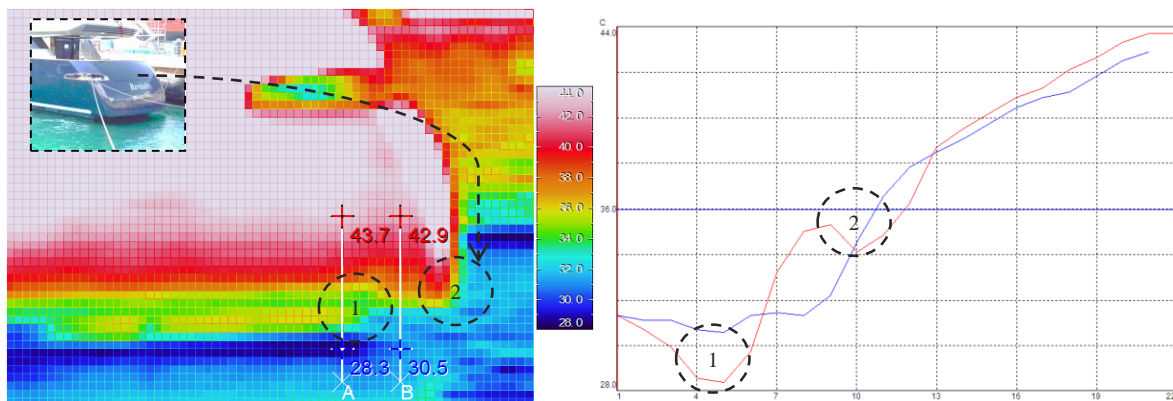
Figure 22: Vertical temperature variation at the stern [Graph: each vertical division is 2^0C]

In Figure 23, we have a very clear view of how hot the stern becomes. The bulwark is the most heated region reaching 61^0C and a close-up of the upper section on the right shows uneven heating within the local plating section. Typically, within the plate there is a high of 60^0C towards the centre and top while a low of 45^0C exists at the bottom. There is a sharp fall of about 10^0C at the intersection of two surface panels. However visually, no significant warping was observed at the stern in spite of the high temperatures. This is probably because the outermost surface is made of panels that have the possibility to expand and relieve the thermal stresses. However, the high temperatures will still continue to be a detriment to coating life.
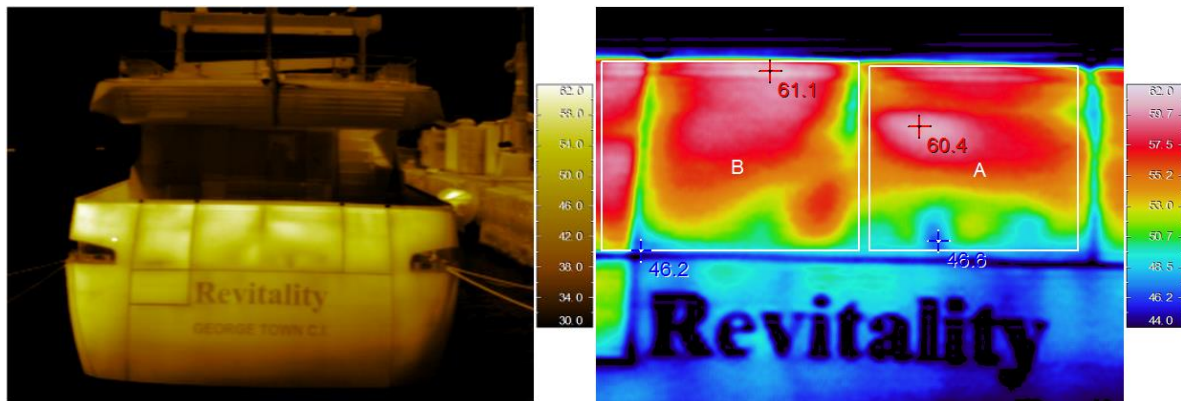
Figure 23: temperature variation across the stern (left) with a close up of the surface (right)

3.4.3   Comparisons between different coloured ships

This section details the comparative measurements made on yachts of the following colours: dark-blue, grey and white, in the month of November. All three ships had glossy surfaces. The ambient air temperature was 10.1^0C and the water temperature was about 8-12^{0}C depending on the distance from the ship.

Table 3: Summary of temperature measurements on different yachts

Yacht Colour	Average High		Remarks
	Starboard	Port	Thermal gradient is much lesser in winter than in summer. The ship surface is still as hot as in summer
Dark-blue	18^0C	54^0C	
Grey	18^0C	46^0C	
White	15^0C	20^0C	

3.4.3.1   Port Side Temperatures

Figure 24: Port side of the dark blue ship [Graph: each vertical division is 7^0C]

Figure 25: Port side of the grey ship [Graph: each vertical division is 7^0C]

Figure 26: Port side of the white ship [Graph: each vertical division is 7^0C]
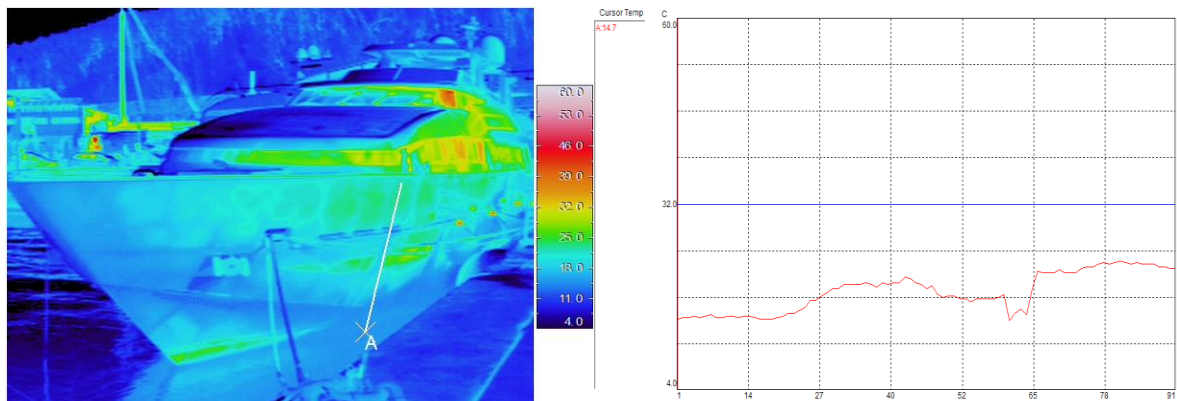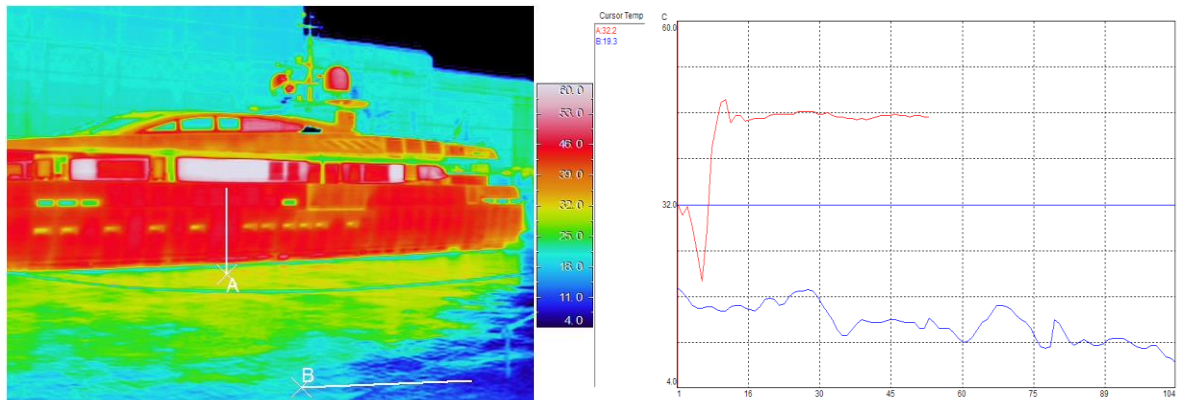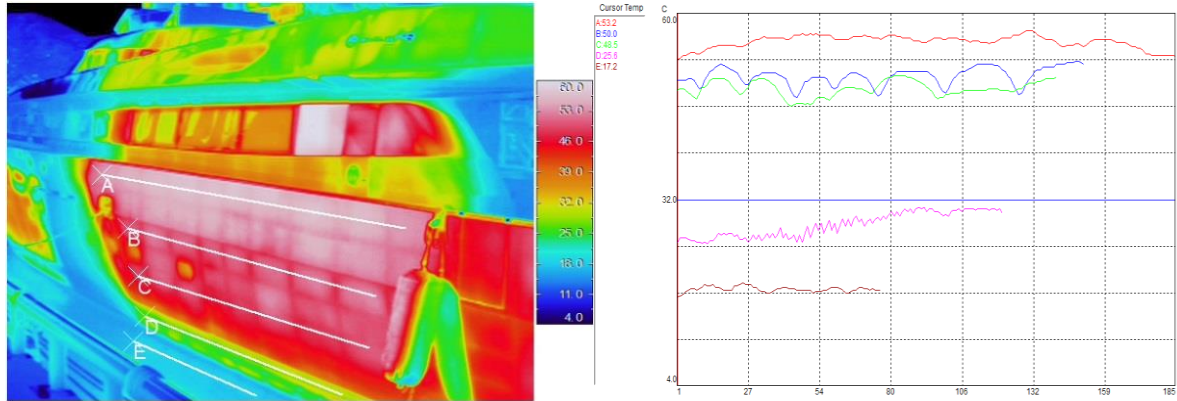
The dark-blue ship is the hottest of the three ships with maximum temperatures on the bulwark reaching 54^0C shown by probe A in Figure 24. This is probably because the sun is closer to the earth in winter, thus making solar radiation more intense. Also, the sun elevation is lower, striking the ship surface more directly than in summer. This is also the reason why there isn't any significant thermal gradient towards the waterline in all three ships, - hence there will be a much steeper change from the waterline temperature to the hull temperature as shown in probe A of Figure 25 where there is a rise of 25^0C! The grey ship reaches an average of 45^0C while the white ship in Figure 26 is the coolest at 18^0C.

3.4.3.2   Starboard Side Temperatures
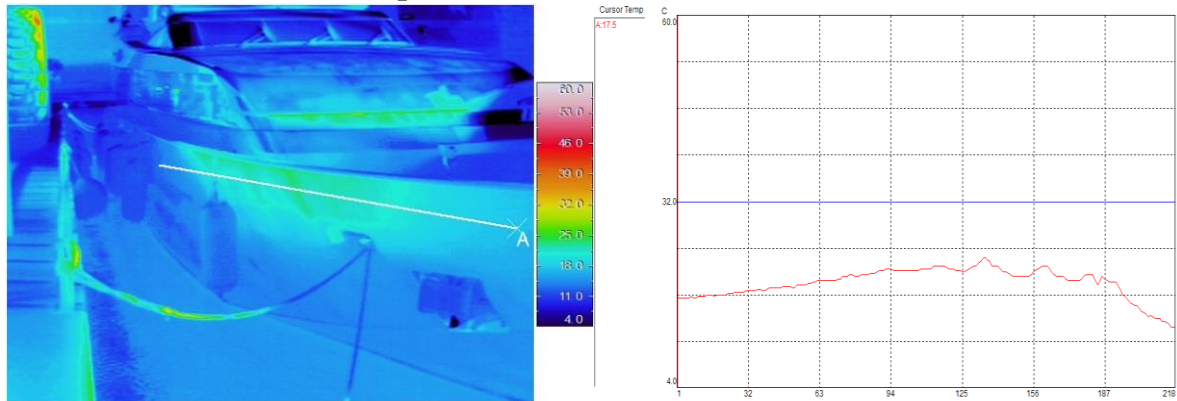
Figure 27: Starboard side of the dark blue ship [Graph: each vertical division is 7^0C]
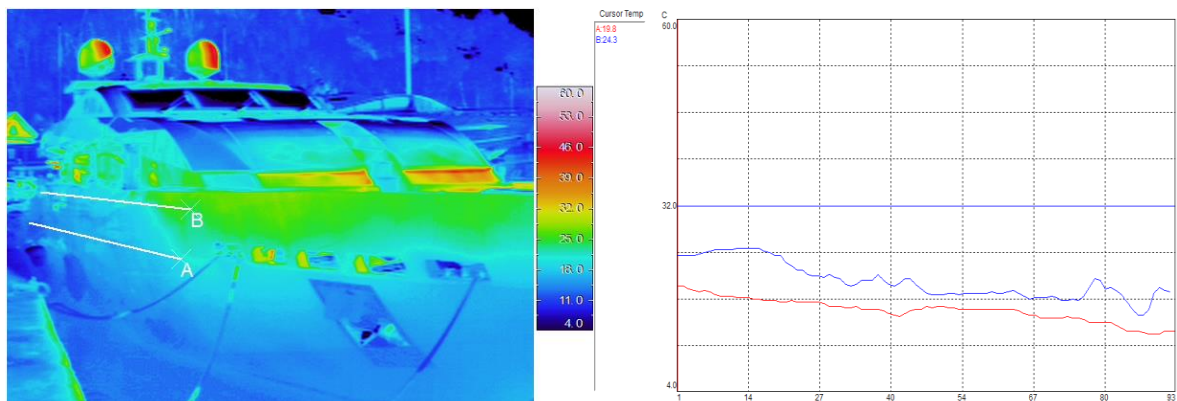
Figure 28: Starboard side of the grey ship [Graph: each vertical division is 7^0C]
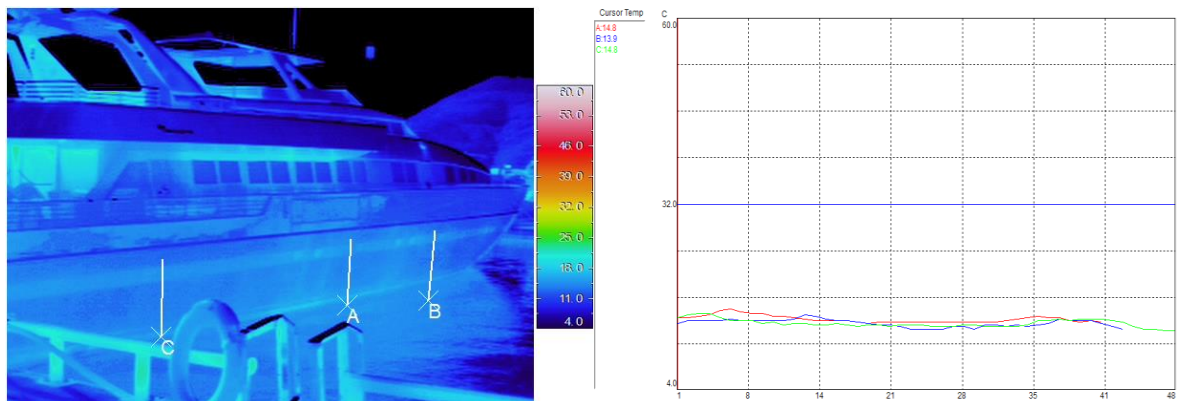
Figure 29: Starboard side of the white ship [Graph: each vertical division is 7^0C]

The starboard side is on the shade side, and thus all three ships are about 18^0C on average with the white ship being the coolest at about 15^0C. There is no significant gradient from the waterline to the bulwark in all three ships. At the bow of the grey ship in Figure 28, some heated areas are seen but these are because of the ship's design with a larger open deck, and the back part of the bulwark is being heated by the sun.

4   EXPERIMENTAL MODELLING

Before proceeding with the theoretical model, it was necessary to make a small scale measurement of the actual thermal conduction properties of the epoxy-aluminium combination, subject to variation in certain parameters.

4.1   Experimental Setup

The setup consisted of a full-scale panel exactly as is found on the target ship, subjected to heating from a halogen lamp to simulate solar heating. The panel was made of two layers. The top layer was epoxy of two different thickness (tested separately). The second layer was Aluminium (ASTM B209 5083 H321) of constant thicknesses in both tests. A collar was also fitted to the entire panel to restrict any expansions in the lateral directions. The long edges were bounded by longitudinal stiffeners and the short edges were bounded by transverse frames.

Table 4: Test plate data of a full scale ship panel

Part	Dimensions
Plate	1000mm x 400mm
Epoxy Layer	Test-1 : 10mm / Test-2 : 20mm
Aluminium 5083 H111 Layer	5mm
Transverse Frames	200mm x 5mm (Web)
Longitudinal Stringer	60mm x 4mm (Web), 60mm x 4mm (Flange)
Lamp	Halogen Lamp capable of 450°C, fixed 500mm from the plate for simulating temperature of 65°C (corresponding to black colour)

Image (left) shows the back panel covered to reduce radiation and natural convection (as in a ship) while image (right) shows the setup of the thermal imaging camera and the halogen lamp.
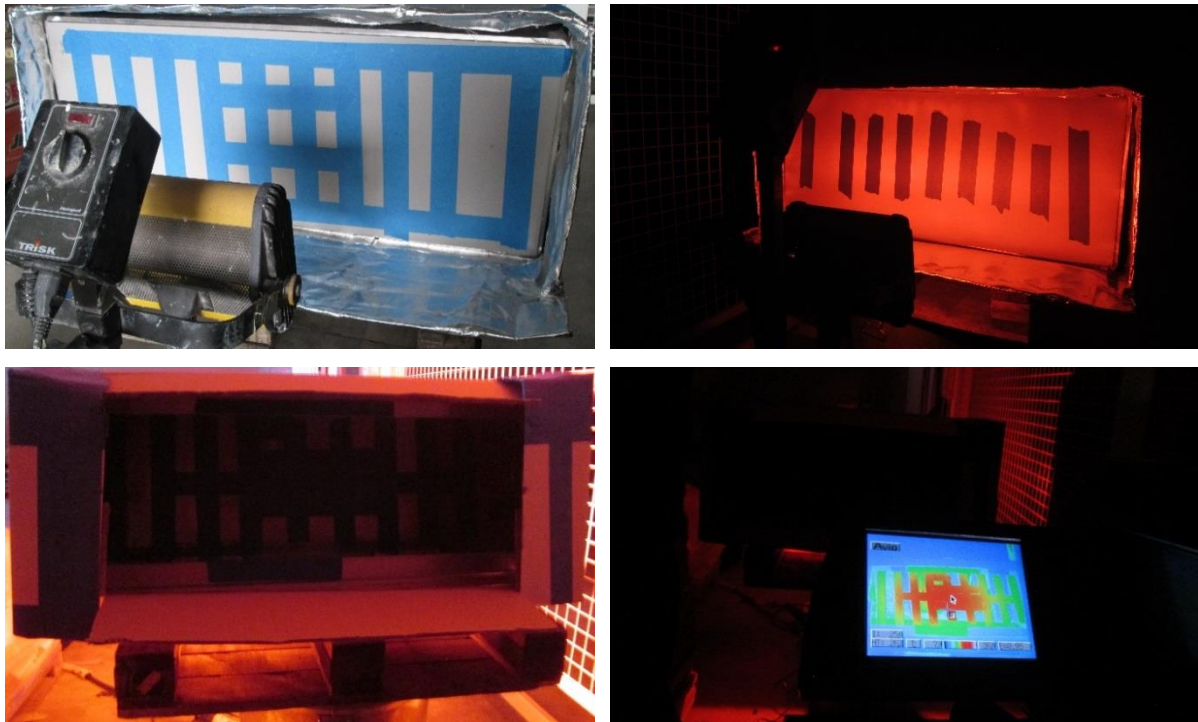
Figure 30: Experiment in progress. Front Side (above) Back side (below)

Table 5: Experimental modelling test results on a full scale ship panel

Test Description	Temperature Difference	Remarks
Test-1: Only Aluminium (5mm)	0.1°C	In the first test, a pure aluminium panel was subjected to thermal loads. Here, the back and front panels practically showed the same temperature, since Aluminium is a very good conductor of temperature
Test-2: Epoxy (10mm) + Aluminium (5mm)	30°C	The difference of temperature between the front and back panel was 30°C, which was double the estimated value. The temperature on the front side increased rapidly in the beginning before slowing down and reaching 64°C on the epoxy surface. This would be a realistic temperature if black paint were used over the epoxy. The corresponding temperature on the back side on the aluminium was 34°C, which heated up very gradually in the beginning, and got even slower as it approached steady state.
Test-3: Epoxy (20mm) + Aluminium (5mm)	40°C	The difference of temperature between the front (68°C) and back panel (28°C) was 40°C in this case which suggests thermal conductivity is not changing linearly as theory suggests.

Calibration tapes were used during the measurement as seen in Figure 30, since it is very difficult to measure the temperature of highly reflective surface such as aluminium, with

thermal imaging. Aluminium is a near perfect reflector and reflects the temperature of the ambient as seen in the back panel. The same process was also adopted on the resin (front side) to have the same relative temperature difference between the front and back sides. The results of the tests are presented in Table 5.

4.2   Inferences

This non-linear temperature difference between the two thicknesses of epoxy can be possibly explained due to trapping of air bubbles during the epoxy curing process. Firstly, Air is a very bad conductor of heat and this most likely reduced the thermal conductivity of the epoxy, by more than 50-70% compared to predictions. Secondly, since the amount of air trapped is inconsistent over the epoxy, and it would also undoubtedly expand when heated, this could be causing the non-linearity. In addition, this reduces the amount of heat reaching the aluminium.

When the heat was turned off, the aluminium continues to stay hot for 30 min before gradually cooling down. This was in spite of the fact that the ambient temperature was 12°C. This could be attributed to the fact the heat slowly passes through the epoxy, reaching its back side interface with the aluminium layer, where there is a transfer of heat energy. There are possibly interface resistances (due to discontinuities between the epoxy-aluminium bond) that further decrease the thermal conductivity of the overall bi-material layers.

It must be kept in mind that if the yacht is in use and the thermal comfort temperatures on a ship are around 25°C, the back face of bare aluminium will be higher than 12°C. In fact in some areas like the engine room, this may be even higher. Therefore, the temperature difference between the epoxy and aluminium would not be 30-40°C and instead reduce to 15-20°C.

It must also be kept in mind that the optimum epoxy thickness should be of the order of 10mm or less. Adding more epoxy increases the ship weight by approximately 1 ton/mm, for a ship length of 40 metres.

Based on the above inferences and observations, the same behaviour was incorporated into the theoretical model, described in the next chapter.

5   THEORETICAL MODELLING

Theoretical calculations are necessary for the development of a simulation model. It provides a conceptual framework to test out assumptions and calculate trends, or identifies any tendencies previously not thought of. Careful consideration must be made to implement several mathematical theories together to describe a system that links specific parameters to a good probability of outcomes, in the overall system output.

Some of the features of the theoretical model are briefly shown in Figure 31 below. The system in question is the motor yacht. Different subsystems such as materials and the way they are structured together is important. Loads are chiefly thermal loads due to solar radiation. The presence of local stresses due to hydrostatic loads is also studied. All of this is within the boundary of the atmosphere and surrounding water (if the ship is in water). Locally, structural boundary conditions will also apply to the plating structure.

Boundary Conditions

Atmosphere, Waterline…

Thermal Boundaries (insulation within ship)...

Plate Simply Supported/ Clamped…

System (Ship)

Scantling (Plating & Frames)

Materials
• Epoxy Filler Layer
• Aluminium (metal)
• Insulation
Hull Paint & Colour…

Loads

Thermal Loads
• Solar Radiation
• Temperature of System / Surroundings
Global loads

Residual Stresses...
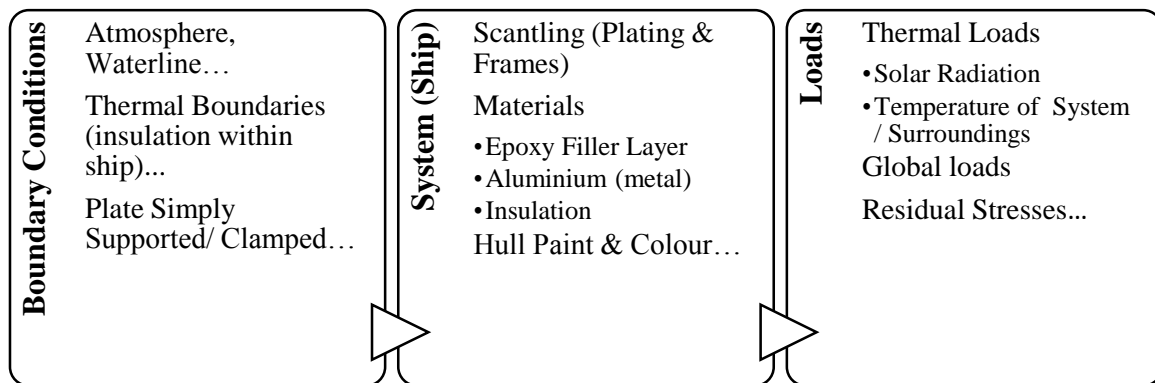
Figure 31: Features of the theoretical model

Understanding the basic theory behind various processes is a critical step and makes the discussions presented in this chapter very relevant and important for future researchers. There is a need to carefully measure and operationalize concepts from theory, then test the relationship between applied concepts and the amount of change observed by varying the parameters (discussed in Section 6.3). The system is subjected to the below parameters.

- Input variables define system attributes such as the colour of the paint, thicknesses of the materials involved, their thermal properties and so on.
- Outputs are primarily temperature. Effects of temperature include deflections and increased energy use for cooling the ship.

The theoretical model has been correlated with experimental measurements described in Section 6.2, to improve the accuracy of model predictions.

Select Theories
- Solar Radiation
- Heat Transfer
- Deflection
  - Plate Theory
  - Beam Theory
  - Bi-Material

Identify strategies to link theories

Create building blocks for each part of the theoretical model

Link all blocks together

Execute theoretical model and analyse output data for correctness and reliability
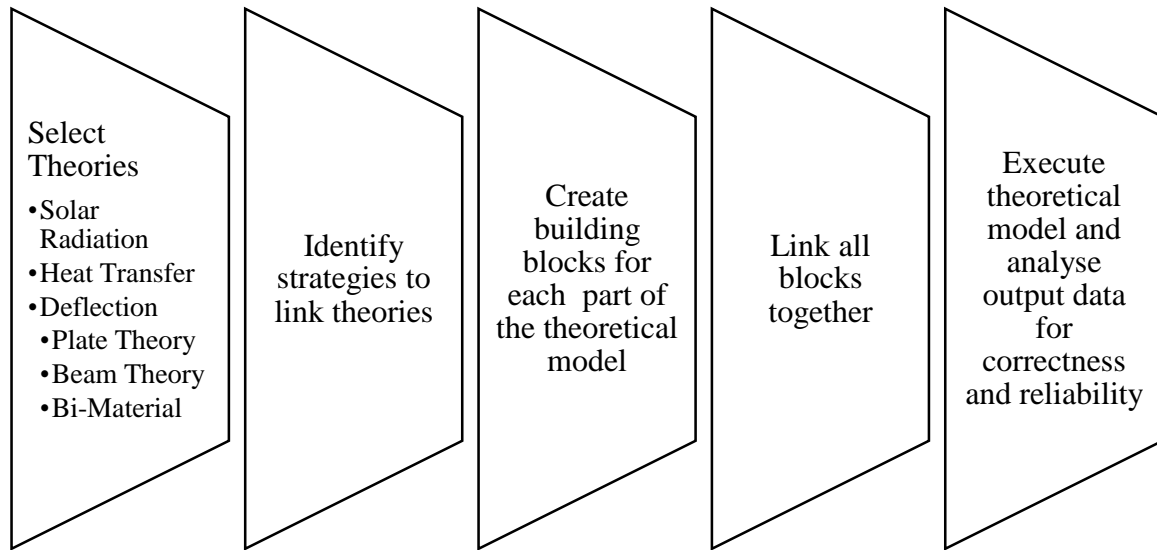
Figure 32: Theoretical model creation strategy

This is especially important in face of the fact that there is hardly any recent literature describing similar analyses on ships, especially on motor yachts. It is possible that such works have been done but are not in the public domain for various reasons. Therefore, this modelling effort would facilitate a documented way to calculate ship surface temperatures based on given input parameters. It is based on well-established scientific literature and empirical findings, and can serve as a design guideline to naval architects.

A suitable model needs to specify,

1. influences on the behaviour of temperature, the impact of different parameters on it and the interaction of different components.
2. which theory forms what part of the model since several theories put together will form part of a theoretical model.

Figure 32 describes the model creation strategy underlying the interconnectivity of different theories or "blocks" that simulate the model. The phenomenon being described is that of solar radiation (which is the input to the model), and temperature and its effects (such as deflection and coating defects), which are outputs from the model. Based on that, the flow of the theoretical model is shown in Figure 33.
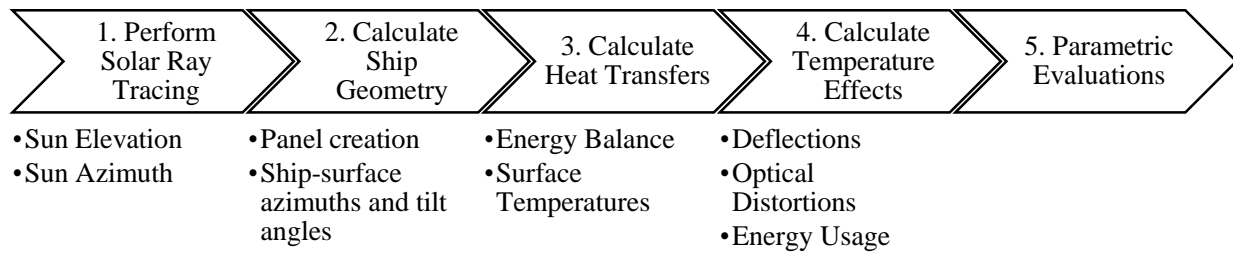
Figure 33: Flow of the theoretical model

1. The model first computes solar radiation from solar ray tracing after location data has been entered. Solar ray tracing is the computation of the sun position (solar azimuth from the North-South axis and solar elevation from the horizontal). Since, the amount of solar radiation is proportional to the sun's position, this is a very important step to begin the calculations.

2. Next the model computes the ship geometry based on the definition of node points. These lie at the intersection of transverse frames and longitudinal stringers. Based on this, it can create surfaces between any four nodes (which serve as vertices). This results in a "panel".

3. Heat transfer about this panel is calculated using the three possible mechanisms of heat transfer and temperatures are evaluated using an Energy Balance method.

4. Effects such as deflections were then calculated using a bimetal plate theory and the composite plate theory which modelled the epoxy-aluminium as an equivalent plate. Increased energy loads due to additional cooling needs for the ship were studied. Since the motor yacht surface is highly reflective, plate bending produces irregular distortions of the reflected image on the hull surface, further destroying the aesthetics of the yacht.

5. Lastly, different parameters were varied to study the effects of changes in temperature and deflections, such that the effects of these parameters could be investigated.

5.1 Solar Ray Tracing Calculations

Solar Radiation strikes the ship surface setting up different heat transfer mechanisms such as emitted radiation, convection to the surrounding air and water, and conduction to the interior of the ship as well as to the waterline. Thus, to model this phenomena, a suitable theory was necessary to calculate the sun position and its relation to the heat flux incident on a surface.

5.1.1 Selection of the solar model

There are several methods in available literature that describe various methods to model solar processes. However, not all of them are easily applicable or are necessary for practicing engineers. Some need a lot of input data (such as meteorological parameters) while others are overly mathematically intensive and meant for other scientific purposes. Keeping these considerations in mind and after a lot of research, the 'ASHRAE model' was chosen.

ASHRAE (American Society of Heating, Refrigerating and Air Conditioning Engineers) publishes a series of standards and data resources such as the ASHRAE Handbook – Fundamentals, which does an excellent review of methods available to calculate solar loads. With a few inputs, which can be found easily on the US State Department of Energy's website (EnergyPlus, 2013), any location in the world can be easily modelled making this model very adaptable. It also includes data for thousands of weather stations which helps to calibrate the mathematical model with local conditions.

ASHRAE (2009) describes design information for modelling energy related processes in residential, commercial and industrial applications. The analogy is thus the same whether it is applied to a building or a ship, which is essentially a structure floating on water. ASHRAE uses annual percentiles to define design conditions, which ensures that it represents the same probability of occurrence in any climate. Monthly information is compiled in addition to annual percentiles to provide seasonally representative combinations of temperature, humidity and solar conditions.

Two important parameters that the ASHRAE model uses is the clear sky optical depths for beam and diffuse irradiances (which are the only location specific inputs). From these two parameters, clear sky radiation for any time of any day of the year can be calculated. *Clear sky*

solar irradiance is the solar radiation incident directly on a surface, in a cloud-free sky. This thus ensures maximum beam solar radiation (directly from the sun) and will result in the modelling the highest possible temperatures. In other words, to model in clear sky conditions (and neglect cloudy days) would generate maximum surface temperatures, which can be considered as a worst case solar loading scenario on the motor yacht.

5.1.2   Description of Equations

Clear sky irradiance parameters are useful in calculating solar related loads for any time of any day of the year. Parameters are provided for the 21st of every month, which is a convenient day for solar calculations because June 21 and December 21 represent the solstices (shortest and longest days) and March 21 and Sep 21 are close to equinox (days and nights have the same length). The flow of equations is described in the next section and references (ASHRAE, 2009).

To design the model, Microsoft Excel was chosen for initial design for its ease of use, since it was necessary to first create a spreadsheet program to test different concepts behind the solar modelling theory. Once the spreadsheet program was working satisfactorily (in predicting the correct surface temperatures as measured from experiments), MATLAB was used to extrapolate the model to calculate temperatures for the entire year.

MATLAB was also essential in enabling parametric studies to be carried out on the model. It is able to work with large matrices, has a simple and effective syntax and has an excellent graphical plotting system. It allows more time on accurately modelling the physical system than spending on lengthy programming. Thus, it allowed for rapid prototyping of the mathematical model. It also has a lot of built in functions that saves time.

5.1.2.1   Solar constant

The starting point is the Solar constant E_{SC} which is defined as the intensity of solar radiation on a surface normal to the sun's rays. A frequently used value proposed by the World Meteorological Organization is $E_{SC} = 1367$ W/m^2. Next, because the earth's orbit is slightly elliptical, the extra-terrestrial radiant flux E_0 varies throughout the year, reaching a maximum of 1412 W/m^2 in January when the earth is closest to the sun and a minimum of 1322 W/m^2

when the earth is farthest away from the sun. For a surface normal to the sun this can be approximated as

$$E_0 = E_{sc} \left(1 + 0.033 cos \left[360° \frac{(n-3)}{365} \right] \right) \qquad (1)$$

Where n is the day of the year (e.g. 1 for January 1st and 32 for February 1st) and the argument inside the cosine is in degrees. Earth's orbital velocity also varies throughout the year so the Apparent Solar Time (AST) has to be determined, which varies with mean time (kept by a regular clock). This variation is called the equation of time and is approximated by the following formula:

$$ET = 2.2918 \left(0.0075 + 0.1868 \, cos(\Gamma) - 3.2077 \, sin(\Gamma) - 1.4615 \, cos(2\Gamma) \right. $$
$$\left. - 4.089 \, sin(2\Gamma) \right) \qquad (2)$$

Where ET is expressed in minutes and

$$\Gamma = 360° \frac{(n-1)}{365} \qquad (3)$$

The conversion between local standard time and apparent solar time is as follows:

$$AST = LST + \frac{ET}{60} + \frac{(LON - LSM)}{15} \qquad (4)$$

Where,

AST: Apparent Solar Time in [decimal hours]

LST: Local Standard Time in [decimal hours]

LON: Longitude of site, [°E of Greenwich]

ET: Equation of Time in [minutes]

LSM: Longitude of Local Standard Time Meridian − negative if in the western hemisphere, [°E of Greenwich]. Standard meridian longitude (LST) is related to the time zone (TZ) as:

$$LST = 15TZ \qquad (5)$$

Where TZ is the time zone expressed in [hours] ahead or behind coordinated universal time (UTC). *Daylight saving time has not been included in these calculations* to simplify the calculations and avoid confusion.

5.1.2.2   Declination

Declination calculation is the next step. Because the earth's equatorial plane is tilted at an angle of 23.45° degrees to the orbital plane, the solar declination angle between the earth-sun line and the equatorial plane varies throughout the year. This is given by:

$$\delta = 23.45 \sin\left(360° \frac{(n+284)}{365}\right) \tag{6}$$

Where δ is in [degrees] and the argument inside the sine is also in [degrees]

5.1.2.3   Sun Position
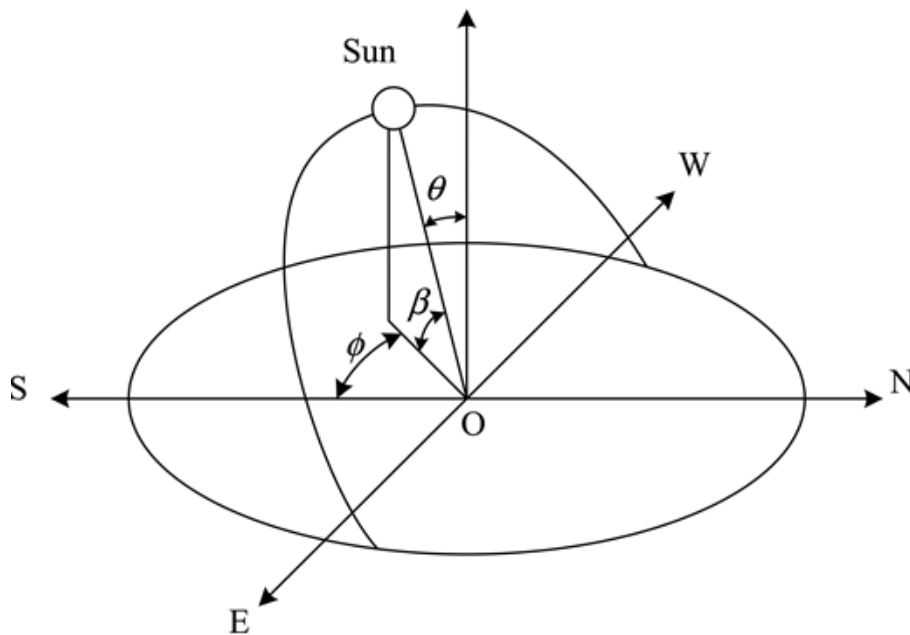
Figure 34: Sun Position parameters, Referenced from (Naraghi & Harant, 2013)

The sun's position is expressed by the Solar Altitude Angle β and the Solar Azimuth Angle ϕ measured from the South (Figure 34). Both of these depend on the local latitude L [°N, negative in the southern hemisphere], the solar declination angle and Hour Angle which is defined as

the angular displacement of the sun east or west of the local meridian due to the rotation of the earth, and expressed in degrees as,

$$H = 15\,(AST - 12) \tag{7}$$

H is zero at solar noon (AST=12), positive in the afternoon and negative in the morning.

The solar altitude angle β is defined as the angle between the horizontal plane and a line emanating from the sun. It varies from 0° on the horizon to 90° if the sun is directly overhead. Negative values correspond to night times. It is calculated by,

$$sin\beta = \cos L\,cos\delta\,cosH + sinL\,sin\delta \tag{8}$$

The solar azimuth angle ϕ is defined as the angular displacement from south of the projection on the horizontal plane of the earth-sun line. *By convention it is counted positive for afternoon hours and negative for morning hours.* At $= 90°$, $\phi = 0°$. For other values, it is given by,

$$cos\phi = \frac{cosH\,cos\delta\,sinL - sin\delta cosL}{cos\beta} \tag{9}$$

5.1.2.4 Air Mass

The air mass *m* is the ratio of the mass of atmosphere in the actual earth-sun path to the mass that would exist if the sun were directly overhead. β is always positive in the daytime.

$$m = \frac{1}{sin\beta + 0.50572\,(6.07995 + \beta)^{-1.6364}} \tag{10}$$

Where β is expressed in [degrees]

5.1.2.5 Clear Sky Solar Radiation

Solar radiation on a clear day is defined by its beam (direct) and diffuse components. These two components are calculated as follows,

$$E_b = E_0 \exp(-\tau_b m^{ab}) \tag{11}$$

$$E_d = E_0 \exp(-\tau_d m^{ad}) \tag{12}$$

Where E_b = beam normal irradiance [W/m²]

And E_d = diffuse horizontal irradiance [W/m²]

τ_b , τ_d = beam and diffuse optical depths which are location-specific and vary during the year. These values have been listed in Table 7

ab,ad = beam and diffuse air mass exponents which are calculated as follows

$$ab = 1.219 - 0.043\tau_b - 0.151\tau_d - 0.204\,\tau_b\tau_d \tag{13}$$

$$ad = 0.202 + 0.852\tau_b - 0.007\tau_d - 0.357\,\tau_b\tau_d \tag{14}$$

5.1.2.6   Transposition to receiving surfaces of various orientations

This section deals with the calculation of solar radiation on the surface of our target ship. The orientation of a receiving surface is best characterised by its tilt angle and its azimuth. Therefore, to proceed, it is first necessary to define the geometry of the ship.
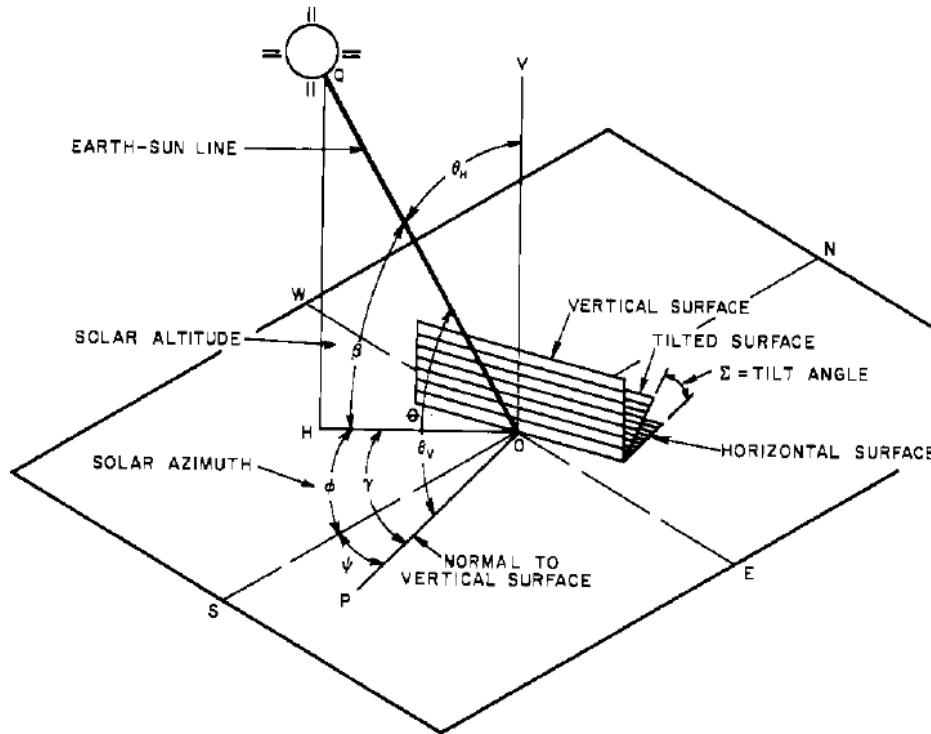
Figure 35: Various solar modelling parameters (ASHRAE, 2009)

5.1.3 Calculation of Ship Geometry

The next step is to analytically model the ship. This is done by providing X, Y, Z coordinates to create an array of nodes. These X, Y, Z coordinates are represented by the longitudinal, transverse and vertical axes positions, respectively. The intersection of a transverse frame and a longitudinal stringer is termed a node. In this way, any 4 adjacent nodes can form a surface which is designated as a "panel". This will enable the creation of a virtual wireframe mesh geometry as visualized in Figure 36.
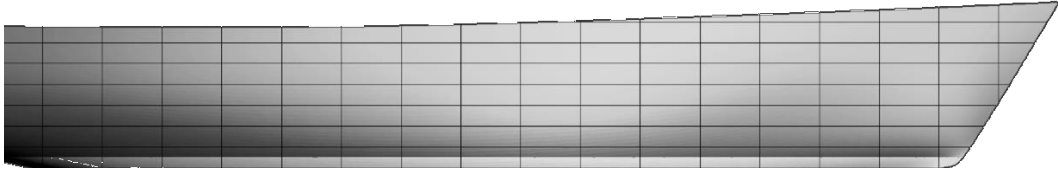
Figure 36: Visualization of the wireframe mesh

Now the tilt angle Σ is the angle between the surface and the horizontal plane. Its value lies between 0 and 180 degrees. Values above 90 degrees correspond to surfaces facing the ground.
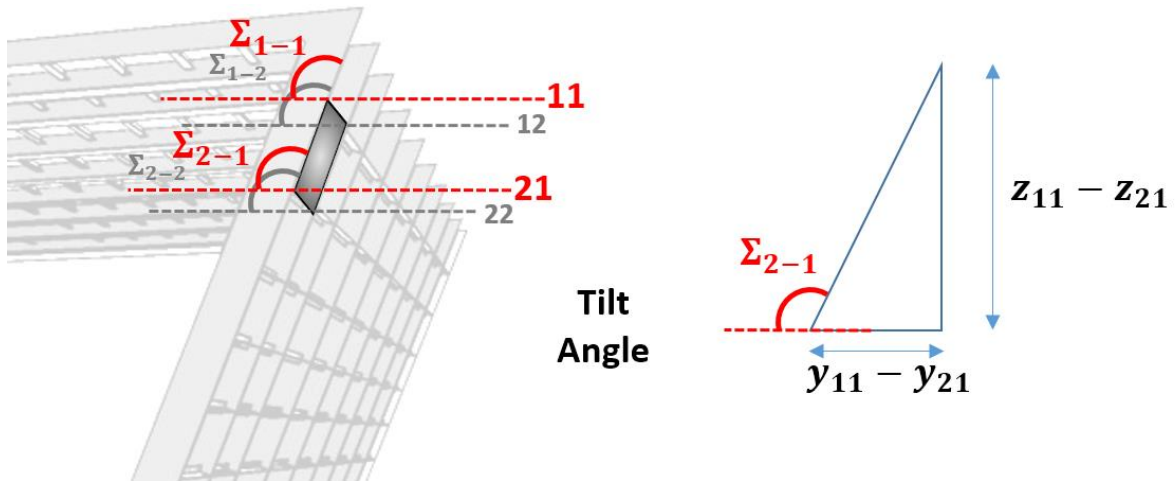
Figure 37: Panel Tilt angle calculation parameters

Since we have already defined the ship geometry, from Figure 37, we can calculate the tilt angle using simple trigonometrical relations. By symmetry, port and starboard will have the same tilt angles.
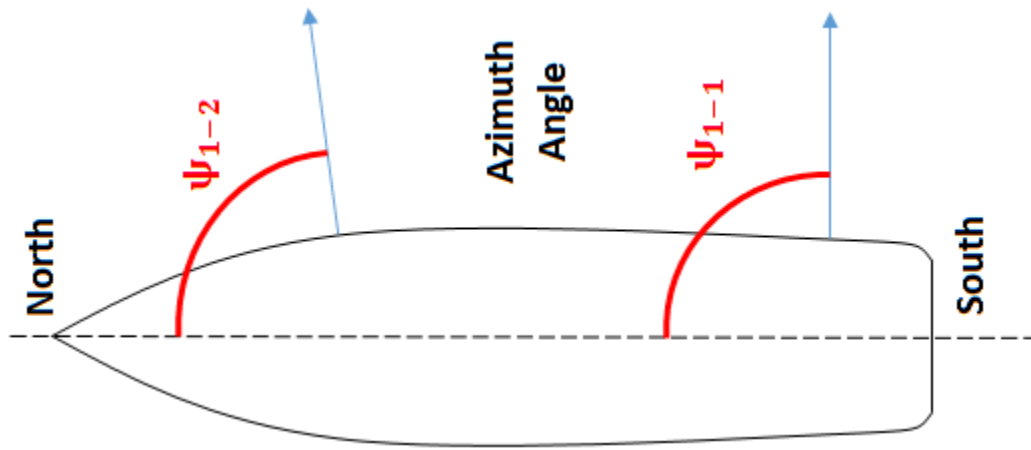
Figure 38: Surface azimuth calculation parameters

The surface azimuth angle ψ is defined as the displacement of the *normal* to the surface on the horizontal plane, from south of the projection. Surface that face west have a positive surface azimuth and those that face east have a negative surface azimuth.

As a last step, it is also important, to correct the surface azimuth with the relative orientation of the ship to the North south axis. Since the surface azimuth is calculated with the assumption that the bow and stern are aligned in the north-south direction, any deviation from this has to be added to the surface azimuth angle.

Next, the surface-solar azimuth angle γ is defined as the angular difference between the solar azimuth and the surface azimuth.

$$\gamma = \phi - \psi \tag{15}$$

Values of γ greater than 90 degrees or less than -90 degrees indicate that the surface is in shade. Finally the angle between the line normal to the irradiated surface and the earth-sun line is called the angle of incidence and is given by,

$$cos\theta = cos\beta \; cos\gamma \; sin\Sigma + sin\beta \; cos\Sigma \tag{16}$$

5.1.4   Calculation of Clear-Sky Solar Irradiance Incident on a Surface

Calculation of clear-sky solar irradiance incident on a receiving surface is the sum of three components: the beam component, the diffuse component and the ground or water reflected component. Hence,

$$E_t = E_{tb} + E_{td} + E_{tr} \tag{17}$$

The beam component is obtained from a straight forward geometric relationship:

$$E_{tb} = E_b cos\theta \tag{18}$$

The diffuse component is calculated from the below relationship:

$$E_{td} = \begin{cases} E_d(Y\ sin\Sigma + cos\Sigma), & \Sigma \le 90° \\ E_d\ Y\ sin\Sigma, & \Sigma > 90° \end{cases} \tag{19}$$

Where *Y* which is the ratio of clear-sky diffuse irradiance on a vertical surface to clear-sky diffuse irradiance on the horizontal is a simple function of the angle of incidence:

$$Y = \max(0.45, 0.55 + 0.437cos\theta + 0.313\ cos^2\theta) \tag{20}$$

Water reflected irradiance for surfaces of all orientations is given by

$$E_{tr} = (E_b sin\beta + E_d)\rho_g \frac{(1 - cos\Sigma)}{2} \tag{21}$$

Where ρ_g is the water reflectance, taken to be 0.07 for large angles of incidence.

At this point, with the calculation of total solar irradiance E_t, this process is repeated for all the panels that form a part of the section that we are dealing with. This gives us the incoming solar radiation heat flux on the entire surface of the ship section under study, for each panel.

5.1.5   Generating design day data

Table 6 gives a normalized daily temperature profile in fractions of daily temperature range. This profile is representative of both dry-bulb and wet-bulb temperature variation on typical design days. A design day is any designated day when the minimum and maximum ambient

day temperatures need to be calculated. This model has been used in the theoretical model to calculate the air temperature that the ship radiates and convects heat to. It has also been compared with local meteorological measurements made during experimental observations, described earlier and seen in the tabular and graphical data below. ASHRAE data for the city of Genoa was used for La Spezia, as it was the nearest weather station with the below details.

To calculate hourly temperatures, one has to multiply the Fraction from Table 6 with the Mean Daily Temp Range, and subtract it from the Monthly Design Dry Bulb Temperatures. Data for 5% Design conditions given below is a typical case.

Table 6: Fraction of daily temperature range (ASHRAE, 2009 - Ch.14, Table.6) with local weather station data (MeteoSpezia, Meteorologial Weather Station website, La Spezia, 2013) for Average Annual Temperature Profiles

Time, h	Fraction	Time, h	Fraction	Time, h	Fraction
1	0.88	9	0.55	17	0.14
2	0.92	10	0.38	18	0.24
3	0.95	11	0.23	19	0.39
4	0.98	12	0.13	20	0.50
5	1.00	13	0.05	21	0.59
6	0.98	14	0.00	22	0.68
7	0.91	15	0.00	23	0.75
8	0.74	16	0.06	24	0.82
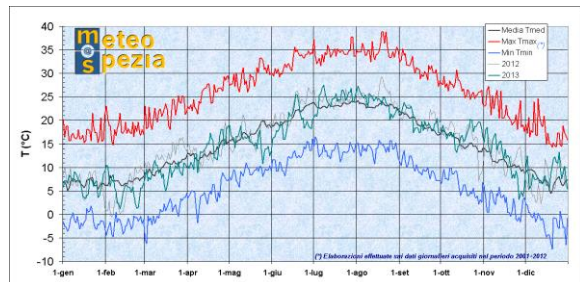
Table 7: ASHRAE solar parameters data for location-specific parameters

	Jan	Feb	Mar	Apr	May	Jun	Jul	Aug	Sep	Oct	Nov	Dec
Beam Optical Depth (Tau_b)	0.325	0.349	0.383	0.395	0.448	0.505	0.556	0.593	0.431	0.373	0.339	0.32
Diffuse Optical Depth (Tau_d)	2.461	2.316	2.176	2.175	2.028	1.892	1.779	1.679	2.151	2.317	2.422	2.514
Monthly Design Dry Bulb Temperatures (5% Design conditions)	16.9	18.8	22.9	26.4	29.1	31.8	33.3	32.4	30	25.7	21.7	17.9
Mean Daily Temp Range - DB	9.7	9.9	10.8	11.1	10.4	9.6	9.5	9.1	9.2	9.9	10.1	9.5

5.2   Heat Transfer and Temperature Calculation

Heat Transfer involves the transmission of energy from one region to another as a result of a temperature gradient. It takes place by three modes: Conduction, Convection and Radiation.
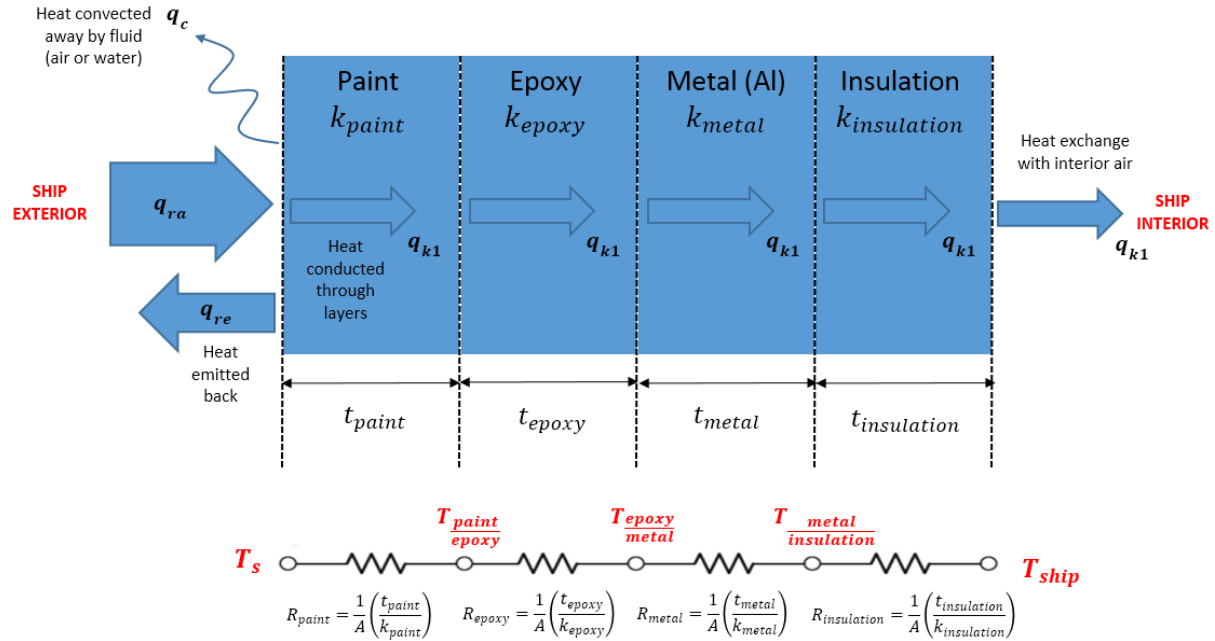
Figure 39: Thermal Circuit of heat transfer over the target ship

Conduction is the transfer of heat from one part of a substance to another part of the same substance, or from one substance to another in physical contact. The heat flux at the hull surface is manifested as a temperature on the surface of the paint. This heat conducts in two dimensions - one towards the interior of the ship passing through the paint, the epoxy filler, the metal and the insulation before interacting with the atmosphere inside the ship; while the other from the bulwark to the waterline over the surface of the hull. Longitudinal variation is negligible for the prismatic section of the yacht. Perfect interfaces have been considered between material layers such as between epoxy and aluminium for instance so as to make the interface resistance negligible. Interfaces resistances are usually set up by surface discontinuities at the interface between two materials.

Convection is the transfer of heat within a fluid by mixing of one portion of the fluid with another. This is found in the interaction of the ship hull with air and water boundaries. *Radiation* is the transfer of heat through space or matter by means other than conduction or

convection, i.e. electromagnetic waves. This is the principal heat input over the hull as a result of solar radiation. The hull in turn emits heat back out to the ambient sky. *The paint colour plays the foremost role in deciding the surface temperature since it absorbs this solar radiation in proportion to its colour.*

We know that the ship surface is exposed to solar radiation. Cleary-sky conditions and light to no wind conditions have been assumed. This ensures that only natural convection has to be modelled. This also means that the surface temperatures will be at their highest. Light wind conditions where applicable for correlating the theoretical model with experiments, are modelled by increasing the surface convective heat transfer coefficient after correlations were made with experimental measurements.

Now thermal analysis can be of two types:

1. A steady-state thermal analysis that determines the temperature distribution and other thermal quantities under steady-state loading conditions. This is a situation where heat storage effects varying over a period of time can be ignored.
2. A transient thermal analysis that determines the temperature distribution and other thermal quantities under conditions that vary over a period of time. (Alavala, 2009)

For the purpose of this thesis, it was sufficient to assume steady state transfer and calculations are made at every hour mark. Generally, two thermal boundary conditions are applied; constant panel heat flux and constant panel surface temperature. The outer surface (the paint) is exposed to solar radiation and convective processes to either the atmosphere or the ocean, i.e. to air and water. The radiation heat exchange with the ambient atmosphere is also taken into account.

The effects of exterior surface paint colour were represented by material properties such as emissivity and absorptivity. Reference colours of black and white were modelled to show the maximum and minimum limits of temperature and deflection. A practical analytical model for predicting heat transfer and temperature development over a panel is shown in Figure 39.

Now the exterior surface reflects and absorbs solar radiation flux and its temperature rises accordingly. This is given by q_{ra} which denotes radiation absorbed by the paint surface.

$$q_{ra} = \alpha A E_t \tag{22}$$

Where, α is the absorptivity of the paint and E_t is given by Equation (17) . Part of this absorbed radiation is emitted back to the ambient sky, denoted by q_{re}. This relation is given by the equation below:

$$q_{re} = \epsilon \sigma A (T_s^4 - T_{sky}^4) \tag{23}$$

Where T_{sky} is given by (Farzaneh-Gord & all, 2009),

$$T_{sky} = 0.0552 \, T_\infty^{1.5} \tag{24}$$

Then heat is transferred by convection to the ambient atmosphere, denoted by heat flux q_c

$$q_c = h_c A (T_s - T_\infty) \tag{25}$$

If the panel is underwater, T_∞ is replaced by T_w (temperature of water). Lastly heat is transferred by conduction q_{k1} to the inside of the ship.

$$q_{k1} = k_{overall} A \left(\frac{\Delta T}{\Delta x} \right) \tag{26}$$

This can be rewritten as,

$$q_{k1} = A \left(\frac{\Delta T}{R_{overall}} \right) \tag{27}$$

Where $\Delta T = T_s - T_{ship}$. Now $R_{overall}$ is given by the relation,

$$R_{overall} = R_{paint} + R_{epoxy} + R_{metal} + R_{insulation} \tag{28}$$

Where,

$$R_{paint} = \frac{1}{A} \left(\frac{t_{paint}}{k_{paint}} \right) \tag{29}$$

$$R_{epoxy} = \frac{1}{A} \left(\frac{t_{epoxy}}{k_{epoxy}} \right) \tag{30}$$

$$R_{metal} = \frac{1}{A}\left(\frac{t_{metal}}{k_{metal}}\right)$$

(31)

$$R_{insulation} = \frac{1}{A}\left(\frac{t_{insulation}}{k_{insulation}}\right)$$

(32)

Where $R_{overall}$ is the total resistance of the composite (paint-epoxy-metal-insulation), t denotes the thickness of the layer in [m] and k denotes the thermal conductivity in [W/mK]

There is also a conduction over the surface from the bulwark to the waterline and this correction also needs to be applied as given by q_{k2} .

$$q_{k2} = \frac{T_s - T_w}{h_w - h_s}C$$

(33)

Here, C is assumed to be equal to 1 because q_{k2} is a surface conduction correlation factor observed during experiments and is applied here in the model to linearize the temperature gradient from the bulwark to the waterline. This is done to simplify the model without which additional calculations would be needed to determine the heat transferred by conduction from one panel to another, through 4 different materials (paint, epoxy, metal, insulation) to arrive at nearly the same result. This would thus be computationally very intensive and unnecessary.

Thus based on all the above heat transfer equations, we can construct an energy balance for the system. We know that the total energy entering a system must be equal to the total energy leaving the system by conservation principles. In other words,

$$q_{in} = q_{out}$$

(34)

This gives us the relation,

$$q_{ra} = q_{re} + q_c + q_{k1} + q_{k2}$$

(35)

Substituting relations from Equations (22), (23), (25), (27) and (33) yields,

$$\alpha A E_t = \epsilon \sigma A \left(T_s^4 - T_{sky}^4\right) + h_c A (T_s - T_\infty) + \left(\frac{T_s - T_{ship}}{\mathrm{R_{overall}}}\right) + \frac{T_s - T_w}{h_w - h_s} \tag{36}$$

Rewriting this equation, we get

$$T_s^4 (\epsilon \sigma A) + T_s \left(h_c A + \frac{1}{h_s - h_w} + \frac{1}{\mathrm{R_{overall}}}\right)$$
$$- \left(\epsilon \sigma A T_{sky}^4 + h_c A T_\infty + \frac{T_{ship}}{\mathrm{R_{overall}}} + \frac{T_w}{h_s - h_w}\right) = 0 \tag{37}$$

This equation can be represented in the form below, which is a quartic or bi-quadratic equation.

$$ax^4 + dx + e = 0 \tag{38}$$

Here $x = T_s$. The solution of this equation will give us the surface temperature and is explained in Appendix-3. Next, we can proceed to finding the individual layer temperatures. Since q_{kl} is the same across any layer, we can determine the unknown temperature by the following procedure,

$$\frac{T_s - T_{ship}}{R_{overall}} = \frac{T_{layer_m} - T_{ship}}{\sum_{i=m+1}^{4}(R_{layer_i})} \quad , \qquad 1 \leq m \leq 3 \tag{39}$$

Or rewriting this in another form,

$$T_{layer_m} = \left(\frac{T_s - T_{ship}}{R_{overall}}\right) \left(\sum_{i=m+1}^{4}(R_{layer_i})\right) + T_{ship} \quad , \quad 1 \leq m \leq 3 \tag{40}$$

Thus in this manner, all interface layers temperatures i.e. $T_{\frac{paint}{epoxy}}, T_{\frac{epoxy}{metal}}, T_{\frac{metal}{insulation}}$ seen in Figure 39 can be calculated. Once these temperatures are known we can calculate the effect due to variation in different parameters and study the effects of temperature on deflections and cooling energy needs.

6   RESULTS AND ANALYSIS

6.1   Solar Ray Tracing

Solar Ray Tracing is essential for determining time and incidence angle of solar exposure on ships. Figure 40 shows the solar ray tracing computed by the theoretical model which correlates extremely well with the external reference provided in Figure 41.
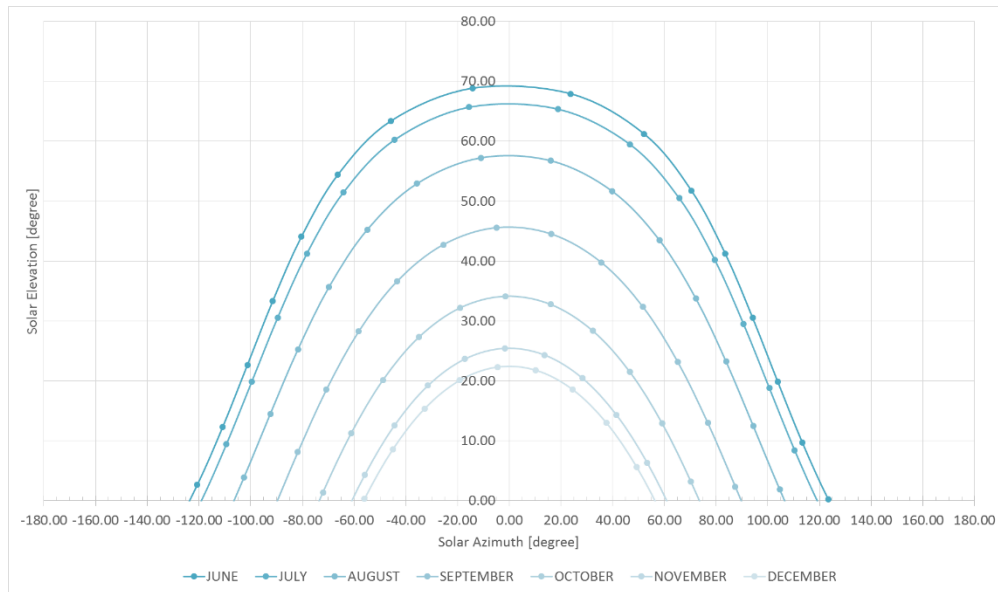
Figure 40: Solar ray tracing computed by the theoretical modelling for La Spezia, Italy
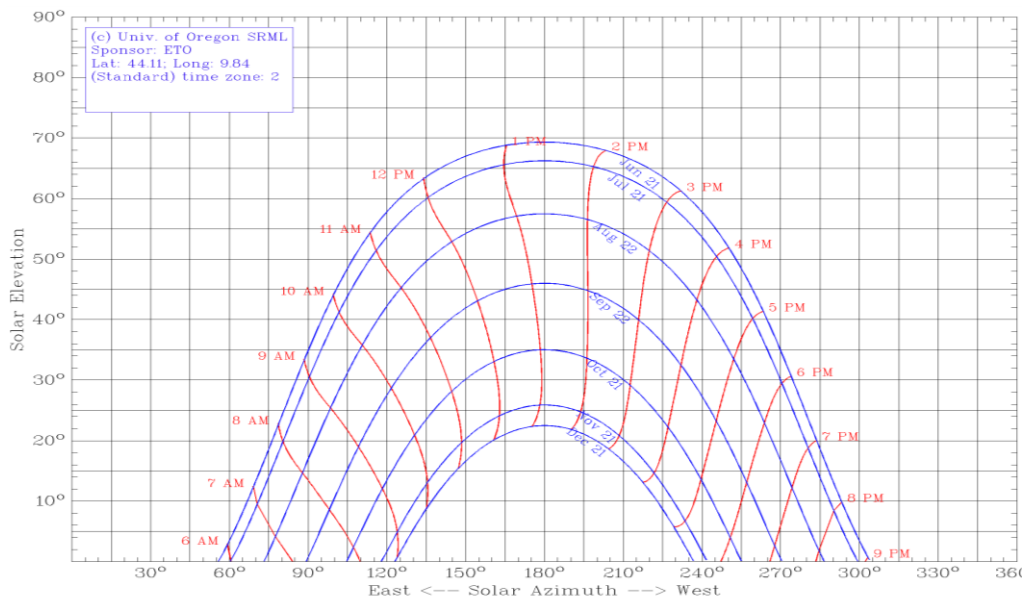
Figure 41: Solar ray tracing - La Spezia, Italy from external reference (UniversityofOregon, 2013)

From this graph it is clear that during the summer months, the time of exposure to the sun is much longer than in winter, about 15 hours. This will result in high surface temperatures for a longer time and consequently, deflections will be clearly visible. In winter, the solar exposure

time is limited to about 9 hours. However, in winter while the solar elevation is quite low, this will also mean that the sun strikes the ship much more directly, i.e. more normal to the surface, resulting in higher surface temperatures. Since deflections are a function of temperatures, this will also cause higher deformations. The theoretical model is swiftly able to calculate the solar azimuth and solar elevation for any location in the world, and compute surfaces temperatures for a target ship.

6.2 Temperature

The graphs below depict the theoretically predicted annual variation of temperature for each hour of the day.
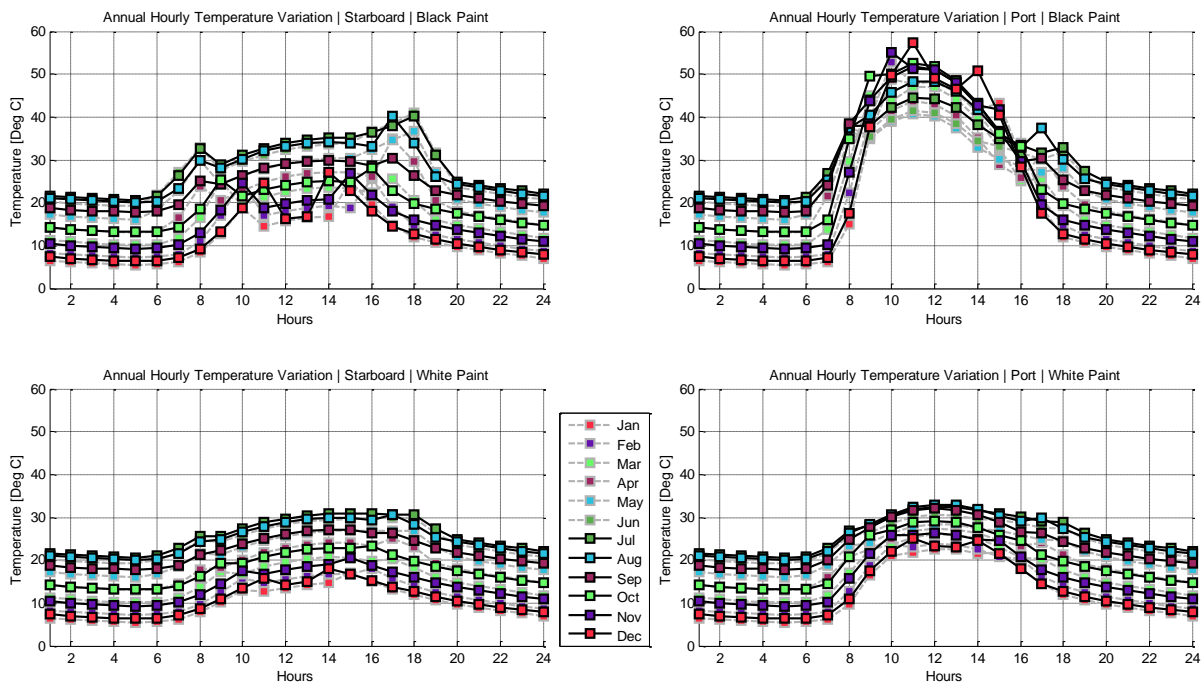
Figure 42: Annual temperature variation predicted by the theoretical model (on bulwark)

The analysis compares the effect of two colours - black and white and its effect on both port and starboard side of the ship. Temperatures correspond to the bulwark, which being a flat surface, is the hottest region on the ship. Since the target ship rests with its port side predominantly exposed to solar radiation, there is also a marked difference in port and starboard temperatures. In the black ship, temperatures can reach 55°C with winter temperatures exceeding summer temperatures by a few degrees. This is because the solar elevation is much lower in winter, causing solar radiation to strike more directly on the ship.

The starboard side which is in shade is nearly 20°C cooler than the port. This will not only set up a thermal stress in the sun exposed area, but the thermal expansion of the ship will be asymmetrical between port and starboard. This will lead to high stress concentrations within the structure. One can also observe peaks at times corresponding to sunrise and sunset. This is because the solar elevation is so low that the sunlight will strike the ship almost normal to the hull surface

In contrast, white paint has very little variation between port and starboard sides, of the order of about 5°C. This examination clearly shows the effectiveness of colour in reducing the surface temperatures.

Figure **43** offers an easy to understand visual comparison between black and white temperature profiles.
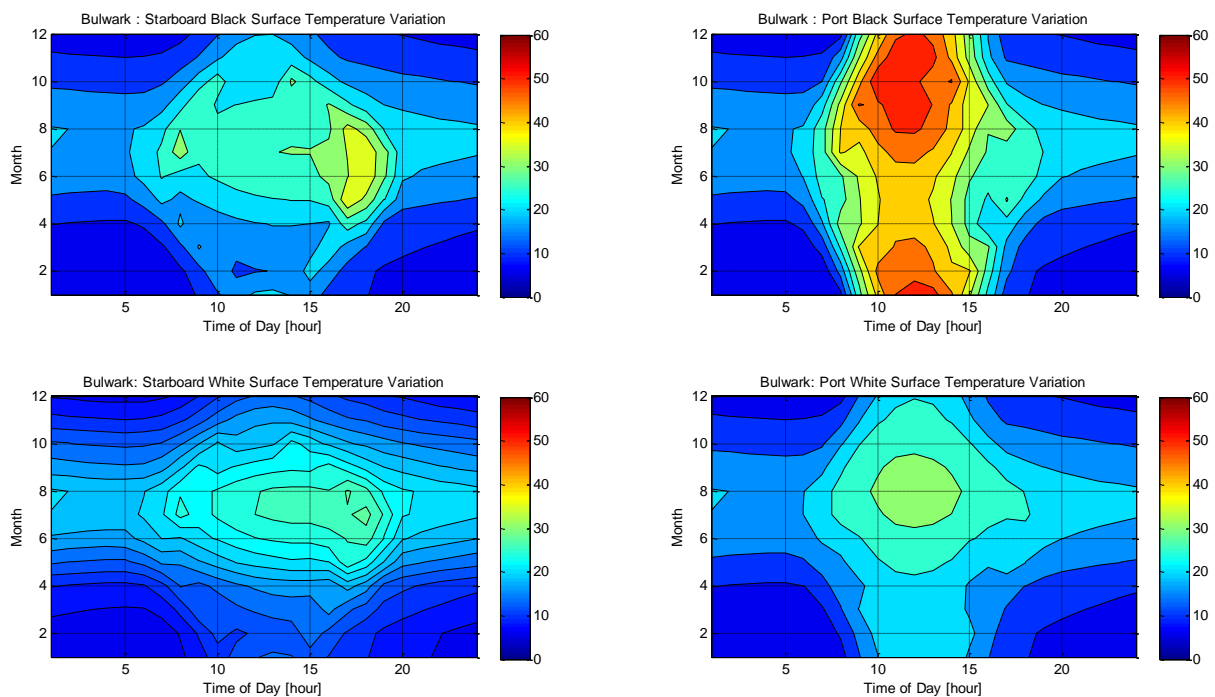
Figure 43: Contour plot of the maximum temperatures predicted (bulwark)

Temperature comparisons between thermal imaging and the theoretically generated temperatures have been discussed in Appendix-1 for various ships. Figure 44 shows satisfactory correlation between both of them for the target ship, bearing in mind that there can be some unavoidable sources of error during thermal measurements and interferences from

other sources, when compared with theoretical predictions (discussed in the chapter on Experimental Measurements).

Nodes 1-7 represent the vertical positions from deck to the waterline, and the figure shows a scatter plot of temperatures at these nodal locations. (E.g. Nodes1-2 represent the bulwark.)
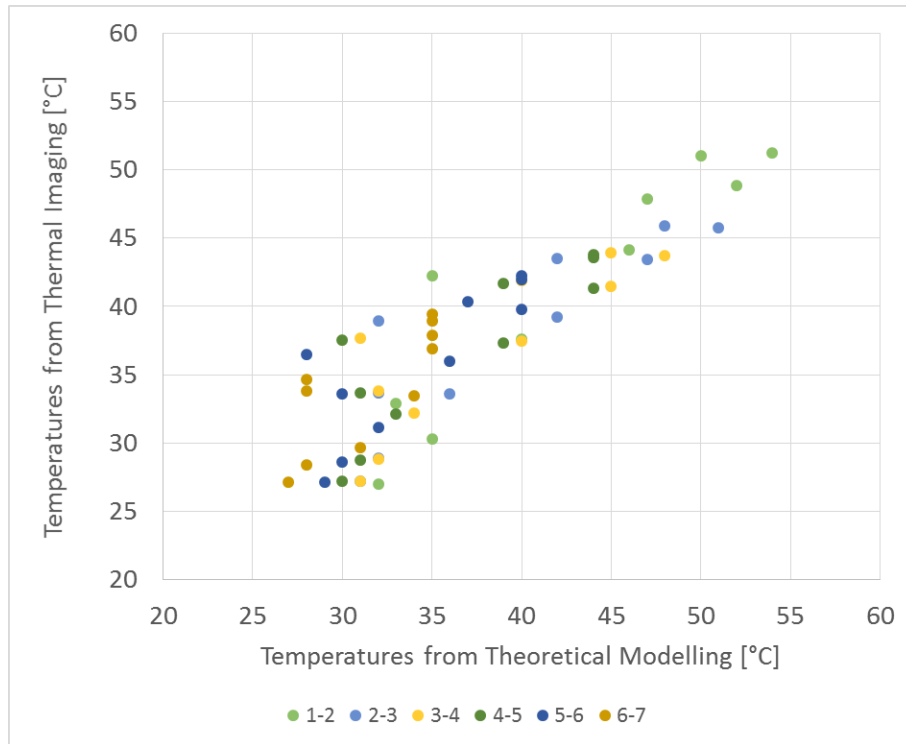
Figure 44: Scatter plot of panel temperatures showing good correlation between thermal imaging measurements and model predictions for the dark blue ship (Aug 2013)

Some important inferences were also made during the correlations. Ships which are berthed next to a dock or other ships are quite influenced by their presence. During summer, the shade side is warmer than predicted since the concrete dock radiates heat. In winter, the docks block the sun (whose elevation is lower in winter) from reaching the shade side causing hull temperatures to be lower than predicted.

6.3   Parametric Analysis

Parametric analyses involve simple evaluations which are statistically significant - certain parameters can be much more significant if they were analysed. On the other hand, they can be much less significant. If neither cases are applicable, that parameter is probably not very important and the theoretical model could be simplified by removing it.

It is very important to consider here that any solution derived from this analysis will have 'cost' as a primary constraint. The ideal solution to reducing plate deformations if a black paint hull is required, is to use a very stiff framing system. However, this would make the boat heavier because of additional metal used, which would then need a bigger engine, which will make the boat heavier adding further to costs and so on. However, if no additional costs are to be borne the solution is then to change to white paint. This creates a technical contradiction where both black paint and a lighter boat are desired. Thus cost as a constraint implies, finding the best combination of components of the system that will come as close as possible to the ideal situation.

However, it is important to note that cost optimization may not necessarily be good enough – it is a balance between competing constraints which will predict performance in relation to a simultaneous change in multiple parameters. This can be used by the naval architect to advise the client on desired qualities versus costs incurred.

6.3.1 Paint Colour
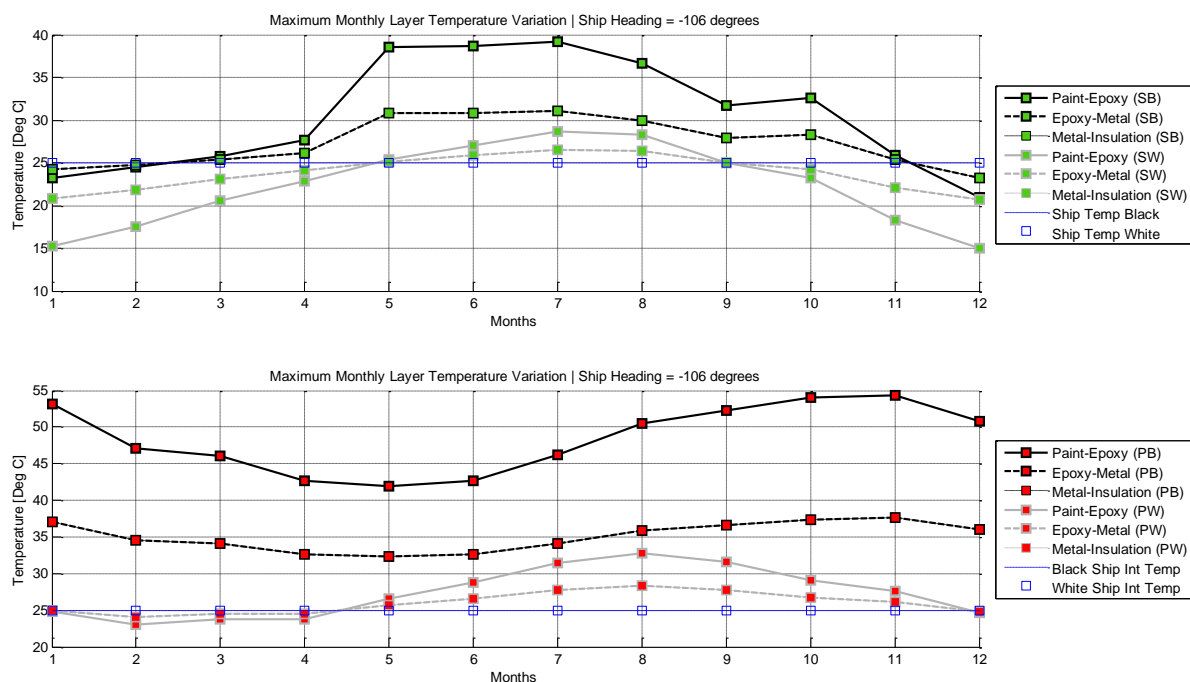
Figure 45: Effect of paint colour on maximum surface temperatures over a year

The parameter of colour is perhaps the most important factor in deciding surface temperatures and resulting deflections. White is not only a 'cool' colour, it also does not show up distortion defects on its surface as much as darker colours such as black do. Figure 45 demonstrates that

the difference between black and white paint can reach 20 degrees in some months. This is a very big difference, not only in creating deformations but also increased HVAC usage thus reducing the energy efficiency of the ship. The colour white is by contrast not only cooler, but has a very low thermal gradient even between starboard and port. The effects of some other colours are described below.

Table 8: Effect of paint colour on solar absorption ratio (TheEngineeringToolbox, accessed on 07 June 2013)

Surface Colour	Fraction of Incident Radiation Absorbed
White smooth surfaces	0.25 - 0.40
Grey to dark grey	0.40 - 0.50
Green, red and brown	0.50 - 0.70
Dark brown to blue	0.70 - 0.80
Dark blue to black	0.80 - 0.90

6.3.2 Annual Variation
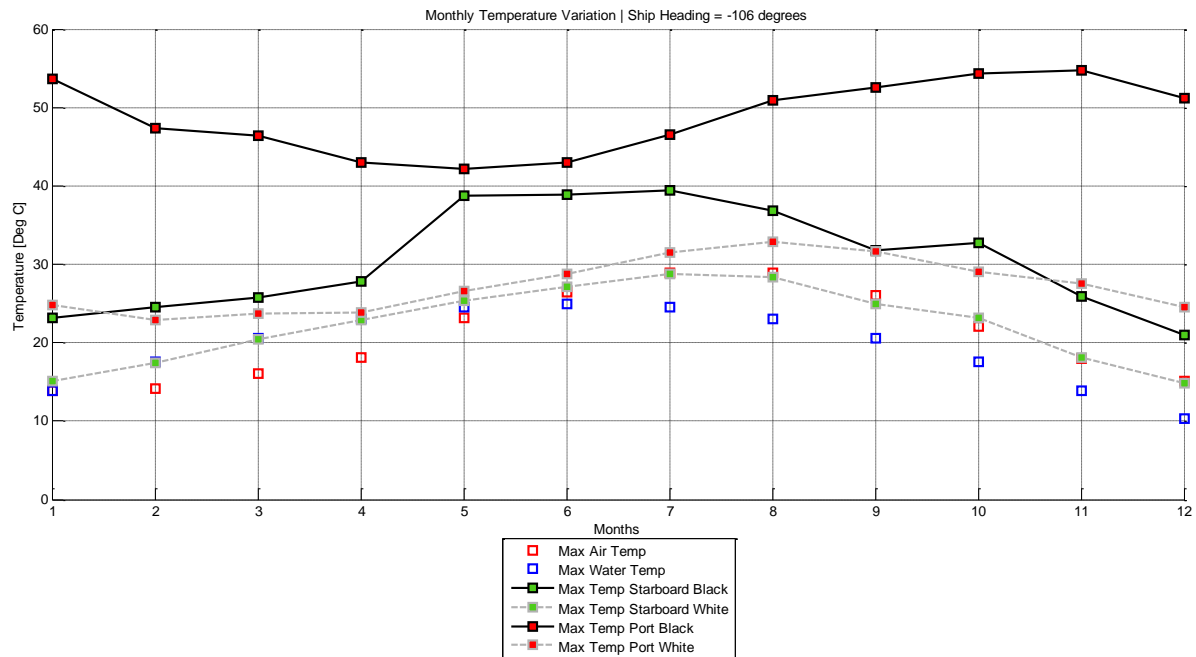
Figure 46: Change of maximum surface temperatures over a year

One of the most significant observations from Figure 46 above is that when the theoretical model was completed in October, it predicted high temperatures throughout winter, especially in the months of November and December. This was subsequently confirmed by thermal

imaging measurements. In fact, the graph of black paint on the port side of the ship, shows a minimum temperature of 42 degrees in May while reaching a maximum of 54 degrees C in November. Thus, it seems that ambient temperature is not as critical as is the intensity of solar radiation, which actually increases in winter since the sun is closer to the earth.

6.3.3 Ship berthed in Water and on Land
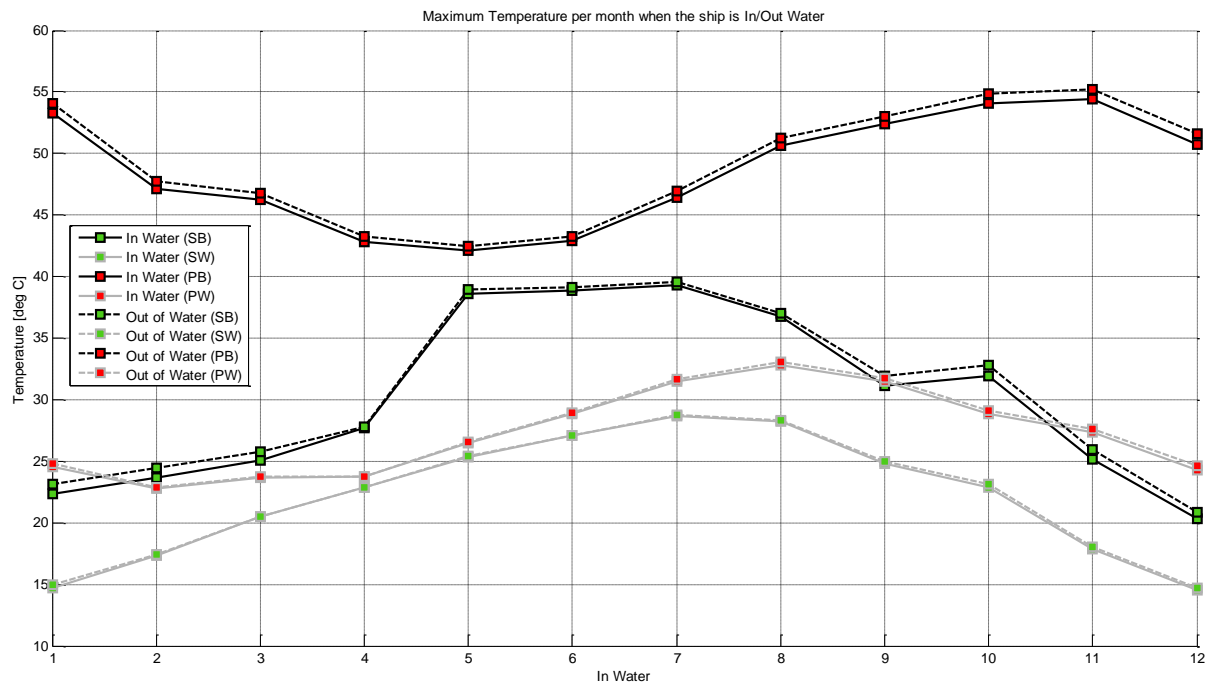
Figure 47: Comparison of maximum temperatures when the boat is in the water and out

The boat is cooler when it is in water due to the large convective heat coefficient of water. But this also leads to a steep gradient from the waterline to the bulwark, which is much lower when the boat is out of water. This is seen in Figure 47 (to read the legend, e.g. PB = Port Black) which shows that the bulwark only has a temperature difference compared to when the ship is out of water as seen. However, while the ship in water has a much lower temperature at the waterline, the ship on land does not. This is what causes the steep thermal gradient.

6.3.4 Site Location

Site location plays a major role in the intensity of solar radiation. A marina in the Mediterranean will have significantly more solar exposure than one in Scandinavia for instance. This could be even more in the Caribbean. Northern latitudes have the sun present at low angles for most of

the day at certain times of the year. Thus, the hull temperatures are quite high during this period while the water is very cold. This even leads to a very steep 30-40°C thermal gradient.

Furthermore, the way the ship is berthed affects whether port or starboard gets heated, and the duration of solar exposure. If the ship is positioned exactly along the east-west axis, the surface temperatures are much lower since the angle of the sun to the hull surface is very oblique. The stern and bow will face the sun directly, however this will be a much smaller area and will be exposed only during sunrise and sunset. At other times, the deck and superstructure will face the brunt of solar radiation but being in lighter colours will be much cooler.

6.3.5   Sun Elevation

At low sun angles, there is a sharp increase in the solar radiation when the sun is at a low altitude because of two reasons,

1. The low sun angle is much more directly incident on the ship surface, resulting in higher beam radiation.

2. At such a low elevation, the angle to the horizontal, i.e. the water surface is also quite small. In other words, the incidence angle is quite large, the reflectivity (or albedo) increases by a very large amount suddenly. This is described by

3.

4. Figure 48,
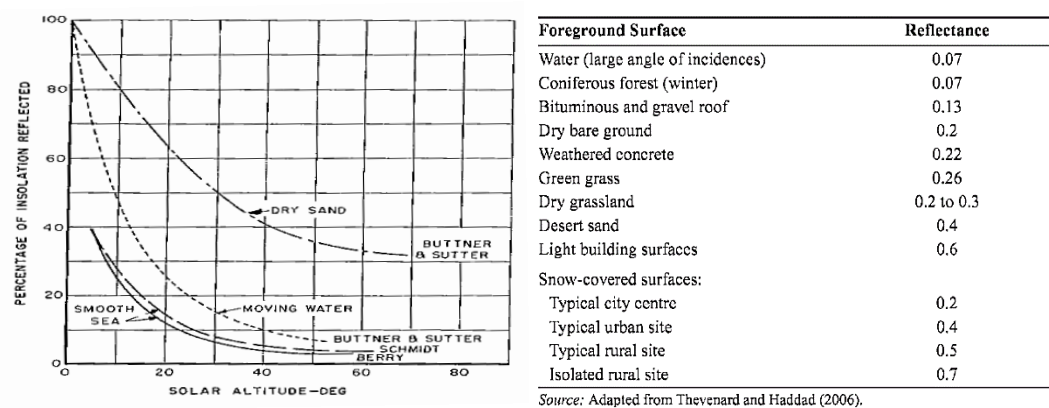
Figure 48: Effect of the incidence angle on the reflectivity of water (left) & (right) ground reflectance values of typical surfaces (Hechtman, 1956), (ASHRAE, 2009)

The theoretical model showing the differences in bulwark temperature after albedo correction in Figure 49. One can clearly see temperature peaks during sunrise and sunset.
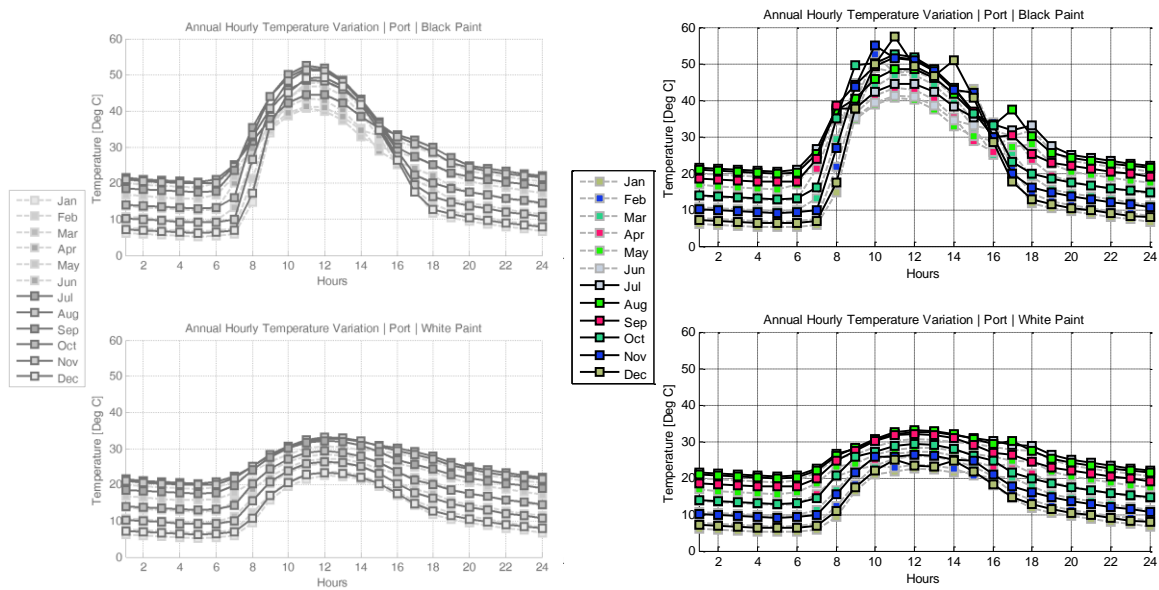
Figure 49: Theoretical model without (left) and with albedo correction (right)

6.3.6   Shaded vs. Sunny berthing condition

The effect of shade has a dramatic influence on the surface temperatures. In Figure 50, one can see a 20°C difference between the shade side (starboard) and the sun side (port). This will cause asymmetrical expansion of the entire ship leading to thermal stresses in certain sections of the ship. To relieve these stresses, those areas will deflect. This is what happens to the plating.
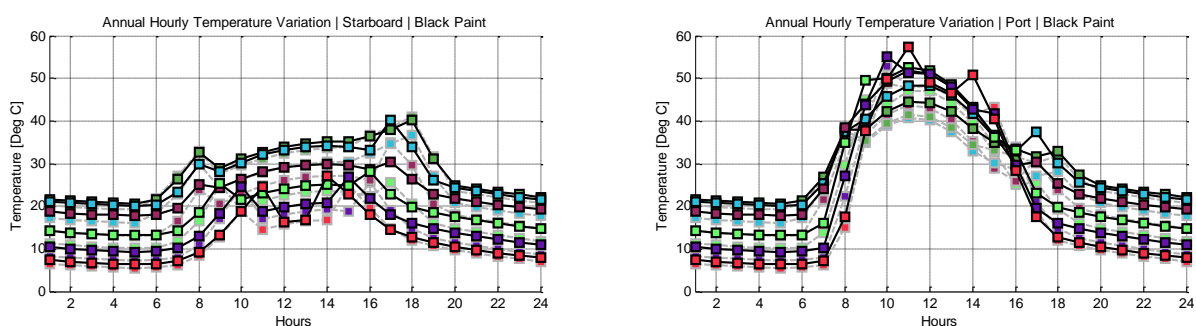
Figure 50: Starboard is in shade while port is on the sun side

In winter, this difference can reach 40-50°C. An experiment carried out showed that it takes about 5 minutes for the surface to cool down to its shade temperature in winter, after its exposure to the sun is cut off by an obstruction.

6.3.7   Effect of varying Epoxy Thickness
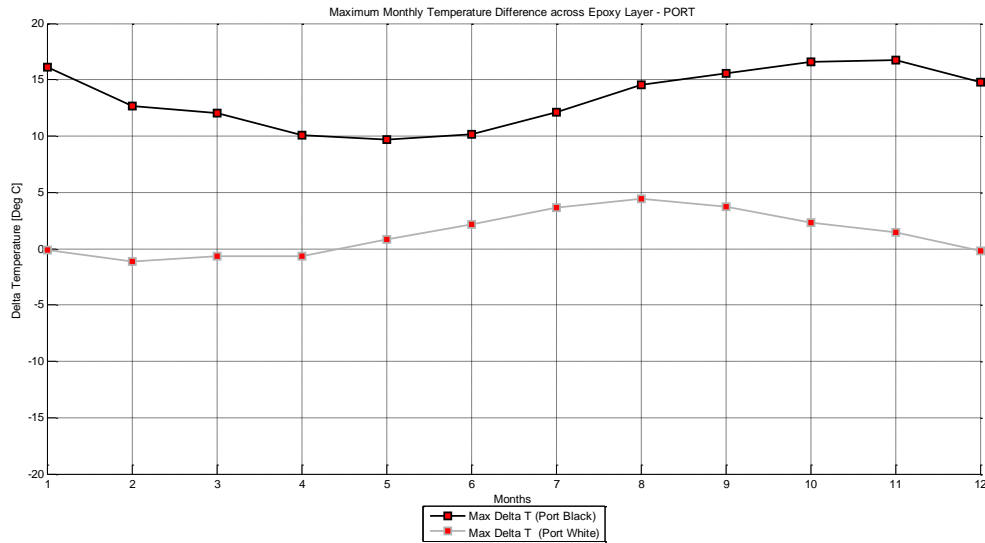
Figure 51: Variation of epoxy thickness and temperature across the epoxy-metal layer

The resin acts as the outside cladding on the aluminium structure. Though it hardly offers any structural strength to the ship structure, when we consider only the area of the plate, it does have significance. Since the aluminium plating is only 5mm thick on the sides, while the epoxy can reach up to 20mm, this creates a bi-material configuration and the combination of epoxy-metal behaves as an equivalent plate. The greater the epoxy thickness, the greater will be the temperature difference across it since it is a bad conductor of heat. In addition, it has double the thermal expansion of aluminium which is stressed by the epoxy when it starts to expand.

Figure 51 shows the temperature variation over the epoxy-aluminium composite when the epoxy and aluminium are 20mm and 5mm in thickness, respectively.

7   EFFECTS OF HIGH TEMPERATURES

Solar radiation induces high temperatures that have several detrimental effects. Some of them are listed below and discussed in detail in this chapter.

- Hull Deformations
- Optical Distortion Effects
- Hull Coating Defects
- Increased Cooling Loads
- Internal Hull Surface Condensation
- Thermal Comfort

7.1   Hull Deformations
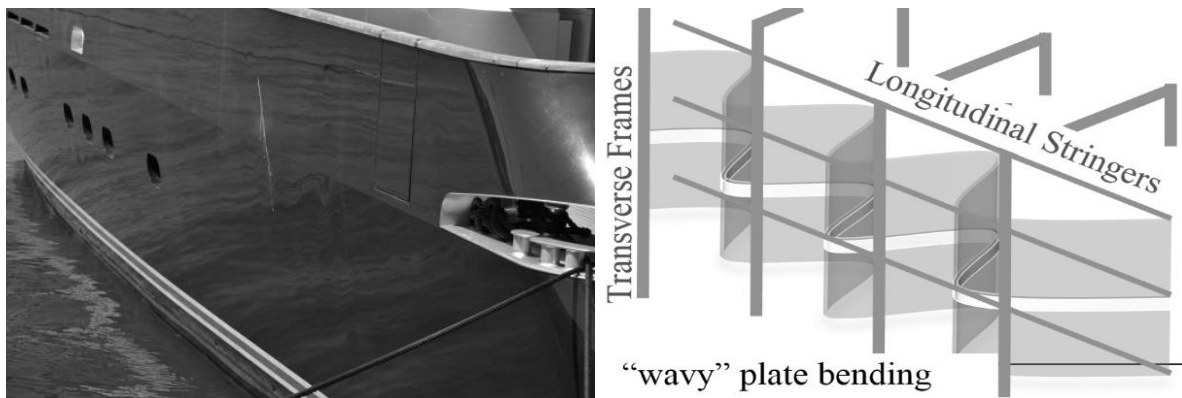
Figure 52: Deformations visible on the aft of the yacht, on the port side.

In

Figure 43, a "wavy" pattern can be seen at the aft of the ship, just under the bulwark. A yacht is a luxury symbol and deflections destroy the aesthetics of a yacht. The largest deflections seem to be in the middle of the plating, which is bound by the transverse frames vertically and longitudinal girders horizontally. These deformations are also seen amidships, and seem to be more pronounced in the region around the portholes that lie between the two accommodation bulkheads. This could mean that the plating between the bulkheads behaves like a beam on simple supports and is being stressed by thermal loads (in addition to hydrostatic loads), while the portholes being a large discontinuity in the structure, represent areas of stress concentration. These deformations are just beneath the bulwark. The water line and bulwark

represent the minimum and maximum temperatures and thus the middle region probably experiences maximum distortions as a result, caught between regions of unequal expansions.

7.1.1 Deformation Measurements

As mentioned before since the target ship was in water, it was practically impossible to accurately measure deformations on the hull surface due to lack of adequate measuring equipment. It is also important to bear in mind that a yacht's surface is quite curved and finding the deflection of a curved shape is quite complicated. While strain gauges would have certainly provided much needed information, budgetary restraints made this option unavailable. Modern techniques like 3D laser scanning, which are becoming both cost effective as well as reliable could have been another option. Some software-based inexpensive solutions can simply use multiple-angle standard camera images and generate a point cloud measurement field (3D model) of the object they scan, called *stereo-scanning*.
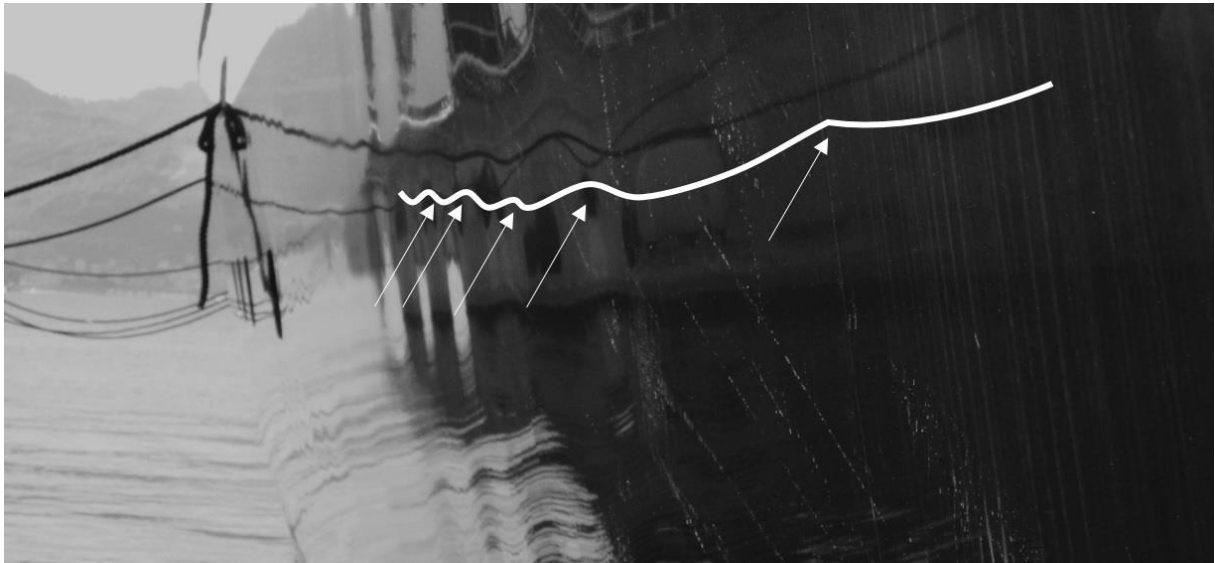
Figure 53: Deflections are clearly visible in this image where one can see the mooring lines rippling in the reflection on the surface of the motor yacht

For this research, it was not possible to procure such tools and instead simple manual measurements have been made. *Thus, these results are only for qualitative purposes, to estimate the range of deflections*. This was still a difficult process, to measure an object moving with respect to the reference at all times, the way a ship does by heaving, rolling and swaying, for example. These measurements were made from both onboard the ship, to cancel the effect

of ship motions, and from a small boat to inspect the hull from close distance. Two approaches were followed which are described in the following sections.

7.1.1.1 Manual Measurement

The first process consisted of placing a flat, 2 meter rigid aluminium baton on the ship hull and measuring the deflection of the central region using a scaled ruler. This was done at several points along the ship, principally in the areas between bulkheads, which had shown the highest thermal gradients and also visually observable deformations. Several data points were taken to compensate for manual errors in this basic measurement process.

Table 9: Summary of qualitative deflection measurements on the dark blue ship in November 2013

Section of ship	Plate Zone	Max [mm]	Avg. [mm]	Remarks
Aft	Bulwark	0.5	0	-
	Mid-plating	6	3	Bulge near engine room bulkhead
	Bottom-plating	2	2	-
Midships	Bulwark	1	0.5	-
	Mid-plating	5	2	4-6mm deflections near portholes
	Bottom-plating	3	2	-
Fore	Bulwark	0.5	0	Bow area under chine not measured
	Mid-plating	2	1	
	Bottom-plating	1	0.5	

Only the port side was measured since the starboard side was moored to quay. However pictures taken appeared to suggest that there were much less visually observable defects, probably due to the starboard side being completely blocked from the sun, i.e. in total shade.
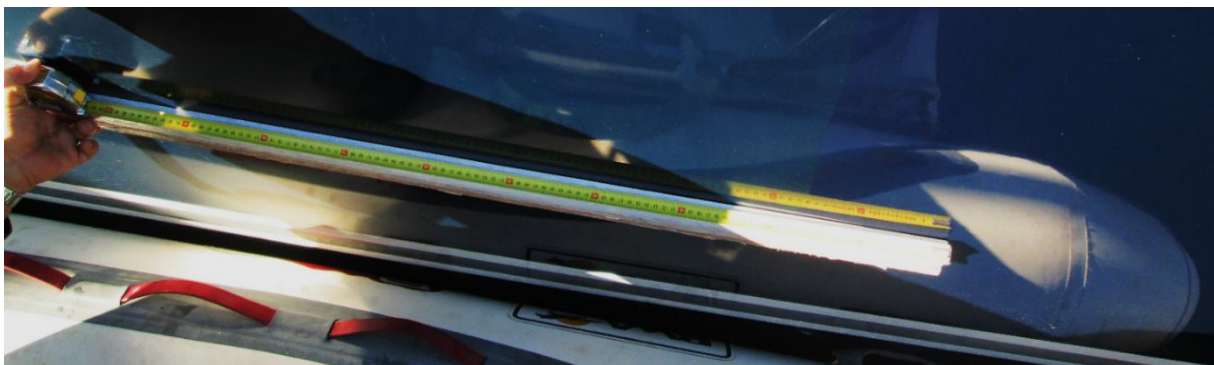
Figure 54: The length of a transversal frame is 1meter and this was used to find the centre of the plate between two transverse frames

Figure 55: Scale measurement of deflections in between two transversal frames

Figure 56: Image showing the author (in black jacket) measuring deformations from a boat

7.1.1.2 Visual Imaging

In the second process, several images were also taken of the port deflections and measured in a drafting program to get a second list of measurements that were compared and averaged with the manual method. Some of these images are described below.
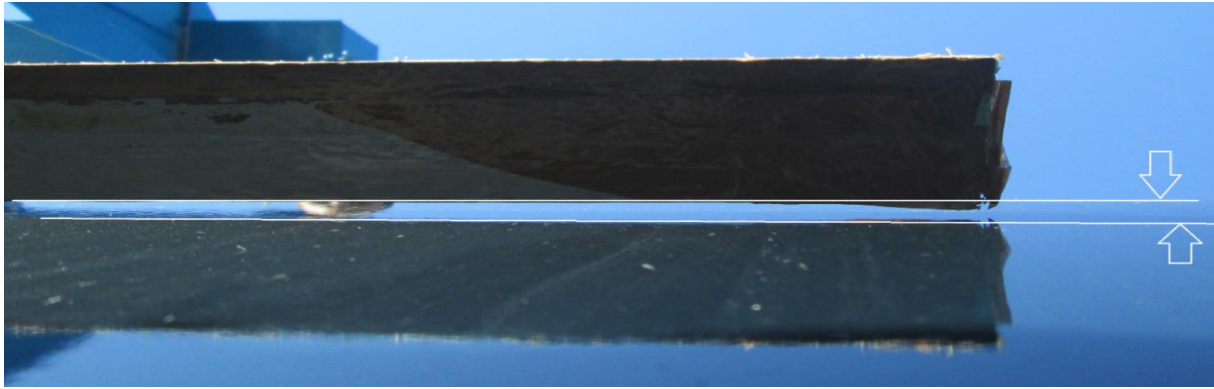
Figure 57: Visual imaging using the baton's reflection on the hull surface

Figure 57 shows the reflection of the baton on the surface of the yacht. Since the distance of the reflection will be equal to the distance of the object from the surface, dividing this apparent gap by a factor of 2 will yield the actual gap.

Figure 58: Visible gap over a porthole clearly visible (midships)

Figure 58 shows the gap apparent over a porthole. As shown in the chapter on experimental measurements, steep thermal gradients were found around portholes. Also, as an opening in a structure, they represent regions of stress concentration. Last but not least, they are located in the middle of two bulkheads, further increasing the deflections in this region.

Figure 59 shows a strange bulge observed at the aft of the ship, near the engine room bulkhead. It is possible that since the greatest distance between bulkheads is found between the engine room bulkhead and the stern, this area might develop multiple deflection mode shapes. Also,

the engine room bulkhead is much stiffer than other bulkheads, making the sections in this region experience high levels of stresses structurally.

Figure 59: Image showing a bulge in the hull plating close to the engine room bulkhead

7.1.2   Deformation Analysis

In this section, deflections due to thermal stresses have been analysed. As already mentioned before, measuring the deflections on the target ship have been quite difficult to achieve and thus it was interesting to see what the theoretical model would predict, to have a frame of reference for comparisons.

Plate Dimensions [mm x mm]	1000x100	1000x200	1000x300	1000x400	1000x500
Bimetal Theory	0.02	0.10	0.21	0.34	0.48
FEM	0.03	0.10	0.21	0.37	0.57
Composite Theory	0.03	0.10	0.22	0.34	0.50

Figure 60: Theoretically & FEM predicted deflections due to effect of only thermal loads

At first only the deflections due to thermal stresses borne out of a temperature difference were evaluated. This is as shown in Figure 60. Plate theory was used to analytically compute a solution and was then compared with FEM to obtain deflections in the centre of the plate. For the plate theory, the epoxy-aluminium bi-material was modelled separately with different theories, first as a bimetal and then second as a composite plate, with suitable calculations to determine the equivalent modulus of the bi-material plate.

As clearly seen, deflections in a single plate are quite low - in the order of less than a millimetre. When compared to the experimental measurements described earlier, these deflection were in the order of 3-4 mm. Thus there must be additional stresses acting on the ship. This could be due to hydrostatic loads acting on the ship in combination with thermal loads on the entire side face of the ship. Normally, due to hydrostatic loads, the bending str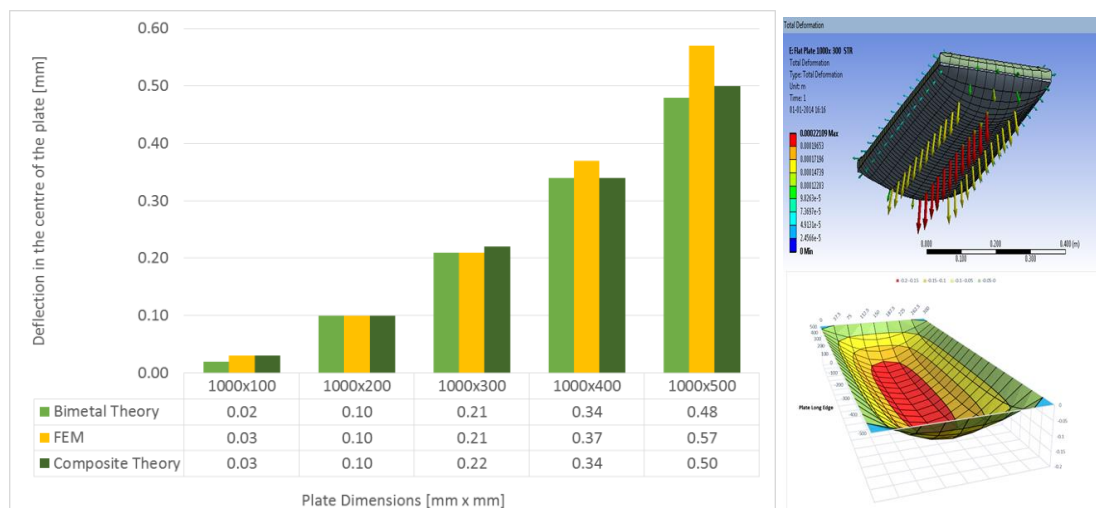esses induce shear along the sides. When the ship is seen as a whole there is mode shape of bending between the stern and the bow due to primary stresses and behaves like a beam on an elastic foundation, i.e. loads acting downwards and buoyancy forces acting upwards.

There however, is a second mode shape between bulkheads that manifests itself in the form of secondary stresses. Typically the deflections measured on the dark blue ship indicate that the maximum deflections seemed to lie between the bulkheads, In fact, there was even a bulge in the plating right next to the engine room bulkhead as seen in Figure 59. Thus this mode shape between bulkheads may also induce additional pressures in the plating which when superimposed with thermal stresses, causes plate deflections of a higher magnitude. Figure 61 presents a theoretical calculation of bending and shear stresses for every section. Thermal stresses are added to these global stresses and a section-by-section picture of deflections calculated by plate theory is shown for both port and starboard sides.

To read the bar graph, for stresses, blue bars indicate compression and red bars indicate tension. For deflections, red bars indicate the plate is bending inwards and blue bars indicate bulges. Length of the bars indicate the magnitude. Deflection mode shapes have been exaggerated for easy visibility. This figure should only be read qualitatively since it is based on theories that include linear approximations. It seems very likely that that since the temperature distribution is asymmetric and conducts through multiple materials with non-linear temperature dependent properties, it is very difficult to build an correct 2-dimensional model for 3-dimensional phenomena.
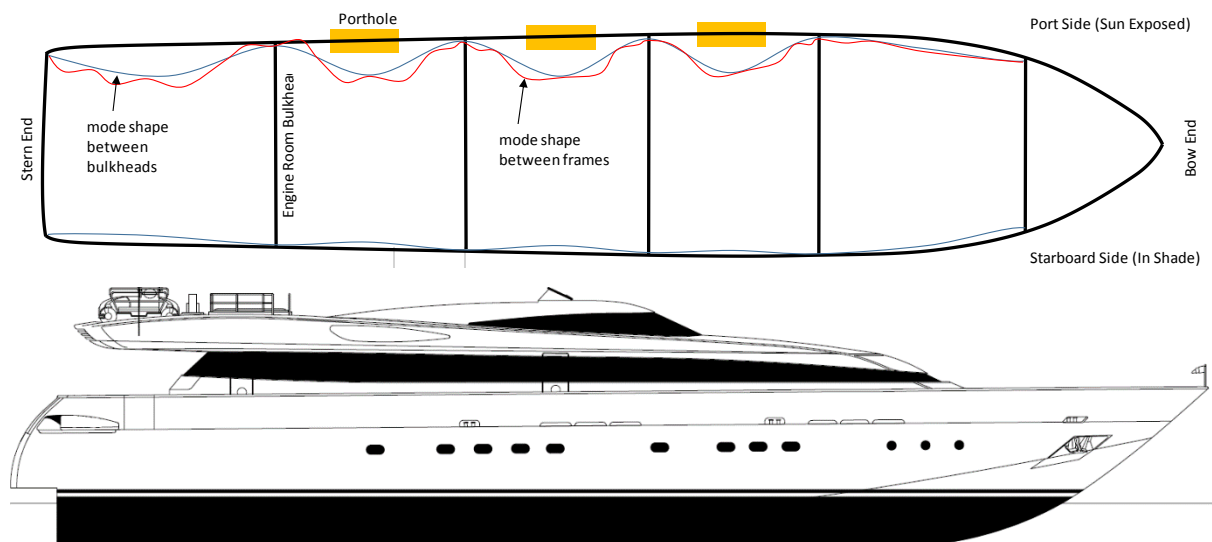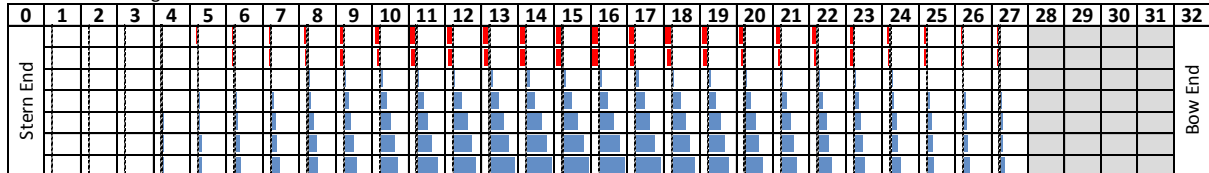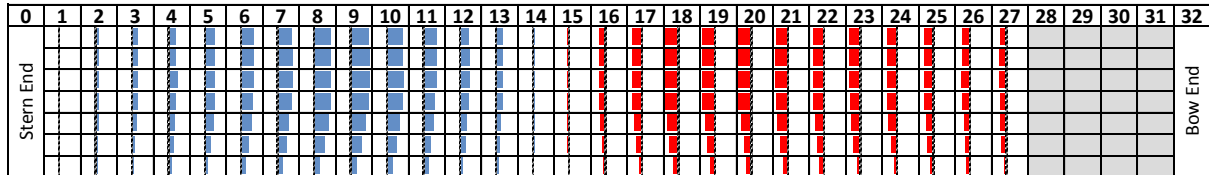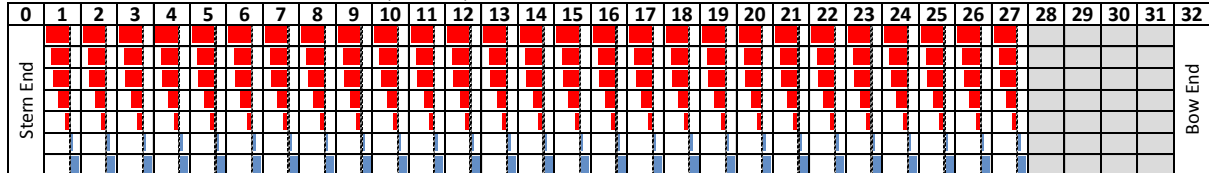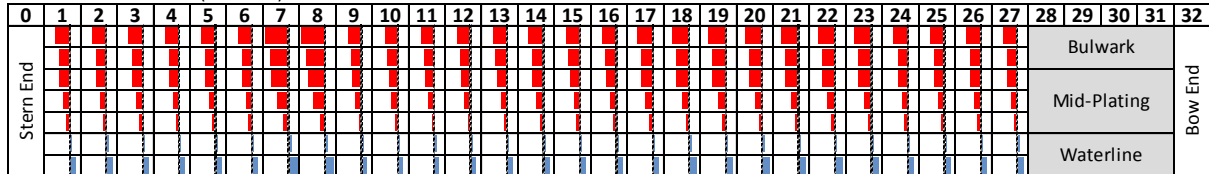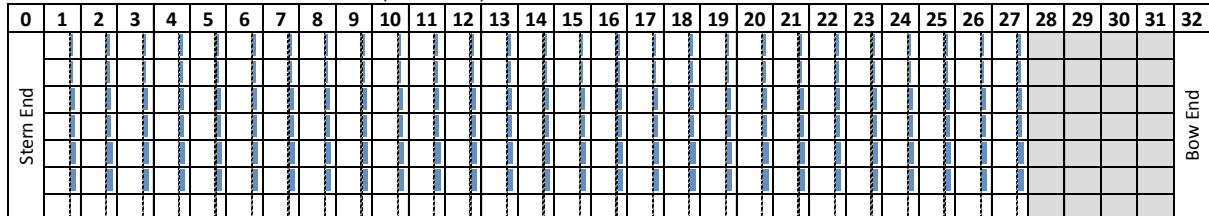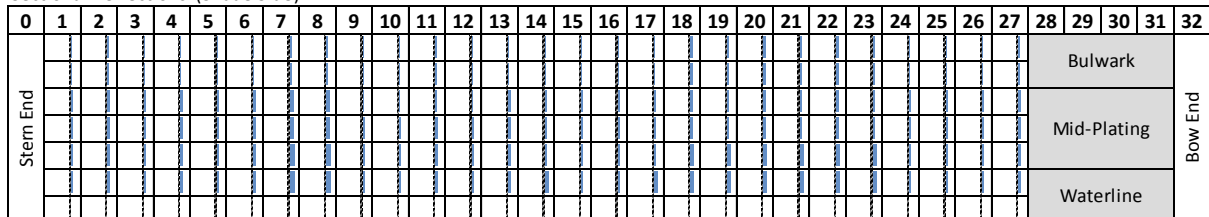
Figure 61: Theoretical estimation of deflection intensity and direction

Thermal stresses in the above model have been calculated with the methods described by (Jasper, 1955) who has idealized the ship as a box-girder and provides methods for calculating the thermal stresses at sections with bulkheads and frames. Portholes have not been modelled but appendix-B of (Hechtman, 1956) provides a method for calculating this. Portholes represent stress concentrations not just structurally but thermally since they have a large thermal gradient around them as explained in in Section 3.4.

Figure 62 shows a FEM vector plot of deflections due to an asymmetrical temperature load on a ship section. The section is an epoxy-aluminium composite and has only temperature loads acting on it. The right side of the section in the figure has been subjected to 60°C while the left is at 10°C, a typical situation in winter. Vectors show the direction and magnitude of deflections. This approach provides a result of 1.5mm of deflection on average on the sun side while shade side is half that. However, while it can compute temperature loads in the vertical and ship interior directions, longitudinal variations are not computed. Any directional temperature distribution will have an impact on structural behaviour and must be evaluated.
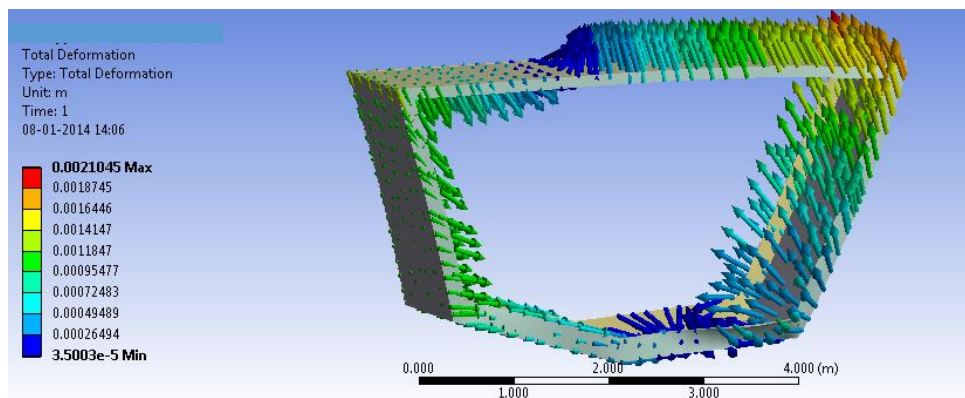
Figure 62: Vector plot of deflections in a ship section subjected to only thermal gradients

7.1.3   FEM Analysis for Future Research

In light of the limitations of a theoretical approach and two-dimensional analysis, the author recommends that an in-depth three-dimensional Finite Element Analysis be carried out on the ship. An FEM analysis will have the following advantages over theoretical modelling:

1. Modelling of solar loads as radiation loads with surface convection properties
2. Material conduction and thermal expansion property variations with temperature
3. Transient analysis as the sun moves over the ship

4. Asymmetric heating of port and starboard sides (the difference reach 50°C in tests)
5. Creep Estimation between different layers

However, the above mentioned advantages will also imply that the FEM analysis must be very carefully carried out. It will be highly complex due to the coupling of thermal and structural loads. In addition, symmetry of structure cannot be used due to the uneven thermal distribution. Solid elements will be needed since the temperature gradient is present longitudinally (from bow to stern), vertically (from bulwark to waterline) and to the interior of the ship.

Therefore, the entire ship should be modelled for a complete analysis. This will mean that the computation time will be intensive and powerful computers will be needed. Also, FEM cannot be carried out without a lot of initial investigations about the structural behaviour under temperatures stresses, which is precisely what this thesis has sought to do.

SINDA 2013, which was launched only recently, is a thermal solver developed by the MSC software company that integrates with PATRAN, and has a unique tool called the Environmental Simulation Module. With this module, it is possible to carry out realistic solar heating simulations on the Earth using the SINDA solver (MSC, 2013). These simulations use a US government worldwide weather database to model realistic terrestrial solar heating, including effects of cloudiness, convection, and both direct & diffuse solar heating. It can be used to calculate annual thermal loads on the ship and also couple it with structural effects due to this solar exposure. Alternatively, ANSYS could be used in a steady-state or transient analysis mode with heat fluxes computed by the theoretical model described in this thesis.

This section has discussed the difficulties associated with theoretical calculation of deformations and the benefits of using FEM as an alternative tool. It would perhaps be a good plan to first perform a ship-scale analysis, idealized as a box girder. By parametrically building the scantling and subject it to thermal loads, deformations on the structure and temperature profiles all over the ship could be determined.

This could then be extended to a ship modelled with actual geometry, by carrying out a design optimization process, which can vary system parameters within constraints of acceptable temperature and deflection. It could be further implemented in evaluating the impact of

proposed solutions on the above parameters. Ship weight and cost could also be evaluated as part of this optimization process.

7.1.3.1 Effect of Creep

One of the assumptions in the beginning of the project was that the cyclic thermal stresses led to a creep phenomenon in the epoxy-aluminium interface. The target ship is nearly 10 years old and bears notable visual deformations even when out of the water and covered from solar radiation exposure (Figure 63). This suggests that creep may have some effect on the structural strength of the yacht hull plating.

Figure 63: Distorted reflection even when the target ship was out of water and in shade

Some research papers (F.S.Jumbo, Ashcroft, & all, 2010) have described detailed FEM and continuum mechanics techniques to analyse thermal residual stresses in epoxy-metal bi-materials. Though they conclude that the effects of creep between the epoxy-metal combination were negligible, the importance of this statement lies in the fact that they conducted experiments on simple plates.

A ship is a combination of plates, frames, stiffeners and bulkheads. When this is subjected to a long term asymmetric heating, there might be a link between creep and deformations in the hull of a motor yacht. Discussions with shipyard personnel have revealed that the target ship did not suffer from such severe deformations, earlier in its lifecycle. When it came to the epoxy-paint interface however, there were severe paint defects seen. This may be due to high temperatures causing the interface to develop high levels of shear stress, forcing the paint to debond from the epoxy and are discussed later in this chapter.

7.1.3.2   Effect of Plate Dimensions

As presented in Figure 60: Theoretically & FEM predicted deflections due to effect of only thermal loads, the effect of increasing the aspect ratio of the plate clearly shows that the longer the length of the plate, and the more square it becomes, the greater the deflection. In fact, FEM results on a plate showed that for large dimension square plates, theoretical calculations are not able to give an accurate prediction of plate deflection under thermal-structural loads.

However, one can still infer that reducing the spacing between longitudinal stiffeners would reduce the plate bending significantly. To reduce the mode shape between bulkheads, an increased web height of both transversal frames and longitudinal stiffeners showed an improvement in the sectional stiffness.

7.1.3.3   Effect of Welding Residual Stresses

Since aluminium welding is a difficult process, a high level of expertise is needed to avoid bad welds, which can lead set up residual stresses. A brief literature review (Matthew Collette, 2012) , (J. Randolph Kissell, 2002) , (Pattee, 1975) reveals that while the yield strength decreases significantly in the Heat-Affected Zone (HAZ), this can be incorporated into the boundary conditions. This is because the edges of the plates are welded to the frames and longitudinals. When exposed to solar radiation induced heating, all metal sections expand and the reduced modulus at the edges will allow the plate to bend in a simply supported mechanism. Further investigation of residual stresses would need a separate in-depth research study.

7.2   Optical Distortion Effects

"Reality is merely an illusion, albeit a very persistent one."   -   Albert Einstein

We have spent several chapters examining the effect of solar radiation, which produces high surface temperatures, leading to thermal expansions and unaesthetic wavy patterns on the hull. However, there is another equally important element. While we have managed to measure and calculate real deflections, it is also very essential to consider *'apparent deflections'*. Apparent deflections are ultimately perceived by our eyes and this section presents a qualitative picture of two optical effects, associated with the perception of deflection.

Figure 64: Surface imperfections can be easily seen in above image where the smooth lines of the mooring lines appear jagged and wavy in the reflections on the yacht's surface

7.2.1   Spherical Mirror Effect

Since motor yachts have highly finished glossy surfaces, these surfaces act like mirrors (Figure 64). In normal conditions, they behave as normal plane mirrors. However, if there are even minor flaws over this profile, they will tend to get exaggerated a lot more, due to the highly reflective surface (Figure 65).
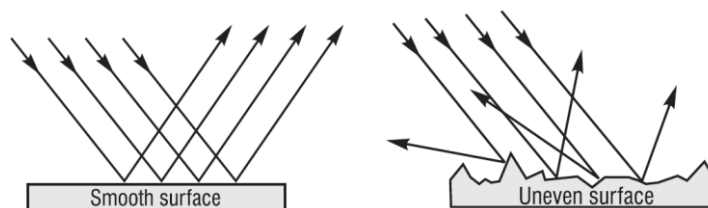
Figure 65: Differences in reflection from a smooth and uneven surface (Pedrotti L. S., 2013)

In fact, due to thermal expansions, when the plate bends between transversal frames, the hull *surface behaves like multiple concave mirrors,* as illustrated in Figure 66.
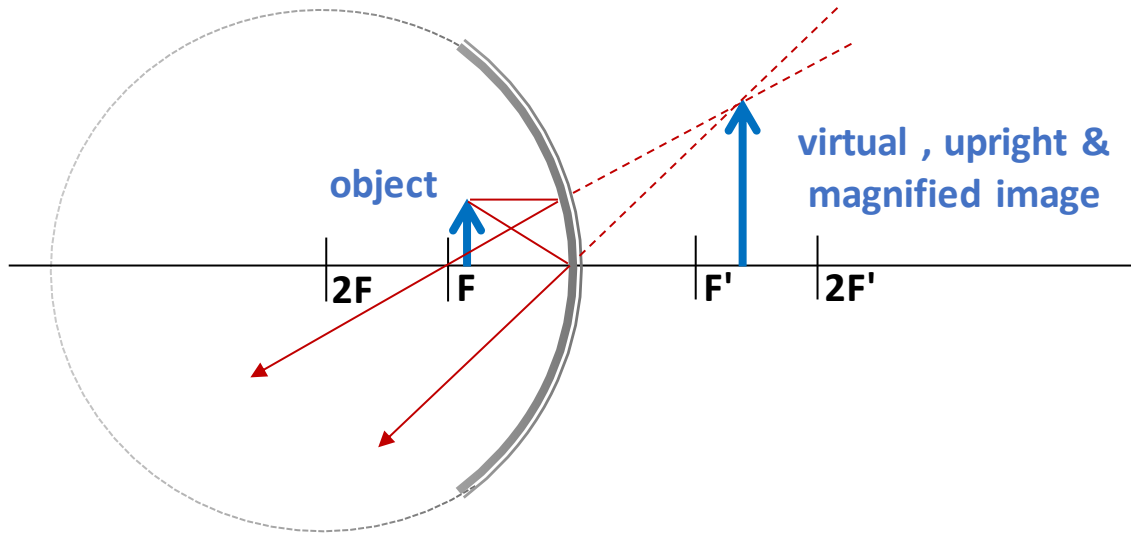
Figure 66: Image showing the working of a spherical mirror

Now a concave mirror always generates a virtual image that magnifies the original object, if the object lies within the focal point. In our case, since the boat's surface is at an angle towards the water, the image of the water close by is reflected off the side of the hull (Figure 67). The higher the plating on the side shell, the further away the wave that is being reflected.
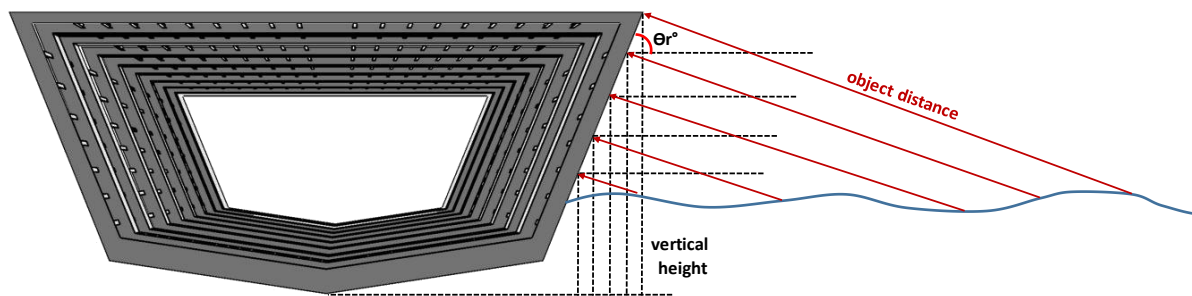
Figure 67: Water reflection off the side of the hull

By knowing the vertical height of the hull surface, we can determine the reflected angle θ_r and calculate the distance of the 'object' that is being reflected, which are water waves in this case.

From the Pythagoras Theorem, we know that the radius of curvature 'R' can be related to the real deflection 'd' and width of the panel 'c' by the geometric relation as shown in Figure 68,

$$R = \frac{c^2 + 4d^2}{8d}$$

(41)
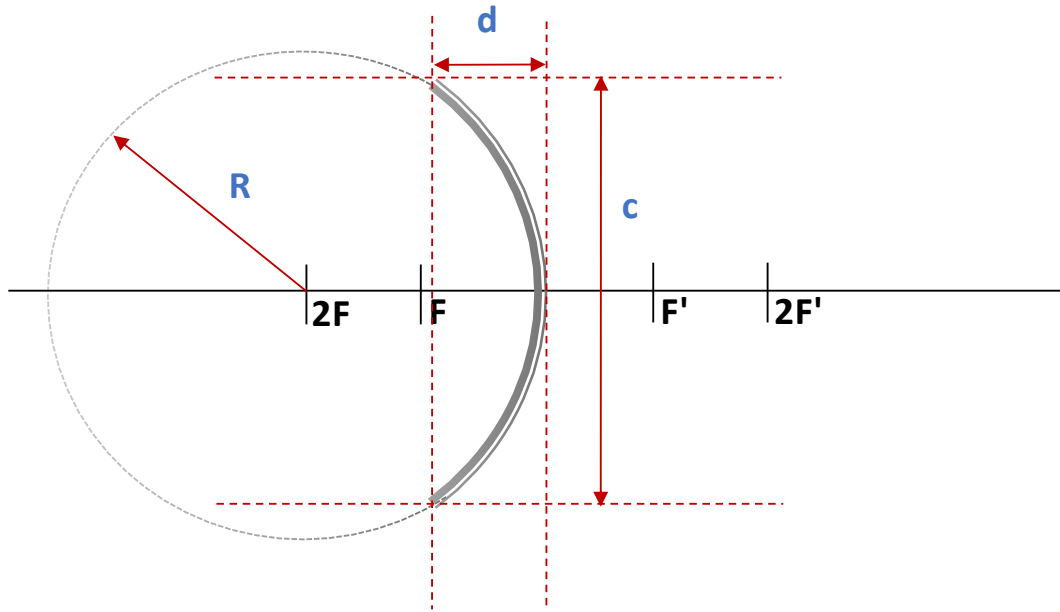
Figure 68: Schematic of a spherical mirror

Once we determine the radius of curvature, the focal length 'f' of the mirror is given by a simple relation,

$$f = \frac{R}{2}$$

(42)

Since object distance is known, the image distance 'd_i' can be calculated by knowing the object distance d_o by the standard Mirror equation,

$$\frac{1}{f} = \frac{1}{d_i} + \frac{1}{d_o}$$

(43)

We also have the magnification ratio M given by,

$$M = \frac{-d_i}{d_o}$$

(44)

To give an idea of the effect of apparent deflection, Table 10 shows a sample calculation for waves i.e. object distance d_o of 5 metres from the hull surface which is reflected in the middle of the plating (about 1.5 metres above the waterline), for a panel width c of 1 metre.

Table 10: Apparent deflection calculations for different values of real deflection

Real Deflection	Radius	Focal Length	Image Distance	Magnification	Apparent Deflection
d	R	f	di	M	d'
[mm]	[mm]	[mm]	[mm]		[mm]
0.0	Infinity	Infinity	Infinity	100%	0.0
1.0	125001	62500	-5435	109%	1.1
2.0	78126	39063	-5734	115%	2.3
3.0	62501	31251	-5952	119%	3.6
4.0	48078	24039	-6313	126%	5.1
5.0	41668	20834	-6579	132%	6.6
6.0	34724	17362	-7022	140%	8.4
7.0	31252	15626	-7353	147%	10.3

As evidently visible, when the radius of curvature R is equal to infinity, it behaves like a plane mirror and there is no magnification. However, the lower the value of R, the greater will be the magnification of the image. Since R is a function of the deflection d of the surface from a flat profile, *the greater the real deflection, the greater will be the 'apparent deflection'*.

Another optical illusion is due to the observer's position. Since the ship can be viewed from different angles and heights, Figure 69 shows a range of object distances based on,

1. Viewing the ship from various possible perspectives - from a range of about 10° - 60° from the stern, and from different distances.
2. A height of 0-3 metres (waterline to bulwark or superstructure level height).

There is also a designated zone given in the figure which suggests a minimum and maximum value based on a typical viewing angle of 30° and a height of 2 metres above the waterline, about 3-5 metres away from the ship.

One can see that, to the observer, the wave reflection seen by surface that is being looked at, shows deflections which are much more pronounced due to the concave mirror effect. This effect diminishes if the ship is looked at perpendicular to the longitudinal axis or parallel to it.
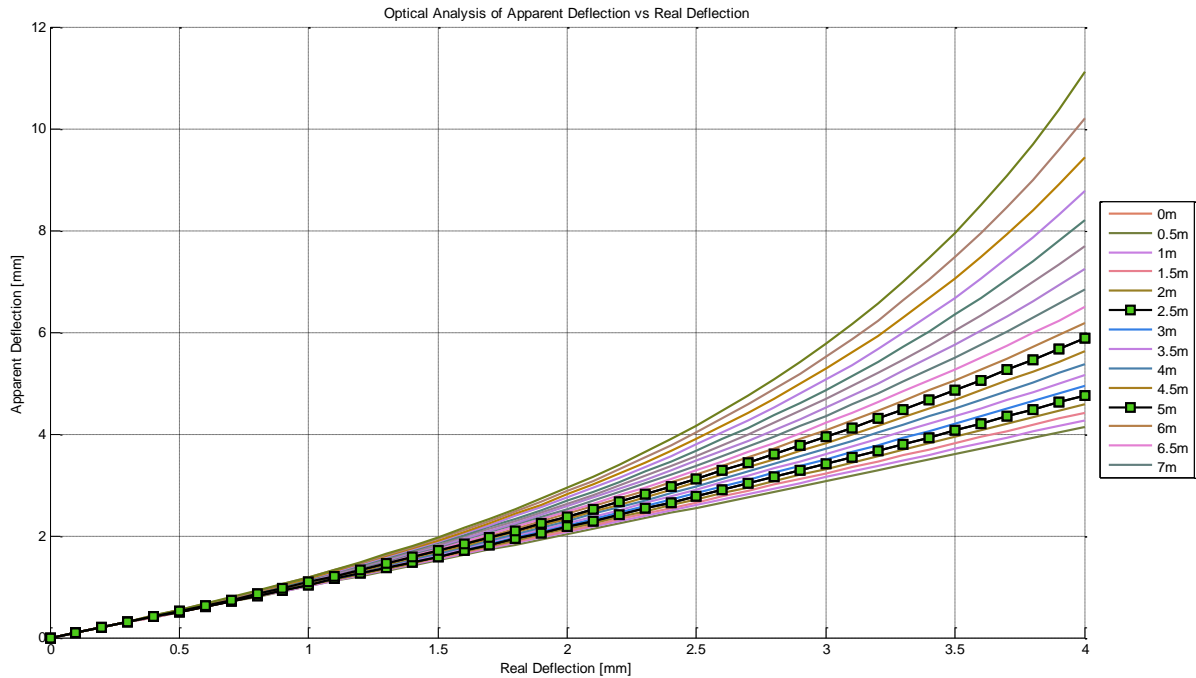
Figure 69: Effect of object distance on the link between real and apparent deflections

From the laws of reflection, we already know that any change in the incidence angle produces twice the change in the reflected angle. For a concave surface, the exit ray angle deviation is different from that of a flat surface. One half of the mirror will increase the exit ray angle while the other half will decrease it by the same amount. Thus, the eyes can visualize 'bands' or waviness along the hull surface very easily (Figure 70).
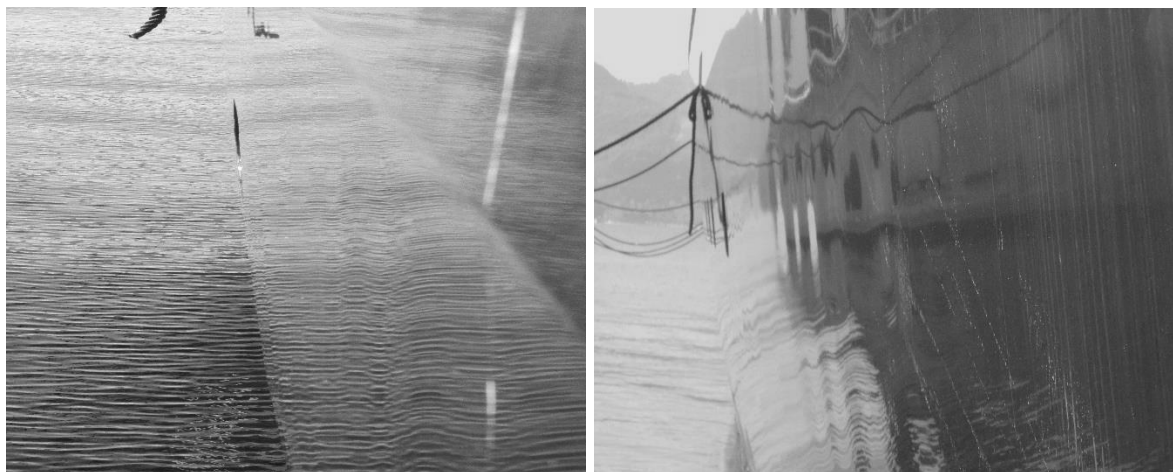
Figure 70: Image showing waviness or "bands" over the same hull surface when seen from two different angles. The distortion of the reflected wave image is also clearly visible

7.2.2   Refraction Effect

Another issue which arises due to the heating of the hull surface is *refraction*. Since the surface temperature of a dark coloured hull can easily reach above 50 degrees, this causes the air immediately in the vicinity of the surface to heat up and expand, causing a boundary layer effect. In this layer, light refracts and bends away from the normal as it passes from a denser layer to a rarer layer. It hits the surface and passes out again to the observer, undergoing another refraction this time bending towards the surface normal. This deviates the reflected ray from the incident ray, which makes reflections on the hull surface look distorted.
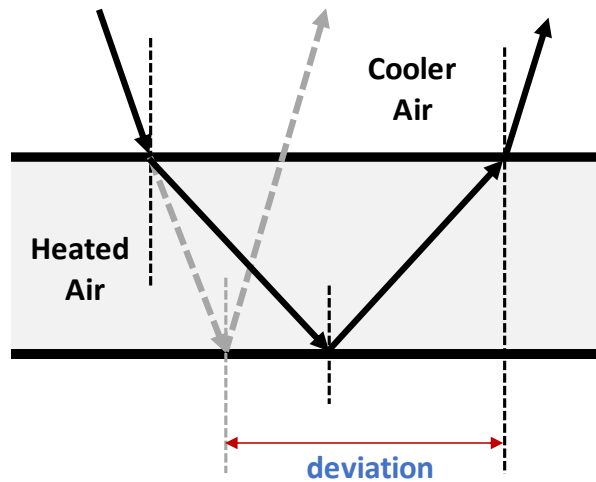
Figure 71: Photo-thermal effect due to refraction

It is understandable that the higher the temperature, the greater will be the heating effect on the air film, increasing the refraction effect.

The human eye can resolve longer wavelength light (1-100mm) from a distance of about 3metres (Kattan, 2009) . At this distance, it is very sensitive to changes in contrast and distortion. From closer distances it can resolve shorter wavelengths of light (0.1-30mm), which allow us to determine whether the surface is dull or brilliant. Thus, even minor defects can be easily spotted by visually.

7.3   Hull Coating Defects

High temperatures over a long time have an adverse effect on the coating surface as seen in Figure 72 and Figure 73. Due to constant expansions and contractions, the paint-epoxy layer is stretched beyond permissible limits and creep at the layer causes the paint to debond. When this happens, the paint either flakes off or loses its shine. Another reason is that if the hull

temperatures become very high, the epoxy or paint can start curing again, causing irreversible damage to the coating surface. In some other cases, if the epoxy is very rigid and does not flex with high temperatures, it can crack, revealing very unpleasant surface defects.

Figure 72: Paint defects due to thermal creep and over-curing in the epoxy-paint layer interface

Figure 73: Paint de-bonding effects due to strong focussing of sunlight on the paint surface

(Kattan, 2009) describes a detailed report on the assessment of yacht coatings. Of the typical faults in coatings, most of them can be attributed to the following causes.

1. Poor vessel design
2. Poor product selection
3. Poor application
4. Poor maintenance
5. Poor climate control
6. Poor worker skill

The discussion of this section is significant because aesthetics has long been the focus of subjective evaluation and detailed solutions have been discussed in Section 8.5.5

7.4   Reduction in Energy Efficiency of Cooling Systems

To calculate energy requirements, it is necessary to determine the amount of energy that must be added or extracted from the space that needs to be heated or cooled. The procedure assumes that the energy required to maintain comfort is only a function of exterior temperature. Since we have already demonstrated a procedure to calculate solar radiation loads in Chapter 5, we can use this to relate paint colour to energy use.

To do this an average value of temperatures will be used to estimate the usage over the year. The second step is to translate this space load on secondary equipment. Thus, this involves the load on the air conditioner, which in turn is supplied electricity by the generator. The last step is to calculate the fuel and energy required to meet both average loads and peak loads.
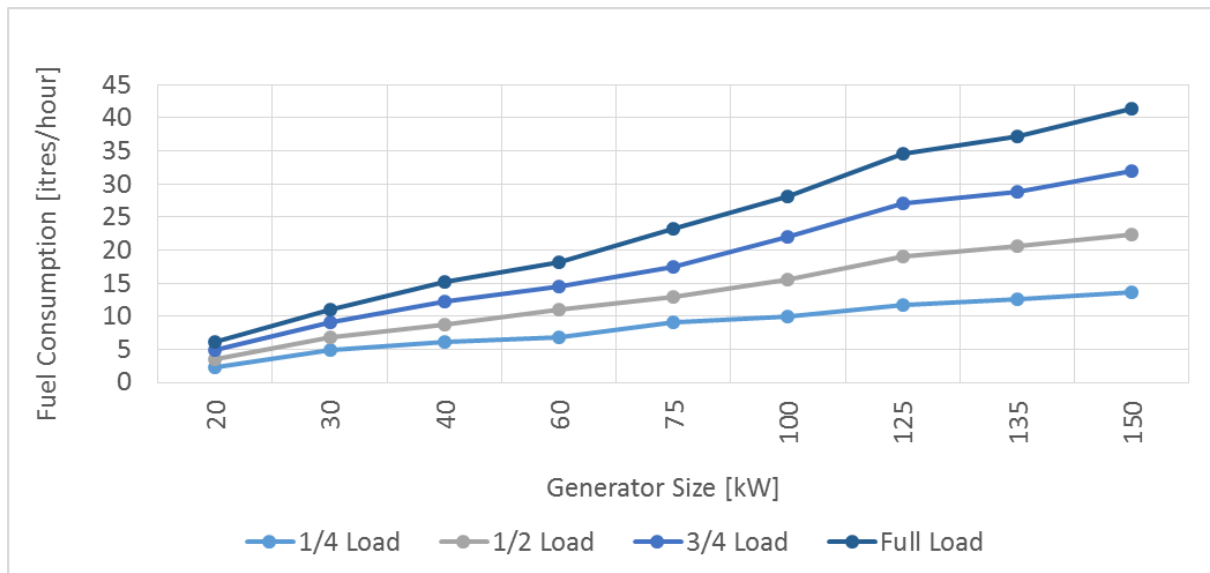
Figure 74: Fuel consumption variation with load (DSS, accessed on 1 Jan 2014)

From Figure 74, it is seen that fuel consumption increases with the load on the generator. On a ship the generator is meant to provide power to a variety of services, however air conditioning loads are the greatest since they have to operate continuously throughout the year.

In the 40-60 metre range, motor yachts typically use 80-125 kW generators. Since cooling loads are proportional to the temperature difference, the maximum difference between white and black hull temperatures is about 50%. This can be approximately calculated to be 5 litres/hour additional fuel consumption for black hulls compared to white, for the same insulation. For 8760 hours of operation in a year (worst case), this would amount to 43,800 additional litres of

fuel a year. This amounts to an extra fuel tank itself. If seen from another perspective, if the ship normally has a range of 700 nautical miles at a cruising speed of 12 knots with a white hull, this would potentially reduce to 650 nautical miles with a black hull.

Effective control of solar radiation is important for energy efficiency because of the high level of internal heat producing devices already present inside the ship. In addition, heat loss takes place through open areas in the superstructure and the hull, at the portholes. Portholes and glass facades should have sun reflecting coats

7.5   Internal Condensation Problems

Moisture inside the ship is a critical issue in corrosion problems involving aluminium hulls. Heat, air and moisture interact in complex ways and these processes together are called hygrothermal processes. Water vapour inside the ship tries to diffuse through conventional insulation and collect in the insulation-aluminium layer.

During sunrise and sunset, when the sun dips below the horizon, there will be a rapid reduction of surface temperature, which will take some time for the air conditioning system to respond to. In this time, condensation can occur in the interstitial layer. This condition would in all probability be amplified for darker colours, since they absorb and emit solar radiation very efficiently. In other words, once the sun sets, black hulls will rapidly lose a large amount of heat, undergoing a large temperature difference.

Moisture could also promote growth of mold that give rise to allergic and asthmatic substances and dust mites. Moisture also degrades the thermal performance of most conventional insulation materials, reducing the energy efficiency.

7.6   Effect on Thermal Comfort

Paint colour has a direct effect on internal ship temperature. Indeed, it is possible to use climate control systems that will maintain equilibrium in temperature and humidity levels. However, these systems will take some time to respond to sudden changes in temperature, seen during sunrise and sunset, and might over compensate with excess heating or cooling. Also, there will be regions of uneven cooling across the ship.

8   DISCUSSIONS AND IMPLEMENTATIONS

"I much prefer to arrive at the wrong solution to the right problem than find the right solution for the wrong problem."

- Peter Drucker, American management consultant, educator, and author

After measuring, modelling and analysing the problem, we have finally arrived at the "problem solving" stage. We know we have a problem and we know the problem needs a solution. With that preamble, this section describes in brief the techniques used to arrive at some solutions to address the issues raised earlier. On no account is this section exhaustive, however it offers a systematic viewpoint of going about conceptualizing, evaluating and implementing solutions.

8.1   Theory of Inventive Problem Solving

Also called TRIZ, this is a systematic and analytical problem solving tool. It is founded on the premise that in any given problem or solution, patterns of technical evolution are repeatable across industries. TRIZ is thus a very large and powerful scientific tool, but to demonstrate its applicability to this problem, only the topics shown in Figure 75 will be covered. This tool was invented by Genrich Altshuller and is based on the study of thousands of patents, which gives it access to a lot of accumulated experience of engineering innovation.
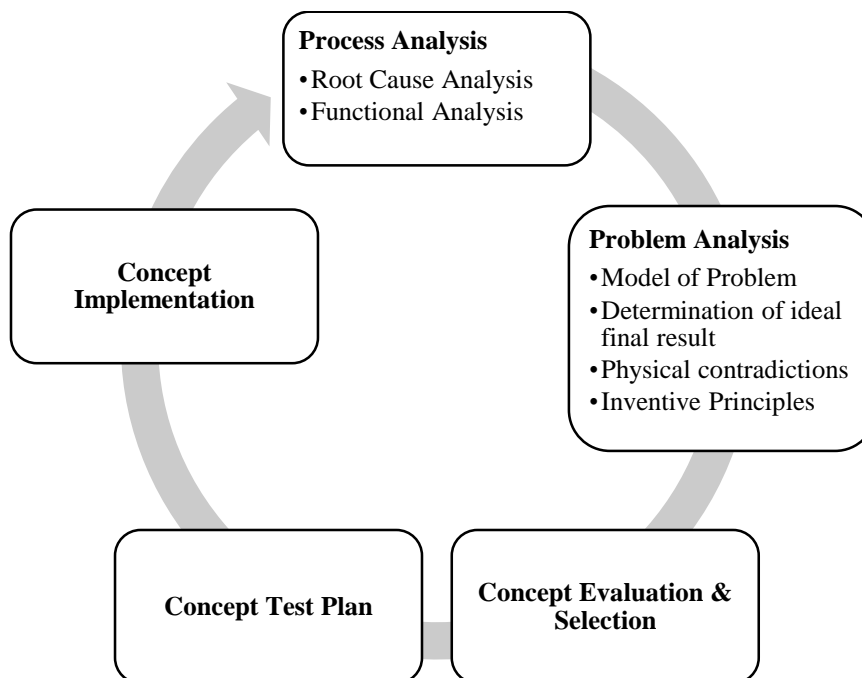
Figure 75: TRIZ Roadmap for problem creation and problem solving

8.2 Process Analysis

SUPER SYSTEM	SYSTEM	SUB SYSTEM
Sun	Paint	Paint Pigment
Atmosphere	Epoxy	Paint Topcoats
Water	Primer	Paint Undercoats
Ship Hull	Metal	Epoxy Fine Layer
Other Ships / Dock	Insulation	Epoxy Coarse Layer
Mooring Fenders	Interior Air	Primer
	Air Conditioner	Stiffners and Panels
	Generator	Insulation Layers
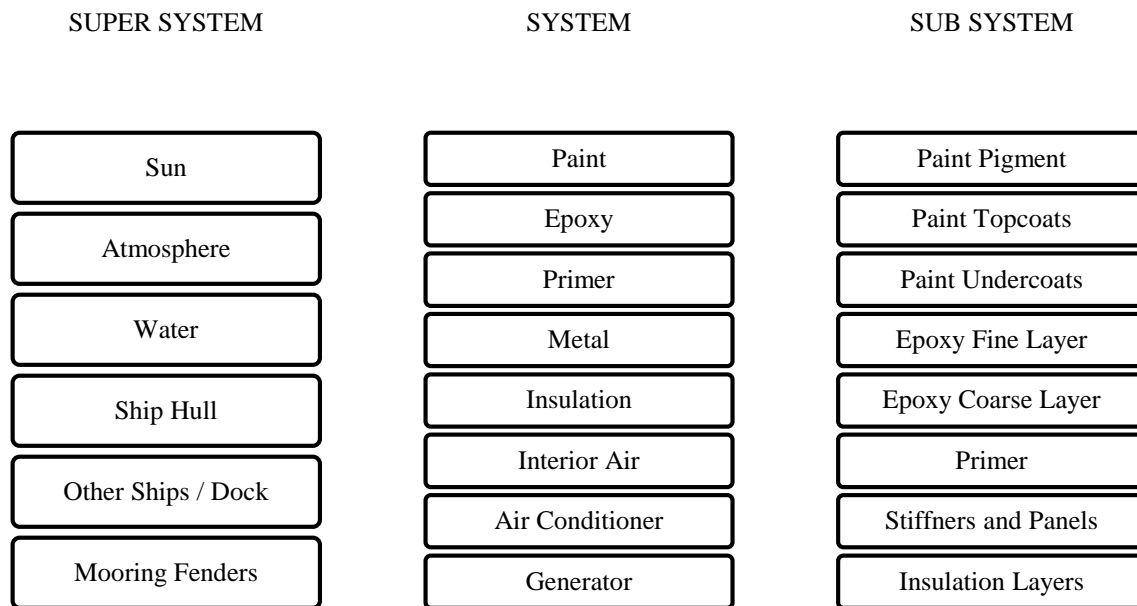
Figure 76: Components defined in the Process Analysis

The process of solar loading on ships can be analysed as shown in Figure 76 depicting the relationship between the super system, system and sub systems. A system is an entity that delivers technical functions, sub-systems are its parts and components, and the super system is the environment surrounding the system. The sun, atmosphere and water act on the paint. The paint-epoxy-metal-insulation form a layered system. Heat conducts through this system and reaches the interior air, which has to be cooled by the air conditioner that is powered by the generator. Other ships and the dock can have a substantial impact on the target ship. At the subsystem level, system macro properties depend on subsystem attributes and they form the parameters that control overall behaviour of the system. (Apte, 2013) and (Salamatov, 2005) can be referred to provide a good introduction to TRIZ and understand the process overview.

8.2.1 Root Cause Analysis

From the analysis carried out in Chapter 6, it is clear that surface temperatures are the primary cause of negative effects such as deflections. For example, structural stresses and thermal stresses act together to produce deflections, as *a function of temperature and local structural stiffness*. The former in turn is due to solar radiation on dark surfaces while the latter is due to

global ship loads. This can be represented in a 'why-why' analysis or a root cause diagram as shown in Figure 77 as an example for aesthetics.

```
                              ┌──────────────────────────┐
                              │   Aesthetics destroyed   │
                              └──────────────────────────┘
                                          │
                              ┌──────────────────────────┐
                              │ Increased visibility of hull
                              │   surface deflections    │
                              └──────────────────────────┘
                                          │
                              ┌──────────────────────────┐
                              │  Uneven surface profile  │
                              └──────────────────────────┘
```

Thermal Expansion of epoxy and metal *(This branch is the same for analysing Increased Cooling Requirement)*	Local loads	Global loads
High thermal expansion levels of material used	Plate expansion restricted at the edges	Hydrostatic loads cause primary stresses
Increase in surface temperatures	Stiffners are rigid	Primary stresses induce secondary and tertiary stresses in the frames and plating.
Increase in absorbtion of solar radiation	Connected to other stiffners and frames	Region between bulkheads behaves like simply supported beams
Choice of dark colour		Region between bulkheads has low stiffness
		Bulkheads stiffer than frames

Figure 77: Root cause analysis of the process

8.2.2 Functional Analysis

Quick solutions like experimenting with the epoxy filler layer thickness or the transverse/longitudinal frame spacing are major decisions and must be weighed well before conceptualizing new solutions. A systematic approach of analysing functions is critical for awareness. Any new solution(s) must continue to perform the original functions, while not hindering the functions of other components in the system. This is briefly shown below.
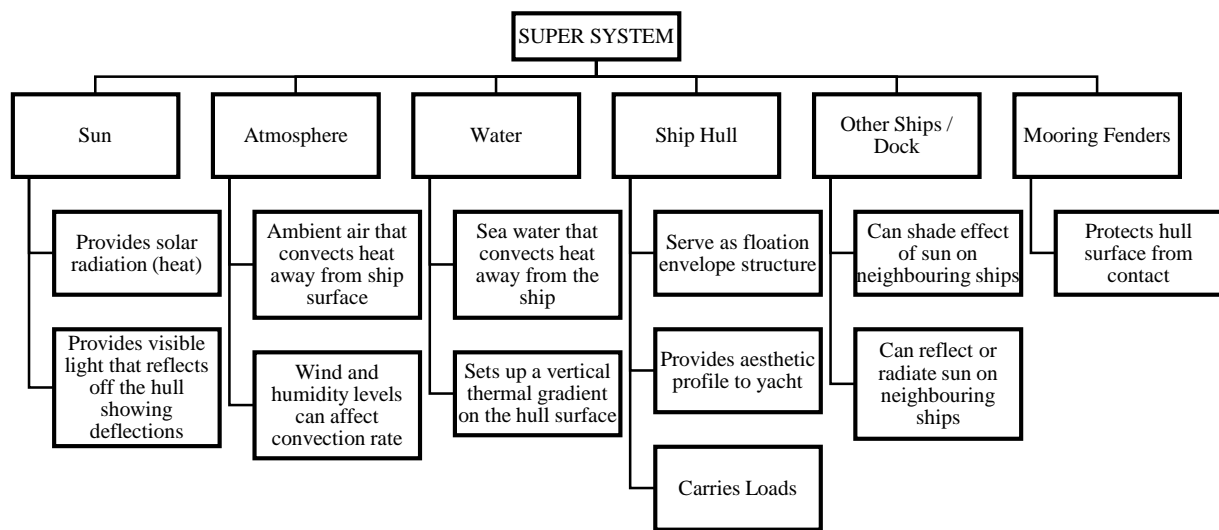
Figure 78: Functional analysis of the super system
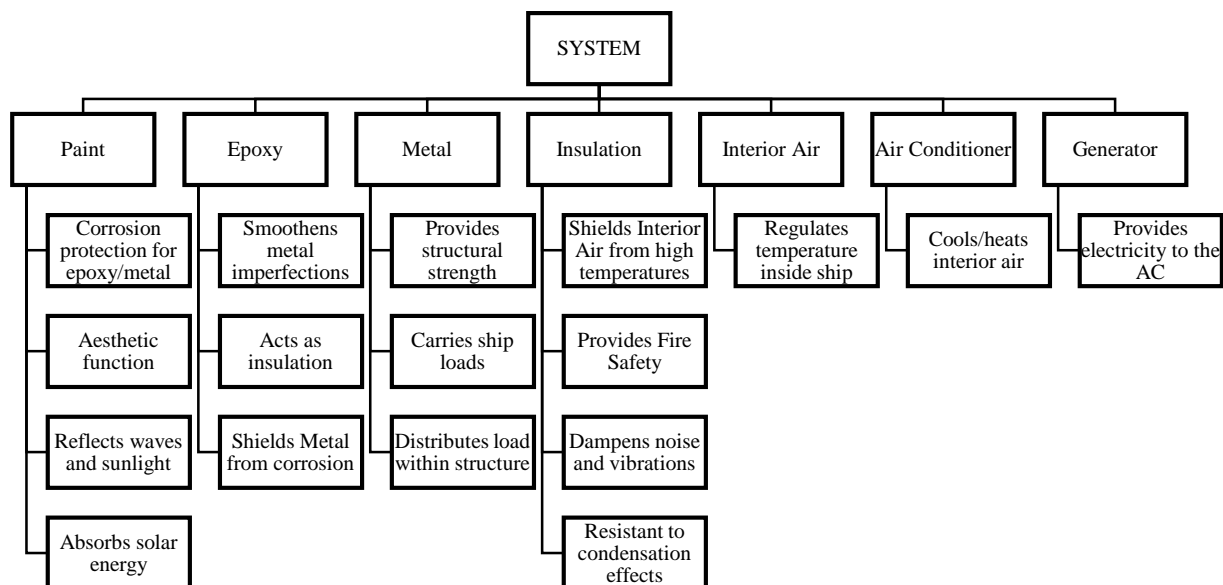
Figure 79: Functional analysis of the system
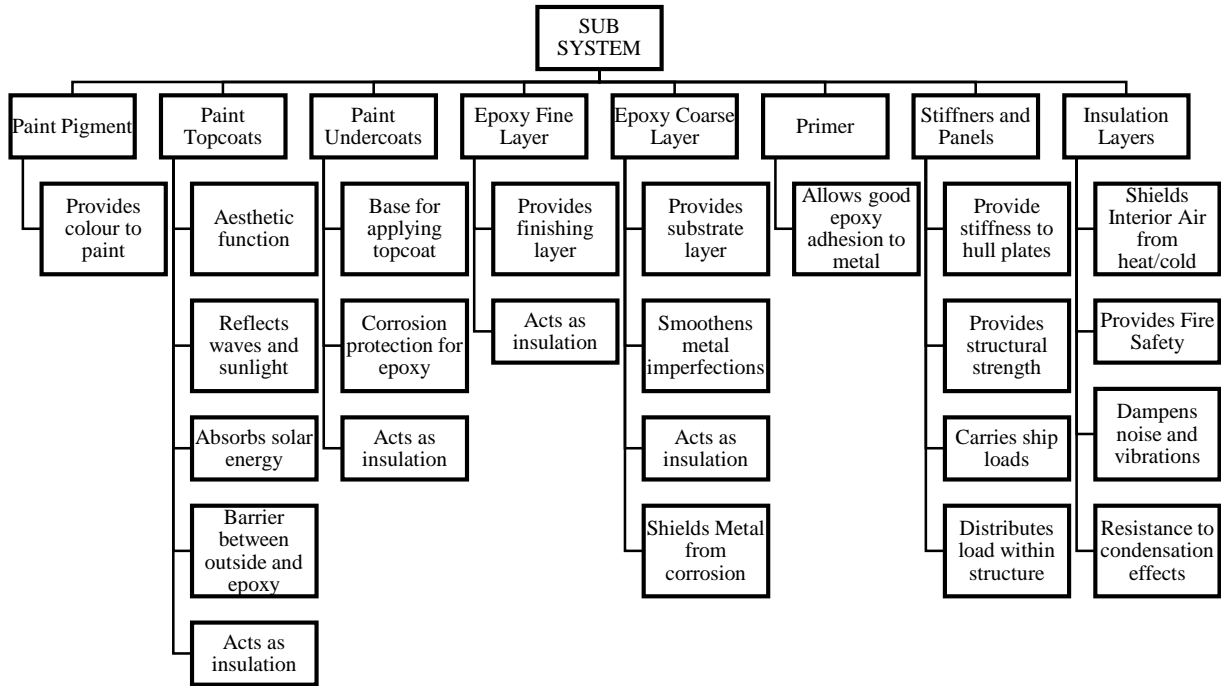
Figure 80: Functional analysis of the sub system

8.3   Problem Analysis

8.3.1   Problem Modelling

Having a black coloured hull and still keeping the hull surface temperatures at the same level as white paint is a technical contradiction. Since the direction from the shipyard is to suggest solutions without involving major changes to the yacht build process, hence this will not involve new system design but instead an *existing system design improvement* of the components described in Figure 76.

8.3.2   Physical Contradictions & Inventive Principles

The process of using TRIZ to generate solutions is described in TABLE 11 below

Table 11: Problem solving process: Applying TRIZ Inventive Principles

Steps	Action	Parameter
Step-1	Identify the contradictions	
Step 2	Look at features in the TRIZ Contradiction Matrix (TrizJournal, accessed on 5 Dec 2013) and identify those important to our consideration	E.g. Black Colour (improves aesthetics) but Heat (worsens)
Step 3	Identify Which Are Improving Features and Which Are Worsening Features	Illumination Intensity (improves aesthetics), Temperature (worsens)

Step 4	Refer to the TRIZ Contradiction Matrix again to learn which of the 40 Inventive Principles may be useful for this problem.	For example, the intersection of Column 18: Illumination intensity and Row 17: Temperature gives the following principles: 32. Colour changes 35. Parameter changes 19. Periodic action
Step 5	Generate Solutions. Repeat process - Select different features and study the matrix for useful principles	These features and principles are described in the next section below

8.4   Concept Evaluation & Selection

Once TRIZ principles are generated, brainstorming by a single person or a cross-functional team of experts can provide many ideas. A technical search combined with studying patent literature can also provide a source of vital clues from other industries. The below table contains a description of solutions generated which are also scored. Higher the score, the more preferred is the solution. Scores are entered as 1,3,7 or 10, 10 being best case and 1 being worst case.

Table 1: TRIZ Principles applied and possible solutions generated

TRIZ principle	Possible Solutions	Time	Cost	Effect	SCORE
1. Black i.e. Colour (improves aesthetics) & Heat (worsens) gives us the intersection of Column 18: Illumination intensity and Row 17: Temperature and gives the following principles:					
32. Colour changes Change the colour of an object or its external environment. Change the transparency of an object or its external environment.	1. Changing the surface texture from glossy to matte may reduce the observability of apparent deflections	7	7	3	147
	2. Instead of black if silver grey is chosen, it is a very good reflector and lies between white and black in terms of surface temperature.	7	7	7	343
35. Parameter changes Change an object's physical state (e.g. to a gas, liquid, or solid.) Change the concentration or consistency. Change the degree of flexibility. Change the temperature.	3. Reducing the thermal expansion properties of the epoxy filler could reduce the bending effects	3	3	3	27
	4. Reducing the epoxy filler thickness could reduce the temperature difference across it and reduce ship weight.	3	7	3	63

19. Periodic action Instead of continuous action, use periodic or pulsating actions. If an action is already periodic, change the periodic magnitude or frequency. Use pauses between impulses to perform a different action.	5. If the ship faces one side all the time, the ship can be turned around periodically so that port and starboard get equally heated, thus reducing the exposure time.	7	7	3	147

2. Temperature (increases) & Stress (worsens) gives us the intersection of Column 17: Temperature and Row 11: Stress or pressure and gives us the following principles:					
2. Taking out Separate an interfering part or property from an object, or single out the only necessary part (or property) of an object.	6. There is a continuous temperature variation throughout the day. Where applicable, if the yacht were lifted out of the water and stored in a covered garage, this could reduce deflections and also prolong coating life	7	7	10	490
	7. Do not berth a black ship in close proximity (5-10) metres next to a white ship or a dark concrete dock as the latter will reflect/radiate additional heat and light onto it and also serve as a visually comparative reference.	3	7	3	63
39. Inert atmosphere Replace a normal environment with an inert one. Add neutral parts, or inert additives to an object.	8. Making the paint reflect only the Infrared component of light while letting visible light by using specific pigments be absorbed could reduce temperatures and still allow black.	7	7	7	343

3. Aesthetics (increases) & Epoxy/metal use (worsens) gives us the intersection of Column 37: Difficulty of detecting and Row 26: Quantity of substance and gives us the following principles:					
3. Local quality Change an object's structure from uniform to non-uniform, change an external environment (or external influence) from uniform to non-uniform. Make each part of an object function in conditions most suitable for its operation. Make each part of an object fulfil a different and useful function.	9. The area in the middle of bulkheads represent stress concentrations and the framing should be made stiffer in this region.	10	7	10	700
	10. The area in the middle of bulkheads represent stress concentrations and the longitudinal stringer spacing should be reduced in this region.	10	7	10	700
	11. The area near the portholes represent stress concentrations and the framing should be made stiffer in this region.	10	7	10	700
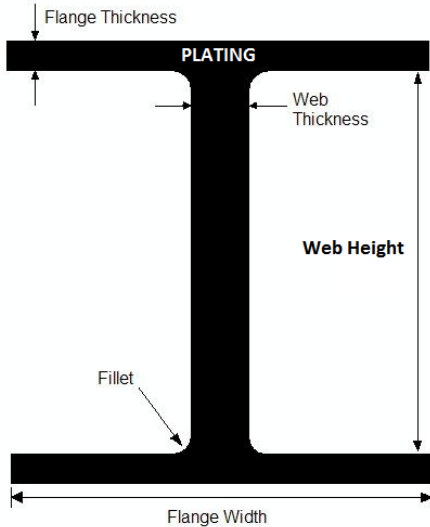
<table>
<tr><td colspan="5">4. Deflection (reduces or improves) & Stresses (worsens) gives us the intersection of Column 12: Shape and Row 11: Stress or pressure of substance and gives us the following principles:</td></tr>
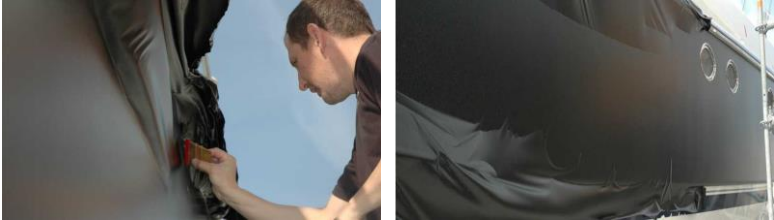</table>

34. Discarding and recovering Make portions of an object that have fulfilled their functions go away (discard by dissolving, evaporating, etc.) or modify these directly during operation. Conversely, restore consumable parts of an object directly in operation.	12. Yachts are left in harbour mainly during the winter months. Thus, solar radiation is high while the ambient water and air temperature is low. Larger and more number of white Mooring Fenders with reflective surfaces can be used to cover the side of the hull exposed to solar radiation.	7	7	7	343
	13. Mooring fenders can be designed to soak up sea water by capillary action using ropes to increase heat removal rate	3	3	7	63
	14. Using vinyl paints as permanent or temporary coatings for aesthetics or topcoat protection, for e.g. White vinyl coating for external storage in winter	7	3	10	210
15. Dynamics Allow (or design) the characteristics of an object, external environment, or process to change to be optimal or to find an optimal operating condition. Divide an object into parts capable of movement relative to each other. If an object (or process) is rigid or inflexible, make it movable or adaptive.	15. If a yacht can be berthed in such a way that it is aligned in the North-South direction, such that the sun hits only the bow or stern region, which have a much smaller area than the side shell, and are also less prone to deflections, this would greatly reduce the visibility of deformations.	7	7	7	343
10. Preliminary action Perform, before it is needed, the required change of an object (either fully or partially). Pre-arrange objects such that they can come into action from the most convenient place and without losing time for their delivery.	16. The application of the epoxy layer is currently done in ambient atmosphere. Use of a climate controlled chamber during epoxy lay-up would prevent thermal expansions during the manufacturing stage itself.	7	3	10	210
14. Spheroidality - Curvature Instead of using rectilinear parts, surfaces, or forms, use curvilinear ones; move from flat surfaces to spherical ones; from parts shaped as a cube (parallelepiped) to ball-shaped structures. Use rollers, balls, spirals, domes. Go from linear to rotary motion, use centrifugal forces.	17. After welding, when the aluminium cools down and contracts, residual stresses are set up in the plating, which cause it to have an initial bend toward the inside. If the plate can be given an initial bend in the opposite direction, and welded, this could cancel out the bending effect.	7	7	7	343

8.5   Concept Test Plan & Implementation

Since motor yachts are luxury symbols which are asserted and advertised by shipyards as a hallmark of achievement, it is evident that any new proposal will have to be thoroughly tested. Such testing can be easy to perform for some of the solutions described and much harder for some others. A test plan for some of the top ranked solutions are described below

Table 12: Test Plan for Selected Concepts

8.5.1 *Solutions to Reduce High Temperatures and Deformations*		
No.	**Solution**	**Implementation Plan**
1	The area in the middle of bulkheads represent stress concentrations and the framing should be made stiffer in this region. (700)	Stiffening the region in the middle of bulkheads, in the middle of the region between the waterline and the deck and in areas with known "hotspots" would be a good remedy for reducing deflections.
2	The area in the middle of bulkheads represent stress concentrations and the framing should be made stiffer in this region. (700)	
3	The area near the portholes represent stress concentrations and the framing should be made stiffer in this region. (700)	One of the best ways to increase the stiffness of a region is to increase the web height in the affected region. Even a 15% increase will increase the moment of inertia by 35% or more. Both the transversal frames and longitudinal stiffeners could be suitably modified. The spacing between longitudinals should also be reduced in the mid-plating region (e.g. from 400 to 300mm), with additional connections between the frames and stiffeners. Such solutions need to be validated by in-depth Finite Element Tools and Experimental observations and model tests.
4	There is a continuous temperature variation throughout the day. If the yacht is not going to be used for several months, where applicable, if the yacht were lifted out of the water and stored in a covered garage, this could reduce deflections and also prolong coating life. (490)		
5	If a yacht can be berthed in such a way that it is aligned in the North-South direction, such that the sun hits only the bow or stern regions, which have a much smaller area than the side shell, and are also less prone to deflections, this would greatly reduce the visibility of deformations. (343)		

5	Making the paint reflect only the Infrared component of light while letting visible light by using specific pigments be absorbed could reduce temperatures. (343)	Low Solar Absorptivity paints that are dark in colour and can still be much cooler than conventional paints of the same colour already exist in the industry today. Mascoat is one such supplier that provides a marine grade thermal insulative paint. While it will still be hotter than white, when compared to conventional black the Mascoat DTM paint (Mascoat, 2013) claims to be 10°C cooler based on a lot of in-house testing on ships. This can have a significant impact on the surface temperature. DuoCoat by DuoMar (DuoMar, 2013) is another alternative. Testing can be in two phases – first a simple laboratory test on a test aluminium panel subjected to heat loads as described in Chapter 4 , and an application on a boat under construction, which can be moved outdoors where it will be exposed to solar radiation. Any one side of the boat can be painted, only in the region between any two bulkheads to ascertain the deflections visually.
6	Instead of black if silver grey is chosen, it is a very good reflector and lies between white and black in terms of surface temperature. (343)	The difference between silver grey and black can be 15°C which is a substantial difference and close to white paint which is about 20°C cooler compared to black. Silver strikes a good balance between aesthetics and manageable surface temperatures. Also, if a two-tone paint scheme or a stripe of a lighter colour can be used in the mid-plating, it could reduce the thermal gradient.
7	Using vinyl paints as permanent or temporary coatings for aesthetics or topcoat protection, or for e.g. White vinyl coating for external storage in winter (210)	Supposing the shipyard decides to only modify the structure while keeping the same paint type (black, white or any colour), it is necessary to test the structure with this paint colour. To paint the whole ship just for a test would take several weeks, and incur huge expenses and intensive labour. An innovative idea could be to use vinyl paints as shown in the images below referenced from (WildGroupInternational, 2013) By applying a black colour vinyl coating even over an undercoat, the effect of solar heating can be quickly assessed. This process of applying vinyl takes about 4 days and can be removed in a day revealing the original paint undamaged underneath – which is an *extremely tedious* job if you try to remove solidified paint. This is not just useful to test the effect of colour, but it can alternatively be applied as a permanent protective barrier over the topcoat or as a quick customization for changing the yacht colour depending on the owner's wishes. It could even be used specifically for outdoor storage in winter when a white or silver coating can be applied to keep the surface cool.

8.5.2   Improving Energy Efficiency

To reduce energy losses, the design process for energy efficient devices must be considered in the beginning of the yacht build project itself. The key components are the heating or cooling loads based on functional areas within the ship, an optimum hull-porthole ratio, and efficient HVAC systems. It would be also a useful approach to benchmark previous ships of different colours and study the below parameters for improving energy efficiency.

1. Minimize ships functional requirements
2. Minimize external and internal loads (paint colour, optimum insulation)
3. Maximize subsystem efficiencies (air conditioner, ducting, generators)
4. Use environmental loads to our advantage (for e.g., dark colours can provide heating during winter)
5. Reuse waste energy from other components such as engine heat
6. Efficient and updated wiring and electrical equipment
7. Minimize impact of heat generating devices by using heat shields, and other confining techniques
8. Separate HVAC systems to address areas with widely different loadings

8.5.3   Reducing Condensation Problems

Condensation problems could be could be alleviated by using special coatings which are applied over all internal aluminium scantlings. They ensure that moisture can never make contact with the bare aluminium hull. In addition, they also provide acoustic and thermal insulation. The Mascoat Marine DTM paint described previously has this feature and can be applied faster than traditional techniques.

8.5.4   Improving Thermal Comfort

For optimum thermal comfort, a detailed calculation must be made for each ship, instead of applying generic rules. This is necessary since a balance is needed between air conditioner equipment and sufficient insulation thickness. The latter is more efficient in retarding large fluctuations in temperature. However, they add to ship weight since they need to be applied over a large area. The air conditioning systems must also be subdivided to cool different areas individually, especially if port and starboard face uneven heating.

8.5.5   Improving Measurement and Assessment of Hull Coatings
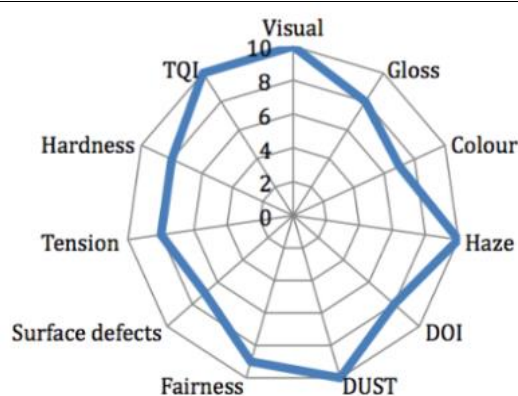
Judging by several efforts to objectify it, there seems to be finally some progress on this front. From the RINA ISO draft on objective evaluation of appearance and BS ISO 11347 (Large yachts. Measurement and analysis of the visual appearance of coatings), there are several proposals presented on different measuring techniques. While experts still haven't agreed to implement all these policies, such standards nevertheless present the shipyard and the owner a common tool for effective measuring techniques for evaluating appearances.

12-point appearance evaluation system ISO draft standard TC 8/ SC 12

The figure above describes a recommended rating system as part of ISO draft (ISO-TC8/SC12). On a scale of 1-10 each parameter is ranked by specialized measuring equipment and a cost is also associated with the finish level. Based on the owner' requirements, an ideal superyacht can have a full 10 point rating on all parameters, or it can have a different combination based on time, budget and agreed levels of quality.

This system might make it possible to define 'beauty' on a project-to-project basis. Since measurement of the above parameters is key to the success of the system, another development called the OFIN Research project (Schneider, 2010) introduces an excellent proposal for objective evaluation of yacht finishes. Alongside old measuring techniques, several new evaluation methods have been suggested.
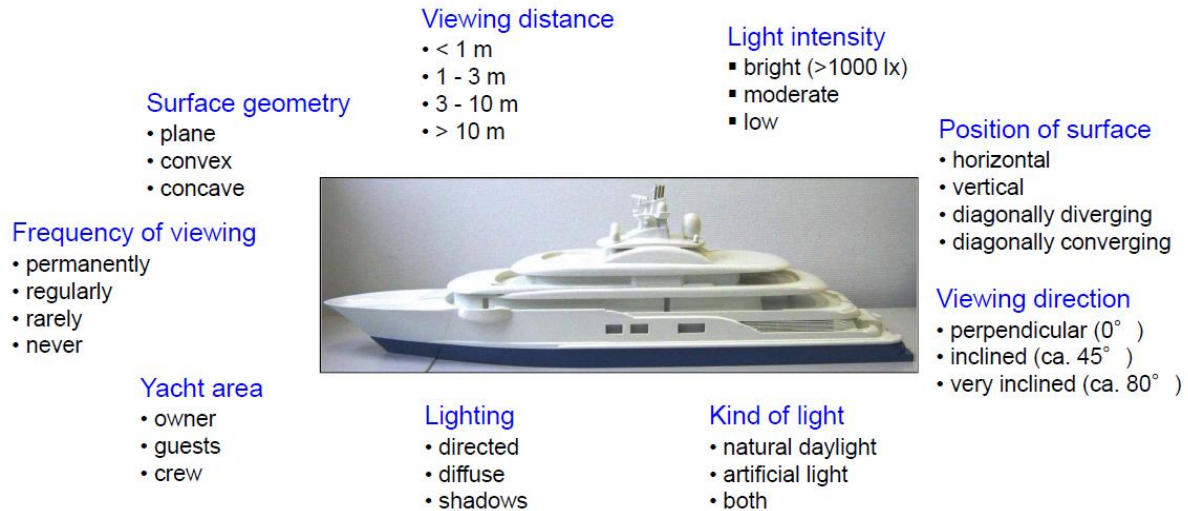
Methods of Evaluation (Schneider, 2010)

One of the many interesting methods is a technique called Defectometry. Initially conceptualized to check paint film levelling and waviness, this technique can be easily adapted for checking deflections and measuring them, by measuring the strip pattern
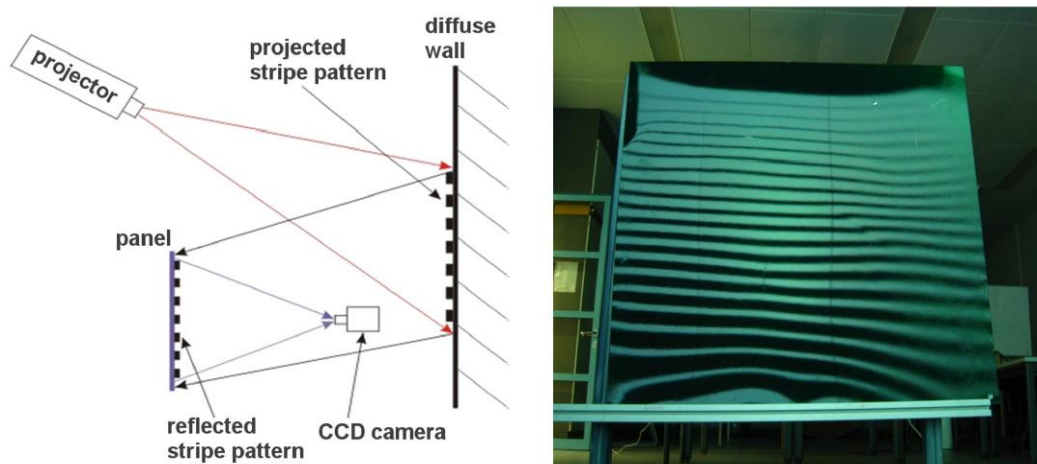
Evaluation of yacht finishes has always been a subject of debate over "*what* is good enough". These new studies and proposals mentioned above are a move in the right direction in the industry, to create an objective understanding of aesthetics. (ISO11347:2012) is a recent standard meant for the assessment of yacht coatings that will hopefully be adopted in the right manner throughout the industry.

9   CONCLUSION

Solar loading in a 6-month period was studied using thermal imaging and a theoretical model was built to simulate the phenomena annually, at any given location in the world. This theoretical model has been quite satisfactory for predicting surface temperatures and has been vital in performing parametric analyses. Without such a parametric analysis, contradictions would have arisen if proposed solutions focussed on only changing one parameter, without studying the effects in other areas. Parameter analysis has further enhanced the understanding of the effect of different variables, such as paint colour, material thicknesses, ship heading etc.

Correlations were made with thermal imaging on the ship, and experimentally on a full scale model plate-panel. This model was found to predict hull surface temperatures quite satisfactorily, and correlates well with actual temperature data measured on the ship. Effects of temperatures on deformations and increased energy consumption for cooling the ship were also evaluated. Deflections have been measured by manual measurements on the ship and analysed theoretically, and with FEM tools. A snapshot of thermal imaging and theoretical predictions made are provided in the figures below.
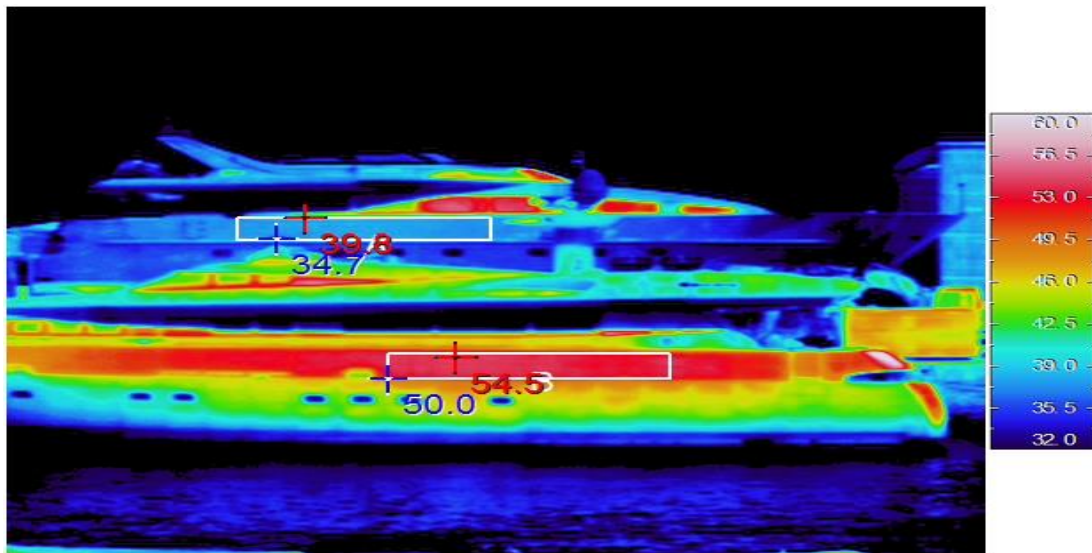
Figure 81: The white ship at 35-40^{0}C is much cooler than the dark-blue ship at 55-60^{0}C even while out of water (windows are ignored since they reflect sunlight and show up as red regions)

Extensive measurements would have been needed throughout the year, in different ship positions for sufficient data. Therefore, specific calculations on Solar Ray Tracing and Classical Heat Transfer theory have been used to create a theoretical model. (Figure 82)
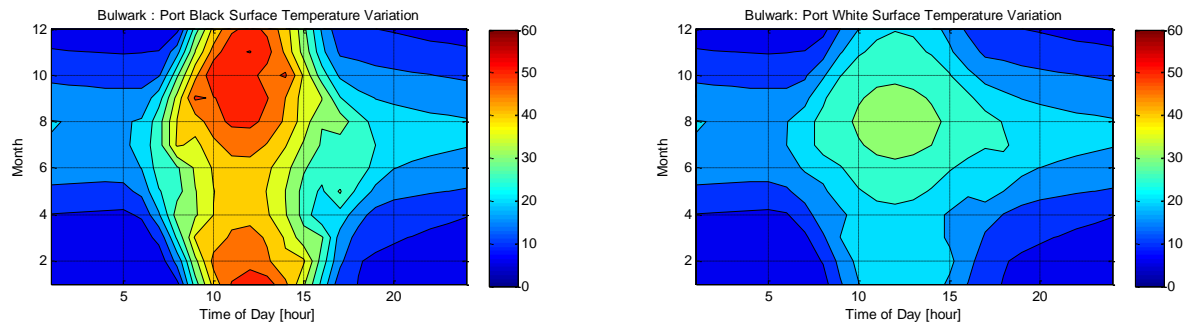
Figure 82: Theoretical prediction of the effect of colour on temperatures (bulwark) over a year

A tabulated summary of results obtained is presented in the table below.

Table 13: Summary of Results

No.	Result
1	Paint colour is the most important parameter effecting temperature. Dark blue or Black hulls are over 20°C hotter than white hulls. They can reach 62°C while white hulls do not exceed 40°C
2	The bulwark is the hottest surface with a linear gradient from the bulwark to the waterline.
3	The ship hull temperatures varies throughout the year, with temperatures reaching a maximum of 54°C in the period from August-December (Figure 82). Winters are slightly hotter than summers since the sun is at a lower elevation and strikes the ship at a more direct angle.
4	Thermal gradients cause expansion of the epoxy-metal bimaterial. Stiffeners restrict the edge movements of the plate but the centre of the plate is free to deform and bends up to 3-4mm on average.
5	It is suggested that hydrostatic loads which cause shear stresses in the side shell are amplified in the presence of thermal stresses resulting in several deflection mode shapes.
6	There exists up to 40°C of difference between port and starboard temperatures. This will cause a lot of uneven expansions and structural issues with areas of stress concentrations.
7	Deflections are seen to be proportional to temperature, with the sun exposed side showing visually detectable deformations in the plate panel between two stiffeners and two frames. The shade side does not suffer from severe deformations but it does have minor defects.
8	It is suggested that creep in the epoxy-aluminium composite plating may possibly take place, since residual deformations were observed even in the absence of solar exposure. This could be the result of long term thermal cyclical loading causing plastic deformations. In addition, it causes the deterioration of the epoxy-paint interface. The test ship was 10 years old.
9	It is estimated that black yachts in the range of 40metres length will consume approximately 5 litres/hour additional fuel compared to white yachts. Consequently, the average range of the yacht could reduce from 700 to 650 nautical miles.
10	Inefficient air conditioning issues and can lead to area with excess cooling, thereby leading to issues like condensation, reduced thermal comfort and increased electricity consumption.
11	Optical issues arise due to deformations over a highly reflective surface such as the hull of a motor yacht. These include irregular reflections and magnifications of surface defects.
12	In conclusion, paint colour leads to high temperatures that leads to a lot of detrimental effects. Several obvious consequences were investigated. Additionally, there can be hidden effects such as the loosening of fasteners due to differential expansion causing increased vibration. It can be extrapolated that these effects have an adverse impact in terms of cost, time and quality.

9.1 Achievements

In the beginning of this project, I was convinced that the application of thermal imaging was vital for this project, and was able to manage it with the help of a specialist who provided it free of cost. It has proved to be an extremely beneficial tool for analysing heating and cooling effects on a ship. Without this, it would have been impossible to make such a large number of measurements in such a short time. Similarly, I have looked at the ASHRAE (2009) solar model that is meant for buildings and have adapted it for ships. I have also built my own model for ship geometry and heat transfer which was coupled to the solar model.

As a result of this research, knowledge of the effects of temperature gradients on the stresses in ship structures is more complete. Design solutions to minimize thermal stresses were developed. Conclusions were drawn on how to restrict the warping distortions of the plating. For generating creative solutions, as a TRIZ Practitioner and with knowledge from my DFSS (Design for Six Sigma) background, I have chosen to apply this tool because it serves the purpose of creating potential design solutions to problems where technical contradictions exist. This was the most appropriate tool for this particular project, where a contradiction between colour and temperature exists. Lastly, it was a rewarding experience to be able to create a quick and simple calculator that will be used as a design reference for naval architects. Future ships in any colour can now be built, with the awareness of associated thermal behaviour.

9.2 Scope of Future Work

A substantial amount of research has been accomplished in the limited time available, yet some future extrapolations of this work can be suggested. The parametric analysis conducted in this thesis can be followed by a multi-objective optimization process. Optimization involves working in a systematic and principled manner to come as close to the ideal operating scenario subject to various constraints imposed on the system. This could be carried out with a detailed thermal-structural analysis, possible only with Finite Element Analysis, unless done with very extensive and expensive experiments. Appendix 7.1.3 lists a brief discussion on this matter.

For more immediate indications of the extreme temperature gradients expected in ships, a project to measure hull temperatures on several ships in services where extreme thermal environments are likely to be encountered, should be carried out. This should also be done in

several locations. Portable thermocouples could be used to obtain temperature data on outside and inside plating where possible. These will allows us to cross check with results from the thermal imaging measurements.

To perform a more in-depth deflection analysis, there were various measuring techniques available. Three-dimensional calculations can be verified by tests carried out on a laid-up ship having strain gauges disposed longitudinally on the hull and on bulkheads, tank ends, and other members. Ideally, 3D scanning techniques will allow robust measurement and analyses.

9.3 Learnings

At the start of any research, goals listed can change over the course of the study. In the end, I was quite satisfied with the way I was able to execute my project plan. In terms of learning, I would say that I have learnt a significant amount about the motor yacht industry and its aspirations balance aesthetics and engineering. This research experience has tremendously improved my knowledge, including research and organizational skills. I have also managed to make reasonable course corrections along the way.

A very large amount of information was necessary to identify long term thermal load behaviour on the ship, and associated structural defects. Consequently, it was not possible to carry out additional detailed analysis with FEM tools in the limited time available. However, important discussions have been made to direct future research using FEM. Several interesting moments also came about during the analysis process. For instance, in the beginning of the project, nobody could have predicted that the target ship was as hot in winter as it was in summer.

Overall, flexibility and course corrections were made at appropriate times during the project. Hopefully now, my work can help future naval architects overcome difficulties associated with dark hulls and owners can be happy with the yachts delivered to them by the shipyard. A change from conservative remedies that are currently being used to more optimized solutions, will enable Baglietto Shipyards to produce superior yachts, with improved aesthetics and engineering. It is hoped that this research project has shown that aesthetics is more than just skin deep.

"It always seems impossible until it's done."

-Nelson Mandela

10 ACKNOWLEDGEMENTS

I would first like to thank my family for standing by me through thick and thin. Their enduring love and presence will always be a source of inspiration.

Joining EMShip has brought with it tremendous learning. This has largely been due to the nature of the course work that stresses on individual thinking and effort. In this regard, this project has been a unique challenge from the outset since it draws on so many diverse engineering fields. Nonetheless, as with the nature of such projects, I have had the pleasure of working with and enjoying the support of some great people. I would like to thank each one of these individuals for their encouragement and contribution.

Steadfast in this regard would be my classmates from EMSHIP, both past and present. It would be fair to say that I have learnt more from them than my books. The same is true of my colleagues at Baglietto. My manager, Mr. Guido Penco would attest to the fact that the wonderful team at Uffico Tecnico Baglietto had a very positive effect on my work and their ship, the 'Revitality", is now quite probably one of the most thermal-imaged motor yachts in the world.

The counsel of my professors has always revitalized my determination to produce a work of quality. Professor Rigo needs special mention for guiding me to EMShip, and Professor Dario Boote for giving me the opportunity to work on such a project. Additionally, I would like to thank the reviewers of this thesis for their valuable inputs.

The author would also like to specially thank Mr. Simeon Simeono, who provided the thermal imaging equipment at no cost and skilfully operated it.

<div align="right">

Vivek Kumar
vivek.kumar.mailbox@gmail.com

</div>

11 REFERENCES

Alavala, C. (2009). *Finite Element Methods : Basic Concepts and Methods.* PHI Learning.

Apte, D. P. (2013). *Introduction to TRIZ.* Retrieved from Innovative Problem Solving: http://www.ee.iitb.ac.in/~apte/CV_PRA_TRIZ_INTRO.htm (accessed on 7 Dec 2013)

ASHRAE. (2009). Climatic Design Information. In ASHRAE, *ASHRAE Handbook-Fundamentals.* ASHRAE.

Beer, F. P. (2012). *Mechanics of Materials, Sixth Edition.* McGraw Hill.

Cengel, Y. (2002). *Heat Transfer, 2nd Edition.* McGraw Hill.

DSS. (accessed on 1 Jan 2014). *Approximate Diesel Fuel Consumption Chart.* Retrieved from http://www.dieselserviceandsupply.com/Diesel_Fuel_Consumption.aspx

DuoMar. (2013). *Thermal Insulating Marine Coating.* Retrieved from DuoMar Progressive Technologies: www.duomar.com (accessed on 14 Sep 2013)

EnergyPlus. (2013). *US Department of Energy - Weather Data - All Regions : Europe WMO Region 6.* Retrieved from EnergyPlus Energy Simulation Software: http://apps1.eere.energy.gov/buildings/energyplus/cfm/weather_data2.cfm/region=6_europe_wmo_region_6 (accessed on 5 Oct 2013)

F.S.Jumbo, Ashcroft, I., & all, e. (2010). Thermal residual stress analysis of epoxy bi-material laminates and bonded joints. *International Journal of Adhesion & Adhesives*, Issue-30 (2010) Pages 523–538.

Farzaneh-Gord, M., & all, e. (2009). *Investigation about the effects of exterior surface paint color on temperature development in above ground pipelines.* Science Direct.

Feng, C., & et all. (2005). *Modeling of long-term creep behavior of structural epoxy adhesives.* International Journal of Adhesion and Adhesives.

Gerard, E. V. (1959). A Long-Range Research Program in Ship Structural Design. *Ship Structures Committee SSC-124*.

Hechtman, R. (1956). *SSC 95 - Thermal Stresses in Ships.* Ship Structures Committee.

ISO11347:2012. (n.d.). *Ships and marine technology - Large yachts - Measurement and assessment of the visual appearance of coatings.* ISO (International Organization for Standardization).

ISO-TC8/SC12. (n.d.). *ISO draft standard TC 8/SC12.* International Standards Organization (ISO).

J. Randolph Kissell, R. L. (2002). *Aluminium Structures - A Guide to Their Specifications and Design, Second Edition.* John Wiley and Sons Inc.

J. Randolph Kissell, R. L. (2002). *Aluminium Structures : A Guide to their specifications and design.* John Wiley and Sons Incorporated.

Jasper, N. H. (1955). *Temperature-Induced Stresses in Beams and Ships.* Washington DC: Navy Department, David Taylor Model Basin.

Kattan, D. R. (2009). *Assesing Yacht Coatings.* Safinah Limited.

Krieth, F., Manglik, R., & Bohn, M. (2011). *Principles of Heat Transfer, 7th Edition.* Colarado: Cengage Learning.

Lyman, P., & Meriam, J. (1964). *SSC 152 - Temperature Distribution and Thermal Stresses.* Ship Structures Committee.

Mascoat. (2013). *Mascoat Marine DTM Paint Internal Report.* Meeting with Mascoat Supplier.

Matthew Collette, R. S. (2012). *Aluminum Ship Structures.* University of Michigan.

MeteoSpezia. (2013, Aug 21). *Meteorologial Weather Station website, La Spezia.* Retrieved from http://www.meteospezia.it/index.html

MeteoSpezia. (2013, 8 28). *MeteoSpezia*. Retrieved from
        http://www.meteospezia.it/riepiloghi.html

Moatsos Ioannis, P. K. (2004). *Structural Reliability Framework for FPSOs/FSUs.*
        Universities of Glasgow and Strathclyde.

MSC. (2013, Oct). *SINDA Release Guides*. Retrieved from
        http://simcompanion.mscsoftware.com/infocenter/index?page=content&id=DOC1047
        5&actp=LIST (accessed on 17 July 2013)

Naraghi, M. H., & Harant, A. (2013). *ASME Digital Collection - Journal of Solar Energy
        Engineering | Volume 135 | Issue 1*. Retrieved from Configuration of Building Façade
        Surface for Seasonal Selectiveness of Solar Irradiation—Absorption and Reflection:
        http://solarenergyengineering.asmedigitalcollection.asme.org/article.aspx?articleid=16
        62243

Paoli, A., Razionale, A., & Saba, D. (2011). *Automation of the finishing process of steel yacht
        hulls based on optical scanning*. Venice, Italy: Proceedings of the IMProVe 2011,
        International conference on Innovative Methods in Product Design.

Pattee, F. M. (1975). *Buckling Distortion of Thin Aluminium Plates during Welding*.
        Massachusets Institute of Technology.

Pedrotti, L. (2013). *Fundamentals of Photonics - Basic Geometrical Optics.* Retrieved from
        SPIE: http://spie.org/x17229.xml

Pedrotti, L. S. (2013). *Fundamentals of Photonics - Basic Geometrical Optics.* Retrieved
        from International Society for Optics and Photonics: http://spie.org/x17229.xml

Rigo, P., & Rizzuto, E. (2002). Analysis and Design of Ship Structure. *SNAME, Ship Design
        and Construction*, Chapter 18, 18-16.

Salamatov, Y. (2005). *TRIZ: The Right Solution at the Right Time : A Guide to Innovative
        Problem Solving.* Krasnoyarsk, Russia: Institute of Innovative Design.

Schneider, M. (2010). *Objective Evaluation of the Visual Assessment of Yacht Finishes.*
        Coating Technology Division, Fraunhofer IPA, Stuttgart: Franuhofer (Joint research
        project OFIN).

ShipStructureCommittee. (2007). *Aluminium Struture Design and Fabrication Guide, SSC-
        452, Section B-8-27.* Ship Structure Committee.

TheEngineeringToolbox. (accessed on 07 June 2013). *Absorbed Solar Radiation*. Retrieved
        from The Engineering Toolbox: http://www.engineeringtoolbox.com/solar-radiation-
        absorbed-materials-d_1568.html

Timoshekno, S. (1987). *Theory of Plates and Shells.* Stanford University: McGraw Hill Book
        Company.

TrizJournal. (accessed on 5 Dec 2013). *Interactive TRIZ Matrix & 40 Principles*. Retrieved
        from http://www.triz40.com/

UniversityofOregon. (2013). *University of Oregon - Solar Calculations*. Retrieved from
        University of Oregon - Solar Calculations:
        http://solardat.uoregon.edu/SunChartProgram.html (accessed on 12 Oct 2013)

WildGroupInternational. (2013). *Vinyl Surface Protection*. Retrieved from Wild Group
        International: http://wildgroupinternational.com/Case-Studies (accessed on 2 Oct
        2013)

Zubaly, R. (1973). Thermal Gradients and Stresses. Part-2, Section-5, P133, P200.

APPENDIX

1 Correlation between Thermal Imaging and Theoretical Modelling

In the first part, the analysis of a dark blue ship in water and a white ship on land has been made. The second deals with the comparison of the same dark blue ship, a different white ship and a grey ship. The data below summarizes the temperatures measured.

Table 14: Comparison between thermal imaging and theoretical modelled temperatures

August Measurement & Modelling Comparison

Dark-Blue Ship / Port Side (sun side)

Thermal Imaging Results							Theoretical Model Results							Error %						
	Panel Node Designation								**Panel Node Designation**							**Panel Node Designation**					
	1-2	2-3	3-4	4-5	5-6	6-7			1-2	2-3	3-4	4-5	5-6	6-7		1-2	2-3	3-4	4-5	5-6	6-7
8	25	25	25	25	25	25		8	40	39	39	39	38	37	8	-62%	-57%	-55%	-55%	-52%	-49%
9	35	32	31	30	28	28		9	42	39	38	38	37	35	9	-21%	-22%	-22%	-25%	-30%	-24%
10	47	42	40	39	37	35		10	48	44	42	42	40	38	10	-2%	-4%	-5%	-7%	-9%	-8%
11	50	48	45	44	40	35		11	51	46	44	44	42	39	11	-2%	4%	2%	0%	-6%	-13%
12	54	51	48	44	40	35		12	51	46	44	44	42	39	12	5%	10%	9%	1%	-5%	-11%
13	52	47	45	44	40	35		13	49	43	41	41	40	37	13	6%	8%	8%	6%	1%	-5%
14	46	42	40	39	36	34		14	44	39	37	37	36	33	14	4%	7%	6%	4%	0%	2%
15	40	36	34	33	32	31		15	38	34	32	32	31	30	15	6%	7%	5%	3%	3%	4%
16	35	32	32	31	30	28		16	30	29	29	29	29	28	16	13%	10%	10%	7%	5%	-1%
17	33	32	32	31	30	28		17	33	34	34	34	34	34	17	0%	-5%	-6%	-9%	-12%	-21%
18	32	31	31	30	29	27		18	27	27	27	27	27	27	18	16%	12%	12%	9%	6%	-1%

(Time of Day shown along left axis of each grid)

Both the thermal imaging and theoretical models show good correlation with an average of 6-8% error. This is excluding the region around 0800h where there is a big difference due to the fact that the ship is surrounded by buildings and natural hilly terrain, and the sun strikes the ship only after reaching a sufficient altitude.
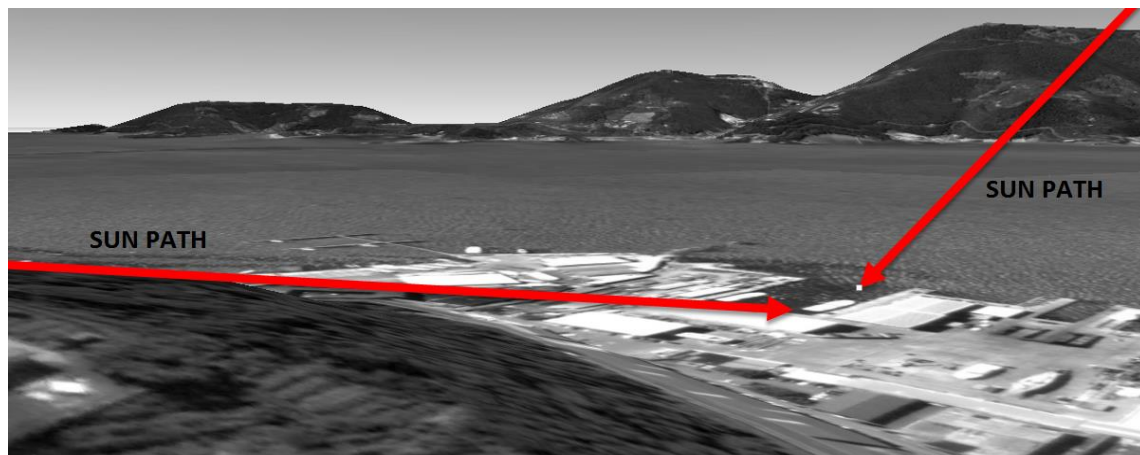

A similar situation is seen at 1700h-1800h where the low sun is blocked out by above hills. To keep in mind is that at very low sun angles, the water surface reflects much more sunlight onto the ship and the temperature can suddenly increase. This causes the sudden appearance of deflections, also manifesting as distorted reflections on the hull.

Dark-Blue Ship / Starboard Side (shade side)

Thermal Imaging Results	Theoretical Model Results	Error %

Thermal Imaging Results

Time of Day	Panel Node Designation					
	1-2	2-3	3-4	4-5	5-6	6-7
8	24	24	24	24	24	24
9	27	26	26	26	25	24
10	30	28	28	27	27	26
11	31	30	29	28	28	27
12	32	31	30	29	28	28
13	33	32	30	30	30	29
14	32	30	30	29	28	28
15	31	30	28	28	27	27
16	32	30	28	28	27	27
17	33	30	28	28	27	27
18	36	33	31	30	28	28

Theoretical Model Results

Time of Day	Panel Node Designation					
	1-2	2-3	3-4	4-5	5-6	6-7
8	30	31	31	31	31	31
9	26	26	26	26	26	26
10	27	27	27	27	27	27
11	28	29	29	28	28	28
12	29	29	29	29	29	29
13	30	30	30	30	30	29
14	30	30	30	30	30	29
15	29	29	29	29	29	29
16	29	29	29	29	28	28
17	37	36	36	36	35	34
18	33	33	32	32	32	31

Error %

Time of Day	Panel Node Designation					
	1-2	2-3	3-4	4-5	5-6	6-7
8	-24%	-28%	-29%	-29%	-29%	-30%
9	5%	1%	1%	1%	-3%	-7%
10	9%	2%	3%	-1%	-1%	-4%
11	8%	5%	2%	-2%	-1%	-5%
12	9%	5%	2%	-1%	-4%	-4%
13	10%	7%	1%	1%	2%	-2%
14	7%	1%	1%	-2%	-6%	-5%
15	5%	2%	-5%	-5%	-8%	-8%
16	10%	4%	-2%	-2%	-5%	-5%
17	-12%	-20%	-27%	-27%	-30%	-28%
18	8%	1%	-4%	-7%	-14%	-12%

There is good correlation here with an average error of 5% except at 0800h and 1700h due to reasons already listed above. The bulwark (Nodes 1-2) is also seen to be hotter than predicted. This maybe because the ship is moored alongside a concrete dock which could be reflecting and radiating heat at the upper parts of the ship. This is quite apparent in the image below.
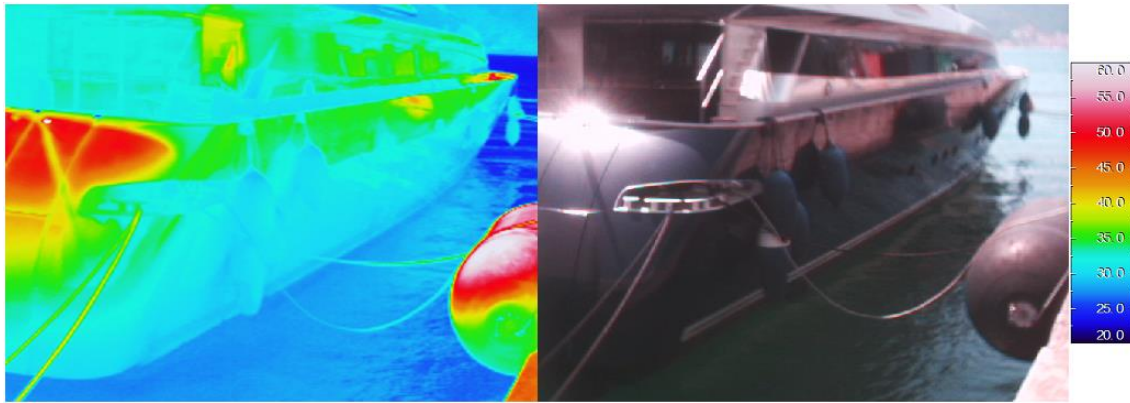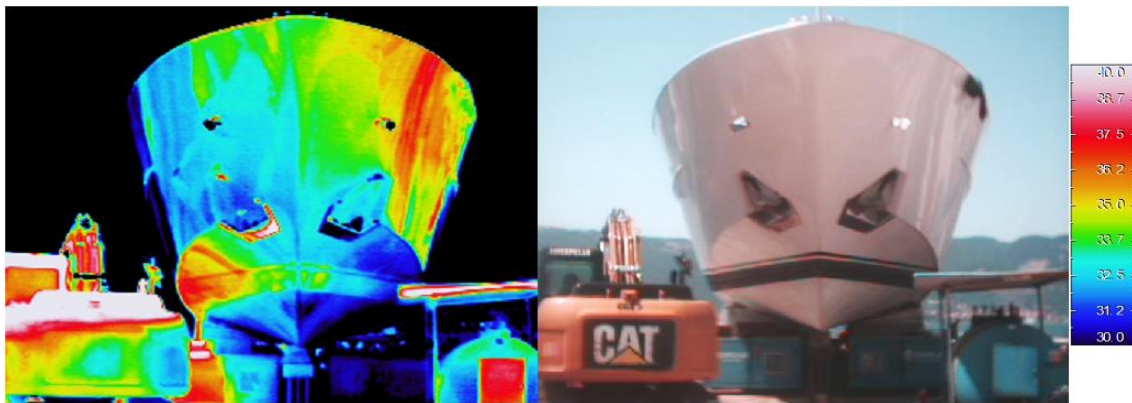

White Ship / Starboard Side (sun side)

Thermal Imaging Results	Theoretical Model Results	Error %

Thermal Imaging Results

Time of Day	Panel Node Designation					
	1-2	2-3	3-4	4-5	5-6	6-7
8	25	25	25	25	25	25
9	29	29	29	29	29	29
10	34	33	33	33	33	33
11	35	34	34	34	34	34
12	37	36	36	36	36	36
13	36	35	35	35	35	35
14	na	na	na	na	na	na
15	na	na	na	na	na	na
16	na	na	na	na	na	na
17	na	na	na	na	na	na
18	na	na	na	na	na	na

Theoretical Model Results

Time of Day	Panel Node Designation					
	1-2	2-3	3-4	4-5	5-6	6-7
8	31	31	30	30	30	30
9	33	31	30	30	30	29
10	36	34	33	33	32	31
11	38	36	35	34	34	32
12	39	36	35	35	34	32
13	38	35	34	34	33	31
14	35	33	32	32	31	29
15	32	30	29	29	28	27
16	28	27	27	27	27	27
17	29	29	29	29	29	29
18	25	26	26	26	25	26

Error %

Time of Day	Panel Node Designation					
	1-2	2-3	3-4	4-5	5-6	6-7
8	-25%	-23%	-22%	-21%	-20%	-18%
9	-13%	-7%	-5%	-4%	-2%	1%
10	-7%	-3%	0%	0%	2%	6%
11	-10%	-5%	-2%	-1%	1%	6%
12	-5%	1%	4%	4%	6%	11%
13	-5%	1%	4%	4%	7%	11%
14	#####	#####	#####	#####	#####	#####
15	#####	#####	#####	#####	#####	#####
16	#####	#####	#####	#####	#####	#####
17	#####	#####	#####	#####	#####	#####
18	#####	#####	#####	#####	#####	#####

This model correlates very well with an average error of less than 5% with the exception of 0800h readings. The bulwark is a bit hotter than predicted. This maybe because in the theoretical model the same ship geometry of the dark-blue ship was used for the white ship which might be different for the bulwark.

White Ship / Port Side   (shade side)

Thermal Imaging Results	Theoretical Model Results	Error %

Thermal Imaging Results

Time of Day	1-2	2-3	3-4	4-5	5-6	6-7
8	24	24	24	24	24	24
9	26	26	26	26	26	26
10	28	28	28	28	28	28
11	30	30	30	30	30	30
12	31	31	31	31	31	31
13	32	32	32	32	32	32
14	na	na	na	na	na	na
15	na	na	na	na	na	na
16	na	na	na	na	na	na
17	na	na	na	na	na	na
18	na	na	na	na	na	na

Theoretical Model Results

Time of Day	1-2	2-3	3-4	4-5	5-6	6-7
8	26	26	26	26	26	26
9	24	24	24	24	24	24
10	25	25	25	25	25	25
11	26	26	26	26	26	26
12	27	27	27	27	27	27
13	27	27	27	27	27	27
14	28	28	28	27	27	27
15	27	27	27	27	27	27
16	27	27	27	27	27	27
17	31	31	30	30	30	30
18	29	28	28	28	28	28

Error %

Time of Day	1-2	2-3	3-4	4-5	5-6	6-7
8	-7%	-9%	-9%	-9%	-9%	-10%
9	8%	8%	8%	8%	8%	8%
10	10%	10%	10%	10%	10%	10%
11	13%	12%	12%	13%	13%	13%
12	13%	13%	13%	13%	13%	14%
13	15%	14%	14%	15%	15%	15%
14	#####	#####	#####	#####	#####	#####
15	#####	#####	#####	#####	#####	#####
16	#####	#####	#####	#####	#####	#####
17	#####	#####	#####	#####	#####	#####
18	#####	#####	#####	#####	#####	#####

The thermal imaging of the white ship on the port side shows significant differences with the theoretical model. This can be attributed to the fact the white was not on water but on land, where ground reflectance was much more due to the concrete floor. Thus, the hull temperatures were higher and there is an average error of 10-12%. This is clearly seen in the image below where although the sun is on starboard (left side in this image), port (right side in this image) is hotter

November Measurement & Modelling Comparison

Dark-Blue Ship / Port Side (sun side)

Thermal Imaging Results	Theoretical Model Results	Error %

Thermal Imaging Results

Time of Day	1-2	2-3	3-4	4-5	5-6	6-7
9	35	32	28	26	24	23
10	46	42	41	38	35	26
11	54	50	46	42	40	28
12	56	54	50	48	40	26

Theoretical Model Results (THM)

Time of Day	1-2	2-3	3-4	4-5	5-6	6-7
9	34	33	33	32	32	31
10	46	44	43	43	42	41
11	53	51	50	50	48	47
12	54	52	51	51	50	48

Error %

Time of Day	1-2	2-3	3-4	4-5	5-6	6-7
9	3%	-4%	-16%	-25%	-32%	-34%
10	0%	-6%	-6%	-14%	-21%	-57%
11	3%	-2%	-8%	-18%	-21%	-66%
12	3%	3%	-2%	-6%	-24%	-84%

For the same ship compared in November, the correlation still holds well, with an average error of about -5%. There is however a difference seen in node positions 4-7. This is probably due to the fact that the ship was moved to a different quay where sunlight was unable to reach the bottom parts of the hull and an overhead crane cast a shadow on several parts of the ship.

Dark-Blue Ship / Starboard Side (shade side)

Thermal Imaging Results	Theoretical Model Results	Error %

Thermal Imaging Results

Time of Day	1-2	2-3	3-4	4-5	5-6	6-7
9	11	11	11	11	11	11
10	15	15	15	15	15	15
11	15	15	15	15	15	15
12	14	14	14	14	14	14

Theoretical Model Results

Time of Day	1-2	2-3	3-4	4-5	5-6	6-7
9	18	18	19	19	19	19
10	21	22	23	22	22	23
11	23	24	25	24	24	25
12	23	24	24	24	24	24

Error %

Time of Day	1-2	2-3	3-4	4-5	5-6	6-7
9	-62%	-68%	-69%	-69%	-69%	-71%
10	-42%	-49%	-50%	-50%	-50%	-52%
11	-54%	-62%	-64%	-63%	-63%	-65%
12	-63%	-71%	-73%	-72%	-72%	-74%

As before, starboard was right next to the dock where no sunlight was able to reach the starboard side and buildings around it blocked the low sun as well (next page).

White Ship - 2 / Port Side   (sun side)

Thermal Imaging Results	Theoretical Model Results	Error %

Thermal Imaging Results

Time of Day	Panel Node Designation					
	1-2	2-3	3-4	4-5	5-6	6-7
9	16	16	16	16	16	14
10	19	19	19	18	18	16
11	22	22	22	22	22	18
12	23	23	22	22	22	18

Theoretical Model Results

Time of Day	Panel Node Designation					
	1-2	2-3	3-4	4-5	5-6	6-7
9	16	16	16	15	15	15
10	19	19	19	19	18	18
11	21	21	21	21	20	20
12	22	22	21	21	21	21

Error %

Time of Day	Panel Node Designation					
	1-2	2-3	3-4	4-5	5-6	6-7
9	1%	2%	3%	3%	4%	-9%
10	-1%	1%	2%	-3%	-2%	-13%
11	3%	5%	6%	7%	8%	-11%
12	4%	6%	3%	3%	5%	-14%

This was a different white ship, 45 metres in length and in water, having a more reflective surface. Accounting for this in the theoretical model, the results showed a satisfactory link with a correlation between both models of around 4%

White Ship - 2 / Starboard Side (shade side)

Thermal Imaging Results	Theoretical Model Results	Error %

Thermal Imaging Results

Time of Day	Panel Node Designation					
	1-2	2-3	3-4	4-5	5-6	6-7
9	11	11	11	11	11	11
10	12	12	12	12	12	12
11	14	14	14	14	14	14
12	14	14	14	14	14	14

Theoretical Model Results

Time of Day	Panel Node Designation					
	1-2	2-3	3-4	4-5	5-6	6-7
9	11	12	12	12	12	12
10	13	13	13	13	13	13
11	14	15	15	15	15	15
12	15	15	15	15	15	15

Error %

Time of Day	Panel Node Designation					
	1-2	2-3	3-4	4-5	5-6	6-7
9	-4%	-5%	-5%	-5%	-6%	-6%
10	-8%	-9%	-10%	-10%	-10%	-10%
11	-2%	-4%	-4%	-4%	-4%	-5%
12	-8%	-10%	-10%	-10%	-10%	-11%

Satisfactory correlation with an average error of about -7%.

Grey Ship / Port Side (sun side)

Thermal Imaging Results	Theoretical Model Results	Error %

Thermal Imaging Results

Time of Day	Panel Node Designation					
	1-2	2-3	3-4	4-5	5-6	6-7
9	33	32	32	32	32	18
10	40	40	40	40	40	22
11	44	43	42	40	40	24
12	46	45	44	43	40	30

Theoretical Model Results

Time of Day	Panel Node Designation					
	1-2	2-3	3-4	4-5	5-6	6-7
9	29	29	28	28	27	27
10	39	38	37	37	36	35
11	45	43	42	42	41	40
12	46	44	43	43	42	41

Error %

Time of Day	Panel Node Designation					
	1-2	2-3	3-4	4-5	5-6	6-7
9	11%	11%	12%	13%	14%	-48%
10	3%	6%	7%	8%	10%	-58%
11	-1%	0%	-1%	-5%	-3%	-65%
12	0%	1%	1%	-1%	-6%	-36%

Another ship was measured which was a 45metre grey yacht moored on its starboard side, such that the sun fell only on the port side. Model shows good correlation with an average error of 5% except at 0900h in the morning due to blocking of the low sun by nearby hills and buildings. Nodes 6-7 which represent the plate near the waterline have a marked difference possibly because of the difference in ship geometry which was not included in the theoretical model (which used the original blue ship geometry).

Grey Ship / Starboard Side (shade side)

Thermal Imaging Results	Theoretical Model Results	Error %

Time of Day	Panel Node Designation					
	1-2	2-3	3-4	4-5	5-6	6-7
9	16	16	15	14	13	9
10	17	17	16	13	11	10
11	17	17	16	13	12	10
12	20	18	17	14	13	13

Time of Day	Panel Node Designation					
	1-2	2-3	3-4	4-5	5-6	6-7
9	13	13	14	14	14	14
10	17	17	17	17	17	17
11	19	20	20	20	20	21
12	21	22	22	22	22	22

Time of Day	Panel Node Designation					
	1-2	2-3	3-4	4-5	5-6	6-7
9	17%	16%	10%	3%	-4%	-51%
10	3%	0%	-7%	-32%	-56%	-73%
11	-15%	-19%	-28%	-57%	-70%	#####
12	-5%	-22%	-30%	-58%	-70%	-72%

As before, since it's moored next to a concrete dock, which blocks the sun reaching the starboard part of the hull, this is much cooler in real life than predicted by the theoretical model.

2   Thermal Camera Details
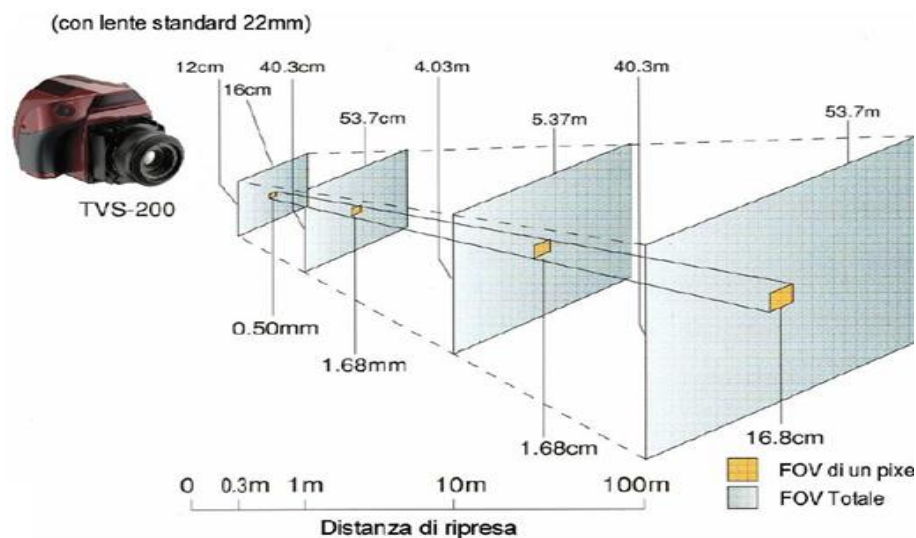
Figure 83: Effect of camera distance from surface being measured on image quality

The Thermal camera being used was the model AVIO TVS-500 had a sensor of 320x240 pixels. It was accurate to within +/- 2°C according to the manufacturer's specifications and had the possibility of taking simultaneous thermal and visual photographs. Figure **83** shows the effect of increasing distance between the thermal camera and the object being measured. At 1metre distance, 1 square pixel is 1.68cm and an area of 53.7 cm^2 can be measured. At 100metres, 1 sq. pixel is 16.8cm but the area of measurement increases to 53.7 m^2. Thus, the closer one is to the measured object, the better the readings but smaller the size of the object that can be measured. Typical distances measured during this project were between 10-50 metres.

3   Solution of a Bi-quadratic Equation

The quartic or bi-quadratic equation of the form, $ax^4 + bx^3 + cx^2 + dx + e = 0$ can be solved as follows. When the coefficients b and c are equal to zero, a and d are positive and e is negative, hence greatly simplifying the determination of the roots.

There is only one real positive root because the derivative of the function $f(x) = ax^4 + dx + e$ for positive values of x (temperature is always positive in the Kelvin scale) is $f'(x) = 4ax^3 + d$ which is always positive, and the function will be strictly increasing in the interval$(0, \infty)$.

To find the roots, we need to evaluate the terms, Δ_0, Δ_1, Q, p, q and S. These terms are given by the following relationships,

$$\Delta_0 = c^2 - 3bd + 12ae = 12ae$$

$$\Delta_1 = 2c^3 - 9bcd + 27b^2 + 27ad^2 = 27ad^2$$

$$Q = \sqrt[3]{\frac{\Delta_1 + \sqrt{\Delta_1^2 - 4\Delta_0^3}}{2}}$$

$$p = \frac{8ac - 3b^2}{8a^2} = 0$$

$$q = \frac{b^3 - 4abc + 8a^2d}{8\,a^3} = \frac{d}{a}$$

$$S = \frac{1}{2}\sqrt{-\frac{2}{3}p + \frac{1}{3a}\left(Q + \frac{\Delta_0}{Q}\right)} = \frac{1}{2}\sqrt{\frac{1}{3a}\left(Q + \frac{\Delta_0}{Q}\right)}$$

There are four roots to a quartic equation. Selecting only the real positive root to the given quartic equation, after the above computations yields,

$$x_{real,+} = -S + \frac{1}{2}\sqrt{-4S^2 - 2p + \frac{q}{S}} = -S + \frac{1}{2}\sqrt{-4S^2 + \frac{q}{S}}$$

4   MATLAB Code Listing

An extract of the main body of the MATLAB program code is presented here.

```matlab
%% Original code written by Vivek Kumar, July-December 2013
%  Master Thesis Project, University of Genoa, Italy, EMSHIP
%% INITIALIZE
clear all ; clc ; close all

%% DEFINE GLOBAL INPUT PARAMETERS

Tship          = 25+273;    % ship internal temperature in degrees [Kelvin]
waterline      = 1300;      % ship draught in [mm]
ship_heading   = -106;      % angle in degrees (-180 to 180, negative for east of north-south
line)
water_reflect  = 0.07;      % water/ground reflectance
solar_const    = 1367;      % [W/m2] Solar Constant E_sc
InWater        = 1;         % 1=Ship is in water, 2=Ship is out of water

% Convective Heat transfer coefficients for a 24 hours period
% Replace with(gentle wind conditions = 20 W/m2K , more windy conditions = 25 W/m2K)
hc_air  = 12*ones(1,24);    % no wind conditions, only natural convection

hc_water = 500*ones(1,24);  % Typical value for water = 500 W/m2K

% Initial Parameters for the Solar Ray Tracing Calculations
% n = no. of days since 1st Jan, calculated for the 21st of every month
n = [21 52 80 111 141 172 202 233 264 294 325 355];

% Local Standard time, ie. hourly time (without considering daylight saving)
LST = 1:1:24;

%% SITE LOCATION DATA + ASHRAE DATA
%Location=Genoa
lat = 44.4111;              % degrees, -ve if in southern hemisphere
long = 8.9328;             % degrees, -ve if west of GMT
TZ = +1;                   % hours +/- of UTC i.e. GMT

% Beam optical depth
tau_b = [0.343 0.38 0.435 0.445 0.462 0.505 0.487 0.477 0.455 0.441 0.373 0.346];
% Diffuse optical depth
tau_d = [2.292 2.097 1.926 1.938 1.942 1.845 1.936 1.964 1.987 1.955 2.168 2.274];
% Month design Dry bulb temperatures
DWB5 = [13.9 14.2 16.1 18.1 23.2 26.4 28.9 28.9 26 22.1 18 15.1]; % (5% design conditions)
% Mean daily temperature range
MDTR = [6.2 6.4 6.7 6.9 7.3 6.5 6.5 6.1 6.8 5.8 5.7 5.9];
% Fraction of daily temperature range
FDTR=[0.88 0.92 0.95 0.98 1.00 0.98 0.91 0.74 0.55 0.38 0.23 0.13 0.05 0.00 0.00 0.06 0.14
0.24 0.39 0.50 0.59 0.68 0.75 0.82];

%% MATERIAL DATA

% 1=black paint, 2=epoxy, 3=aluminium, 4=insulation, 5=white paint
% 6=gray paint

% Thicknesses in [mm] for each material
thk    = [1    10  5    60   1   ];
emis   = [0.9  0   0    0    0.9 ];
% Material properties (some elements are zero because they are not needed)
absorb = [0.95 0   0    0    0.3];
cond   = [0.2  0.1 200 0.2 0.2 ];
alphaT = [55e-6 55e-6 23.6e-6 55e-6 55e-6];
YMod   = [0    10  70   0    0   ];

length = 1000; %in mm, for panel length

%% SHIP GEOMETRY CALCUALTIONS
run('Cal_ShipGeometry')

% Input = Ship x,y,z data for intersection of frames and longitudinals
% Output = Panels calculated from 4 point node data with
% tilt and azimuth angle calculated for each panel;
% ship_heading, azimuth_star_corrected, azimuth_port_corrected;
```

```matlab
%% SOLAR RAY TRACING CALCULATIONS
run('Cal_SolarTracing') % This runs the i,j,k loop beforehand to speed up the program

%% PARAMETRIC EVALUATION

for InWater=1:2 %1 = In water, 2=Out of water

    if InWater==2; %if out of water, temperature of fluid under waterline is same as air
        Tw(i,j)=Ta(i,j);
        waterline=0;
    end

    % for SH = 1:12; ship_heading=30*(SH-1);

    for epoxy_thk=1:20

        thk(2)=epoxy_thk; % thickness is varied from 1-20mm
        % 0.001 to convert mm to metres, Resistance for each layer/material
        Res = 0.001.*thk./cond;

        % Total layer resistance for black paint
        Rsum(1) = Res(1)  +   Res(2)+Res(3)+Res(4);
        % Total layer resistance for white paint
        Rsum(5) = Res(5)  +   Res(2)+Res(3)+Res(4);


        for i = 1:12 % Loop to start no. of months

            for j=1:24 % Loop to start number of hours in a day

                for k = 1:10 % Loop to start calculations for every panel in station

                    run('Cal_DifferentPaints')

                end % k-loop (for number of panels/nodes)

            end % j-loop (no. of hours in a day)

            % Calculates temperature for ship in water and out of water
            InWater_MaxSurfTemp_star(InWater,i)=max(max(Ts_star(i,:,:,1)))-273; %Black
            InWater_MaxSurfTemp_star5(InWater,i)=max(max(Ts_star(i,:,:,5)))-273; %White

            InWater_MaxSurfTemp_port(InWater,i)=max(max(Ts_port(i,:,:,1)))-273; %Black
            InWater_MaxSurfTemp_port5(InWater,i)=max(max(Ts_port(i,:,:,5)))-273; %White

        end % i-loop (no. of months)

        %%
        EpoxyMaxDeflection_star(epoxy_thk)=max(max(deflection_star(:,:,1,1))); %Black
        EpoxyMaxDeflection_star5(epoxy_thk)=max(max(deflection_star(:,:,1,5))); %White

        EpoxyMaxDeflection_port(epoxy_thk)=max(max(deflection_port(:,:,1,1))); %Black
        EpoxyMaxDeflection_port5(epoxy_thk)=max(max(deflection_port(:,:,1,5))); %White

        %Calculate minimum deflections
        EpoxyMinDeflection_star(epoxy_thk)=min(min(deflection_star(:,:,1,1))); %Black
        EpoxyMinDeflection_star5(epoxy_thk)=min(min(deflection_star(:,:,1,5))); %White

        EpoxyMinDeflection_port(epoxy_thk)=min(min(deflection_port(:,:,1,1))); %Black
        EpoxyMinDeflection_port5(epoxy_thk)=min(min(deflection_port(:,:,1,5))); %White

    end % epoxy_thickness-loop (from 0-20mm)

end % For in water or out of water


% Plot All Graphs
run('Plotting2')

%% ///////////////////////// END OF PROGRAM /////////////////////////////
```
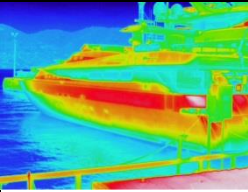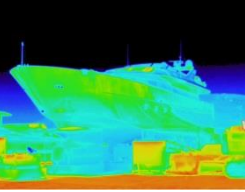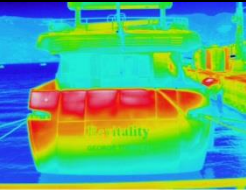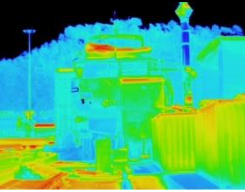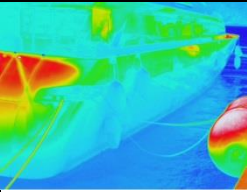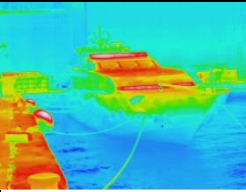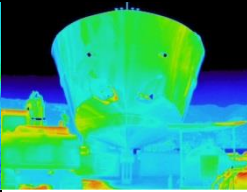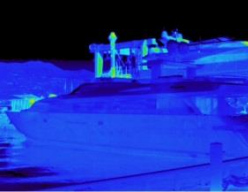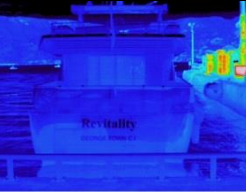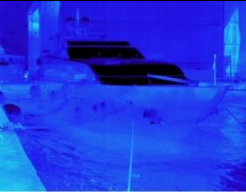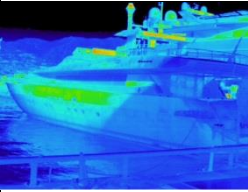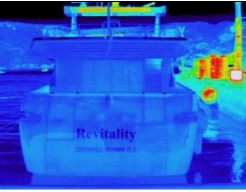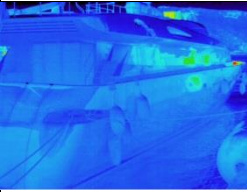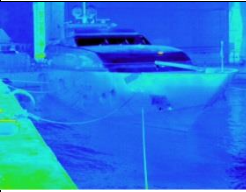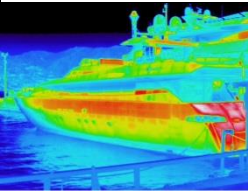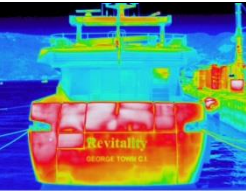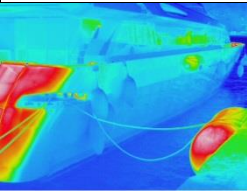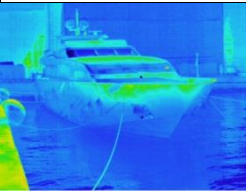
5   Thermal Imaging Comparison of the Dark-Blue Vs White Ship (Aug, 2013)

Time of Day	Blue Ship [Port]	White Ship [Port]	Blue Ship [Stern]	White Ship [Stern]	Blue Ship [Starboard]	White Ship [Starboard]	Blue Ship [Bow]	White Ship [Bow]
0800				Not Available				
0900								
1000								
1100								
1200								

Time of Day	Blue Ship [Port]	White Ship [Port]	Blue Ship [Stern]	White Ship [Stern]	Blue Ship [Starboard]	White Ship [Starboard]	Blue Ship [Bow]	White Ship [Bow]
1300								

6   Thermal and Visual Observations on the Dark Blue Ship (Aug, 2013)

Time of Day	Blue Ship [Port]		Blue Ship [Stern]		Blue Ship [Starboard]		Blue Ship [Bow]	
0800								
0900								
1000								

Time of Day	Blue Ship [Port]		Blue Ship [Stern]		Blue Ship [Starboard]		Blue Ship [Bow]	
1100								
1200								
1300								
1400								
1500								

Time of Day	Blue Ship [Port]		Blue Ship [Stern]		Blue Ship [Starboard]		Blue Ship [Bow]	
1600								
1700								
1800								

7   Thermal and Visual Observations on the White Ship from (Aug, 2013)

Time of Day	White Ship [Port]		White Ship [Stern]		White Ship [Starboard]		White Ship [Bow]	
0800			Not Available	Not Available				

Time of Day	White Ship [Port]	White Ship [Stern]	White Ship [Starboard]	White Ship [Bow]
0900				
1000				
1100				
1200				
1300				